CIAMTIS

U.S. DOT Region 3 University Transportation Center

Extending the Service Life of Rigid Pavement Joints with Self-Healing Sealants

January 18, 2024

Prepared by:

Sandra Milev, Mohammad Shadab Shaikh, Shivani Agrawal, Christopher J. Kloxin, Alexander S. Brand, Jovan Tatar

PennState College of Engineering

LARSON TRANSPORTATION INSTITUTE

DISCLAIMER

The contents of this report reflect the views of the authors, who are responsible for the facts and the accuracy of the information presented herein. This document is disseminated in the interest of information exchange. The report is funded, partially or entirely, by a grant from the U.S. Department of Transportation's University Transportation Centers Program. However, the U.S. Government assumes no liability for the contents or use thereof.

1. Report No.	2. Government Accession No.	3. Recipient's Catalog No.
CIAM-UTC-REG17		

4. Title and Subtitle	5. Report Date
Extending the Service Life of Rigid Pavement Joints with Self-Healing Sealants	December 31, 2023

6. Performing Organization Code

7. Author(s)	8. Performing Organization Report No.
Sandra Milev; Mohammad Shadab Shaikh, Shivani Agrawal, Christopher J. Kloxin, Ph.D.; Alexander S. Brand, Ph.D., P.E.; Jovan Tatar, Ph.D.	

9. Performing Organization Name and Address	10. Work Unit No. (TRAIS)
University of Delaware 127 The Green Newark, DE 19716	

11. Contract or Grant No.

69A3551847103

12. Sponsoring Agency Name and Address	13. Type of Report and Period Covered
U.S. Department of Transportation Research and Innovative Technology Administration 3rd Fl, East Bldg E33-461 1200 New Jersey Ave, SE Washington, DC 20590	Final Report, 02/01/2020 – 12/31/2023

14. Sponsoring Agency Code

15. Supplementary Notes

Work funded through The Pennsylvania State University through the University Transportation Center Grant Agreement, Grant No. 69A3551847103

16. Abstract

As transportation agencies largely neglect joint sealant maintenance in concrete pavements, water infiltration into the deteriorated joint and subgrade often results in base softening, erosion, and faulting, posing a significant financial burden on taxpayers. To improve the durability performance of concrete pavement sealants, an elastomer with self-healing ability was designed by incorporating dynamic disulfide bonds. The effects of monomer type, type of initiator/catalyst and its concentrations on the polymer network were analyzed to understand how they influence material properties and eventually polymer self-healing. The performance of the new self-healing sealant was characterized under typical environmental and load conditions experienced by pavement joints. The sealant exhibited satisfactory performance across several aspects (modulus, strength, adhesion, hardness, fatigue) with self-healing efficiency of 78%. However, before implementation, critical concerns regarding residual deformation and UV resistance must be addressed.

17. Key Words	18. Distribution Statement
sealants, self-healing, concrete pavements, dynamic covalent bonds	No restrictions. This document is available from the National Technical Information Service, Springfield, VA 22161

19. Security Classif. (of this report)	20. Security Classif. (of this page)	21. No. of Pages	22. Price
Unclassified	Unclassified	100	

Form DOT F 1700.7 **(8-72)** **Reproduction of completed page authorized**

Table of Contents

List of tables

List of figures

CHAPTER 1

Introduction

One of the key difficulties faced by highway agencies today is how to evaluate, maintain, and improve existing pavements to match today's trends toward heavier traffic loadings, and larger traffic volumes, rather than how to design and construct new pavements. In fact, maintenance, repair, and rehabilitation are the most reported road-related expenses (Liu et al., 2010). Throughout its service life, concrete pavement is constantly subjected to traffic pressures as well as stresses caused by temperature and moisture changes. As the temperature and weather vary, the concrete expands and contracts. These environmentally induced stresses are released through cracking, particularly at the weak points in the concrete (Teller et al., 1936). Implementation of the joint system is necessary to manage the position and geometry of transverse and longitudinal cracking in concrete pavements. This implies that concrete will crack irrespective of the presence of joints but if joints are present they provide a guided path to release stresses in the form of cracks.

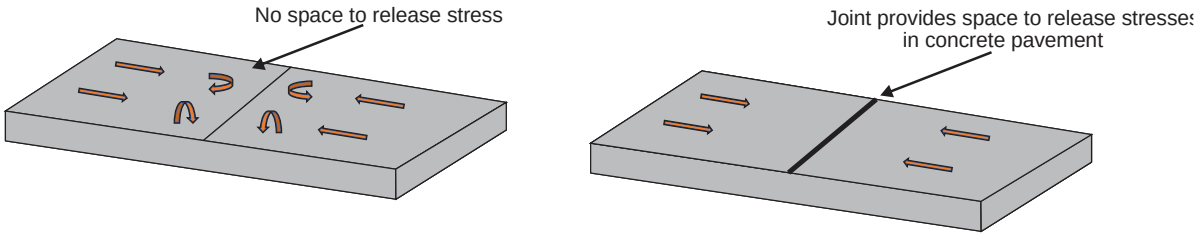

Figure 1. Joints in concrete pavements

There are various caulking and sealant materials that are used for concrete pavement joints, such as silicones, polysulfides, urethanes, and acrylics. All of these sealants have advantages and disadvantages related to curing, adhesion, ultraviolet (UV) light resistance, and intended application. Acrylics are generally used in low-movement joints, adhere to a variety of substrates, cure slowly and exhibit some shrinking after curing (Lu et al., 2022). Polysulfides possess excellent chemical resistance and perform well in submerged applications, but they have poor recovery after moderate cyclic movements and limited UV stability (Foster, 1987). Silicones have excellent movement capabilities, heat stability and UV resistance, and good adhesion to several substrates; however, a primer is recommended on cementitious substrates to improve adhesion. Polyurethanes adhere to a wide variety of substrates and have good toughness and abrasion resistance, but poor UV resistance (Lu et al., 2022).

Although conventional sealants mentioned above possess many advantages, numerous challenges such as long-term performance, reliability, and sustainability are involved with their application (Mphahlele et al., 2017; Peterson et al., 2012). The ability to repair micro-cracking, delamination, and other defects in-situ would be of great importance for extending the service life of construction sealants. Furthermore, environmental impact and waste management of plastics are identified as critical issues that should be addressed (Paolillo et al., 2021).

Research on polymers with dynamic covalent bonds has grown over the past decade due to their ability to repeatedly repair damage before failure occurs. Self-healing ability is appealing for polymers since these materials can be exposed to a harsh environment and load conditions during their service life, which can lead to the accumulation of damage over time (Van Der Zwaag, 2014). So far, considerable research efforts have been focused on developing different polymers with covalent adaptable networks (CANs) that can break and reform when exposed to heat, light, and other stimuli. It has been shown that CANs have the potential for application in many fields: sensors, probes, coatings, etc. One of the big challenges related to introducing these polymers as commercial products is related to synthetic processes that are in most cases difficult to implement in manufacturing. Furthermore, for applications in infrastructure, understanding durability performance under environmental conditions is essential for the transition of these materials from the lab into industrial products. For example, some polymers may be adequate in terms of functionality and load-carrying capacity, but if they are susceptible to rapid degradation, their use is limited. During their service life, polymers used in construction are exposed to a variety of environmental conditions: moisture, UV radiation, various chemicals, freeze-thaw cycles, etc. As a result of this exposure, their properties deteriorate over time.

Among different polymeric materials, covalently crosslinked polymers (thermosets) are preferred when good mechanical properties, resistance to environmental degradation, thermal stability, chemical resistance are required by the service loadings and environment. However, as a result of their cross-linked structure, thermosets have the disadvantage of not being recyclable and healable due to the permanent nature of crosslinks once the polymerization reaction is complete. In the last few decades, advancement in the development of engineering materials is driven by the need for energy-efficient solutions that would promote sustainable use of resources (Guimard et al., 2012). To achieve this goal, research has been focused on extending the life span and development of recyclable polymers. CANs are a new class of polymer, that can change their topology under thermal stimuli (Montarnal et al., 2011) . They are considered to have the potential to overcome issues related to processability and provide repairability and improved long-term performance (Kloxin & Bowman, 2013). Under specific stimuli, CANs can rearrange their structure by exchange reactions while maintaining a constant degree of cross-linking at all temperatures lower than degradation temperature (Capelot et al., 2012), (Montarnal et al., 2011). This unique property of CANs allows the polymer to surpass the limitations of covalently cross-linked (thermosets) and physical networks (thermoplastics). They are designed to combine the superior mechanical properties of thermosets and the processability of thermoplastics.

For applications in infrastructure, the ability to adjust material properties to meet specific service requirements is a highly attractive feature. For example, by adjusting stoichiometry, using different monomers, or changing cross-linking density, the modulus can be varied to satisfy load-carrying capacity at room temperature for structural applications (Zhang et al., 2019), or low modulus requirement of non-

structural sealants. These same parameters (polymer network stiffness, crosslinking density) in addition to catalyst type and content, temperature, also affect the self-healing ability. A decrease in backbone stiffness increases the mobility of polymer segments, which enhances self-healing. Overcoming trade-off between mechanical properties and self-healing according to the intended application, developing scalable and low-cost synthetic processes, are essential for the transition of these materials into commercial space.

OBJECTIVES

The objective of our research was to investigate the potential of self-healable polysulfide sealants to extend the service life of rigid pavement joints. The self-healing ability of the sealant is enabled by the disulfide dynamic polymer network. Disulfide bond exchange was employed due to the commercial availability of compounds with disulfide bonds with some of them having the ability to exchange bonds at room temperature. The research was conducted to address the following project objectives:

- **Objective 1**. Synthesize a sealant with repeatable self-healing abilities that will extend the service life of joint seals

- **Objective 2** Determine how changes in type of monomer, type of initiator/catalyst and its concentrations affect the polymer network and ultimately, material properties and self-healing.

- **Objective 3.** Characterize the performance of the new self-healing sealant under typical environmental and loading conditions experienced by pavement joints

CHAPTER 2

Literature review

General Joint Sealant Classifications

There is a wide variety of sealant materials with different properties in the modern construction market, such as polyurethane, polysulfide, silicone, rubberized asphalt, and preformed compression sealant. However, these various types of sealants employed to seal pavement joints can be broadly classified either as cold-poured, hot-poured, or preformed sealant (Figure 2).

- *Cold-poured sealant.* This category of sealants is known to have good adhesive strength, cohesive strength, low modulus, reduced temperature sensitivity, but are highly expensive. Some of the cold-poured sealants include polyurethanes, polysulfides, silicone, and modified epoxies. The most adopted type of sealant by many agencies is a single-component cold-pour silicone.
- *Hot-poured sealants*. This category of sealants is expected to lose the elastic properties when they are overheated, examples of which include asphalt mastics filled with latex, butyl, or reclaimed rubbers.
- *Preformed sealants*. These set of sealants are presumed to be inserted and compressed by a special device. Examples of preformed sealants include molded strips of styrene, urethane, polychloroprene, neoprene, and other synthetic rubbers. The advantage of using preformed sealants is that they are ready for application without the need for on-site heating, mixing, curing. Their effectiveness depends on the lateral pressure during their service life.

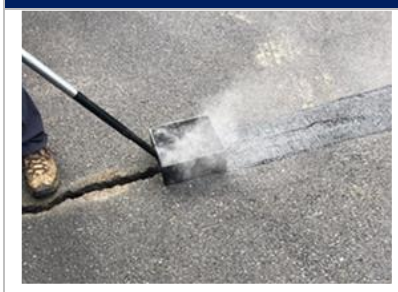

Pen DOT (2024)

a)

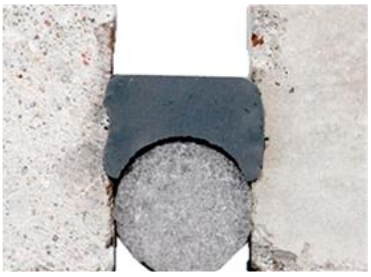

(ACPA, 2018)

b)

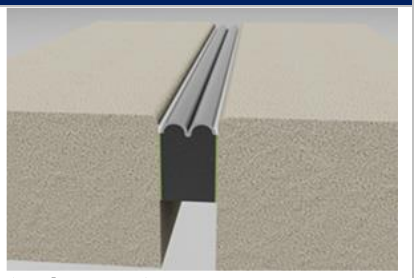

(Wabo, 2024)

c)

Figure 2. Typical image of: a) hot-poured sealant, b) cold-applied sealant, and c) compressed sealant installed into a pavement joint

Historically, hot-poured sealants have been widely adopted for concrete pavement joints. However, the cold-applied sealants – silicone-based in particular – and the preformed sealants according to ASTM D5893 and ASTM D2628, respectively, have gained increased attention in recent years and have become a favored choice by many state DOTs (Lynch et al., 2000). Hot-applied sealant materials are flexible at a relatively

low cost and possess a good sealing features; however, due to aging and water penetration, there is a reduction of flexibility and the adhesion strength in the sealant-concrete interface (Bakhsh et al., 2013). The hot-poured sealants have a capability to last for a long time if installed adequately; according to an FHWA study, it was shown that hot-applied sealants could last for 9 years with an efficiency of up to 75% (Smith & Romine, 1999). Another study conducted by the California Department of Transportation (Caltrans) stated that hot-poured rubber joint sealants were still performing well even after 10 years (State of California Department of Transportation, 2008).

The cold-applied sealants were developed after hot-poured sealants and can render better bonding and expansion characteristics. They are also easier and safer to apply and are less sensitive to changes resulting from aging or temperature effects compared to hot-poured sealants (Brown, 1991; Lynch et al., 2002). However, the cost is higher than hot-poured sealants but can provide a longer service life. A research study carried out in Arizona shows the excellent performance of the cold-poured silicon sealants that served up to 20 years (ARA, 2013): after about 31 million equivalent single axle loads (ESALs).

The third category of sealants, preformed compression sealants, are designed to remain tight in the joint even at the maximum opening of the joint (during summer) and to resist the compressive stresses. The effectiveness of preformed sealants depends on their ability to remain in compression ACPA, 2018; Bakhsh & Zollinger, 2015). Preformed sealants are more resistant to deterioration from exposure to sunlight, weather, oils, chemical, heat, abrasion, and impact, and hydrostatic pressure compare to other sealants; however, they are the most expensive to use for pavement joints. According to the field study conducted by the Michigan Department of Transportation (MDOT) on various concrete pavement joint sealants, it was concluded that preformed compression sealants show a better performance than other sealants (Eacker and Bennett, 2000). Two recent studies, one from FHWA's long-term pavement performance (LTPP) SPS-2 experiment in Arizona (ARA, 2013) and the other study conducted by pavement preservation product manufacturer Crafco in Spokane, Washington (Lynch et al., 2013), show that preformed sealants can achieve a service life more than 20 years if properly installed. Previously, there has not been any factual evidence to prove the effective longevity performance of preformed sealants but these recent findings confirm that joint sealants could serve for a very long time.

Moreover, according to Biel & Lee (1997) and the American Concrete Pavement Association (ACPA) (ACPA, 1995; ACPA, 1993; ACPA, 2018a), the criteria for selecting and evaluating a sealant product lies in its elasticity, modulus, adhesion, cohesion, compatibility, weatherability, and jet fuel resistance. The elasticity illustrates the ability of a sealant to regain its original size after being stretched and compressed by traffic and thermal effects. Modulus describes the change in internal stresses in a sealant while being stretched and compressed over a range of temperatures and dynamic traffic loading; a low modulus is desirable, especially in cold-weather climates. The elasticity and the modulus of a sealant define its deformability under stress. Adhesion describes the ability of the sealant to adhere to the concrete joint while cohesion refers to the ability of the sealant to resist ripping from tensile stresses. The sealant must be compatible with the substrate to prevent loss of adhesion, adverse reactions with the substrate, discoloration, and degradation of the material. Weatherability describes the ability of a sealant to resist deterioration from ozone or UV radiation. Lastly, jet fuel resistance is the ability of the sealant to resist degradation in contact with jet fuel, which is relevant for airfield applications. When some materials are in contact with jet fuel swelling may occur, causing the material not to return to its original state nor adhere to reservoir walls. To

ensure optimal performance sealant should possess the ability to deform at low temperatures, while avoiding excessive softening at warmer temperatures to prevent flow out of the joint.

Table 1 below gives a full description of the available joint sealing materials and their relative specifications used for maintenance practice in various DOTs (ACPA, 2018a; Dispenza, 2014; FHWA, 2019). As shown in Table 1, new types of sealant materials have been widely used in concrete pavement joints, including silicone, polysulfide, polyurethane, and other high-performance elastic polymer materials (Feng, 2009). Among them is the polyurethane sealant materials, which are divided into polyether and polyester types. The polyether polyurethane is more pronounced for sealing concrete joints compared to polyester polyurethane, which easily hydrolyzes. After curing, a series of excellent mechanical and durability properties can be achieved from this type of sealant materials, due to the presence of strong polar groups such as -NCO and -OH in the molecular structure of polyurethane, hence making the sealant material useful. These properties also include wear resistance, good oil resistance, high and low-temperature resistance, and strong adhesive and cohesive bond deformation performance (Liu et al., 2019). However, the problem of degradation still affects the polyurethane sealants especially in a humid or moist environment, hence, the polyurethane sealants have poor heat and moisture resistance. Likewise, the easy pulverization and the yellowing under long-term solar radiation also affect the durability of polyurethane sealing materials (Caihua, 2003; Liu et al., 2019).

Another recent cold-applied sealant is polysulfide sealant. Through the vulcanization reaction, the polysulfide sealant compound is formed by polymerizing metal peroxide and liquid polysulfide rubber. The polysulfide joint sealant can be divided into the single-component type and two-component type, or non-sag type and self-leveling type according to fluidity and packaging form. Polysulfides possess good durability and mechanical properties such as corrosion resistance, low-temperature flexibility, good aging resistance, wear and tear resistance, water tightness, and excellent airtightness. The two-component type is most commonly adopted for joint sealing due to the slow curing and high non-sagging tensile modulus associated with the single-component type (Wang et al., 2011; Liu et al., 2008).

Silicone oxide polymer is another type of silicone sealant polymerized from a series of polydimethylsiloxane with different molecular weights. The similarity of this silicon-oxygen bond structure with inorganic silicate not only results in an excellent water- and aging-resistant material but also results in outstanding bonding, good resistance to low and high temperatures, and elasticity (Wang et al., 2011; Liu et al., 2008). However, similar to the polyurethane and polysulfide material, the application of silicone oxide sealants is also limited to a certain extent due to the high cost of production and poor embedding resistance and oil resistance of silicone materials.

In summary, the new categories of joint sealant have been greatly improved in terms of aging resistance, adhesion, environmental adaptability, elastic deformation, and other factors as compared to the traditional joint sealant. The selection of the appropriate sealant depends on factors such as anticipated joint movement, climate, and the specific performance requirements of the application. Regular maintenance and following manufacturer recommendations are essential to ensure the long-term effectiveness of concrete pavement joint sealants.

Table 1. Description and specifications for common joint sealing saterials (ACPA, 2018a; Dispenza, 2014; FHWA, 2019).

Category	Material type	Specification(s)	Description
Liquid, Hot-applied sealants (Thermoplastic material)	Polymerized/Rubberized Asphalts	ASTM D 6690, Type I (AASTHO M 324)	Moderate climates, 50% extension at 0°F (-29°C)
		ASTM D 6690, Type II (AASTHO M 324)	Most climates, 50% extension at -20°F (-29°C)
		ASTM D 6690, Type III (AASTHO M 324)	Most climates, 50% extension at -20°F (-29°C) with other special tests
		ASTM D 6690, Type IV (AASTHO M 324)	Very cold climates, 2000% extension at -20°F (-29°C)
Liquid, Cold-Applied Sealants (Thermosetting) - Single component	Silicone	ASTM 5893, Type NS	Non-sag, toolable, low modulus
		ASTM 5893, Type SL	Self-leveling (no tooling), low modulus
		ASTM 5893, Type SL	Self-leveling (no tooling), ultra-low modulus
		DOW CORNING CORP., (2002)	Jet Fuel Resistant
	Nitrite Rubber	N.A.	Self-leveling (toolable), non sag
	Polysulfide	N.A.	Self-leveling (no tooling), low modulus
	Polymeric low modulus	N.A.	Self-leveling (no tooling), low modulus
Liquid, Cold-Applied Sealants (Thermosetting) – Two-component	Elastomeric polymer (polysulfides, polyurethanes)	Fed Spec SS-S-200E Type M	Jet-fuel resistant, jet-blast resistance machine-applied fast cure
		Fed Spec SS-S-200E Type H	Jet-fuel resistant, jet-blast resistance hand-mixed retarded-cure
Solid, Cold/Ambient Applied sealants	Lubricant	ASTM D 2835	Used in installation of preformed compression seal
	Polychloroprene Elastomeric (Neoprene)	ASTM D 2628	Jet-fuel resistant preformed compression seal
Expansion Joint Filler Materials/Preformed Isolation	Performed filler materials	ASTM D 1751 (AASHTO M 213)	Bituminous, non-extruding, resilient
		ASTM D 1752, Type I-IV (AASHTO M 153)	Sponge rubber, cork, and recycled PVC
		ASTM D 994 (AASHTO M 33)	Bituminous
Preformed Polychloroprene Elastomeric Materials (Compression Joint Seals)	Preformed compression seals	ASTM D 2628	Jet fuel resistant

Category	Material type	Specification(s)	Description
Preformed Polychloroprene Elastomeric Materials (Compression Joint Seals)	Lubricant adhesive	ASTM D 2835	Jet fuel resistant
Backer Rod Materials	Closed-cell	ASTM D 1330, type C	Standard polyethylene foam
		ASTM D 5249	
		ASTM D 5249	Cross-linked polyethylene foam
	Opened-cell	Not recommended	Polyurethane foam
	Bicellular	ASTM D 5249	Outer cross-linked; inner: open-cell foam

Note 1: ASTM D 1190 was withdrawn in 2002 and replaced with ASTM D 6690 (Type I)
Note 2: ASTM D 3405 was withdrawn in 2002 and replaced with ASTM D 6690 (Type II)
Note 3: The use of preformed compression seals in resealing operations will depend on the condition of the joints
Note 4: Only closed-cell backer rods are recommended. A few agencies no longer use backer rods because of concerns that they trap moisture in the joint.

Types of Joint Sealant Damage

Joints are the weakest link for any concrete pavement and bridge structure. Joint failure is the leading cause of water damage to the substructures of pavement, loss of support, and inadequate load transferability (Al-Qadi & Abo-Qudais, 1995; Biel & Lee, 1997; Lima & de Brito, 2009). According to Miller & Bellinger (2003) the joint seal damage is expressed as any condition which allows the passage of water or corrosive chemical material or incompressible materials from the surface to the pavement joint. The joint sealant failure depends on the properties of the material used, joint movements, and sealant installation (Choi et al., 2017). Based on a compressive literature review, besides aging, the failure of these sealants has been associated mainly to failure by cohesive and/or adhesive failures (Chang & Lee, 2002; Fincher, 1983; Lee, 1994; Lima & de Brito, 2009; Odum-Ewuakye & Attoh-Okine, 2006; Price, 1984; Wallbank, 1989). However, according to Miller & Bellinger (2003) and Lamarre et al. (2016), four other types of joint seal damage were identified and reported, some of which are extrusion or intrusion failure, substrate failure, failure due to loss of sealant properties, and impregnation of incompressible material into the sealant joint.

The integrity of any pavement joint sealant relies heavily on the adhesion between the sealant interface and the substrate wall and the cohesion of the sealant material itself. These are the two most prominent failure mechanisms in concrete pavement joints and the relationship existing between other modes of failure. Furthermore, according to many research studies on joint sealing, another critical factor is the installation of sealant (Ioannides et al., 2004; Lynch et al., 2013; . Improper installation of sealants could amount to premature debonding from traffic and weather effects, presence of debris, moisture, and humidity (Gurjar et al., 1998; Gurjar et al., 1997; Hawkins et al., 2001). The joint walls should be cleaned through one or more techniques such as air blasting, water-blasting, and sand-blasting to achieve sound installations for

sealant installation at the concrete joints (Cho, 2013; Gurjar et al., 1998; Morian and Stoffels, 1998). Table 2 demonstrates the summary of causes and factors affecting sealant failure (Ramadani et al., 2014).

Table 2. Common factors, causes, and failure types of joint sealants (Ramadani et al., 2014)

Factors	Cause	Failure type
Traffic or load related factors	Slabs vertical displacements while traffic passes (Particularly in case of joints with faulting) - sealants elongation cycles	Adhesive and cohesive Failure Pumping and faulting
Material properties related factors	Low cohesiveness quality	Cohesive failure and torn failure
	Low bond strength between sealant material and joint reservoir	Adhesive failure
	Lack of sealant material's extension capacity	Cohesive/adhesive/torn failure
Climatic factors (Solar radiation, temperature changes, etc.)	Weathering and aging (Stiffening and losing flexibility	Crack initiation in the middle of the sealant - Cohesive Failure
Factors related to construction/installation	Joint wall dirtiness before installation	Premature Failure (Adhesive)
	Existence of moisture at the joint wall before installation	
Joint distresses	Spalling, corner breaks, etc. directly damage the sealant	Sealant damages and failures
Pavement/Joint and sealant design-related factors	Sealant size and geometry (depth to width ratio)	Affects stress distributions, lead to fatigue - Cohesive Failure
	Joint width too wide (extraction) during winter; preformed sealant not in compression but in tension	Sealant displacement
	Joint width too narrow during summer; Sealant in excessive compression	Sealant press/damage
Sealants chemical reactions	Destructive chemical reactions between sealant materials and fuel/engine oils particularly the jet fuels in airfields	Stiffening - Cohesive Failure

Adhesion failure

The joint seal damage due to adhesion failure is also referred to as the loss of bond between the sealant and the side of the pavement joint. This kind of failure is associated with the uneven surface preparation, tensile stresses from the joint movement which exceeds the capacity of sealant bonding to the concrete surface, and weak bed configuration (Choi et al., 2017; Li et al., 2014). Adhesive failure is more common than cohesive failure and more pronounced when silicone sealant is used (Biel & Lee, 1997). Failure due to adhesion may also be due to joint reservoir walls, if not cleaned and dried before installation. The walls with debris or moisture will decrease the amount of contact area between concrete slab and sealant in which the sealant adhere to the debris instead of the slab (Gurjar et al., 1997; Li, 2011; Ramadani et al., 2014).

The integrity of any pavement joint sealant relies heavily on the adhesion between the sealant interface and the substrate wall. The strength of this adhesion is dependent on their interaction with each other and on many other variables. The strength of adhesion should be strong enough to overcome all the static and dynamic stress applied to the sealant-pavement interface (Odum-Ewuakye & Attoh-Okine, 2006). This static and dynamic stress could be thermal movement, traffic loading, distress such as faulting in the pavement. Gurjar et al. (1998) investigated the adhesive bond between the joint sealant and concrete surface and found that concrete substrate, temperature, humidity during curing, and sealant type were pertinent factors.

Cohesion failure

Unlike the adhesion failure, which is the rupture between the sealant and concrete, cohesion failure signifies the breakage or cracks with the sealant materials itself when the stresses within it exceed the strength of sealant (Li et al., 2014). The cracks within the sealant can occur in either the longitudinal or transverse directions. This kind of failure is associated with joint movements, traffic loads, poor sealant quality, presence of air voids in the sealant, and improper multi-component sealant mixing (Choi et al., 2017; Li et al., 2014). A combination of these stresses (horizontal and vertical), aging, and material properties causes internal micro-cracking, and once the micro-cracking begins, the problem often grows to a larger scale until macro-cracks develop eventually. Consequently, the macro-cracks will later occur to the entire sealant depth until the sealant fails (Gurjar et al., 1996; Gurjar et al., 1997; Li, 2011). According to Biel & Lee (1997), cohesive failure is most common in polyvinyl chloride coal tar and rubberized asphalts.

If the adhesive strength is higher than cohesive strength, cohesive failure may happen over time. Conversely, if cohesive strength is higher than adhesive strength, adhesive failure occurs over time due to aging. An illustration of join adhesion and cohesion failure is shown in Figure 3.

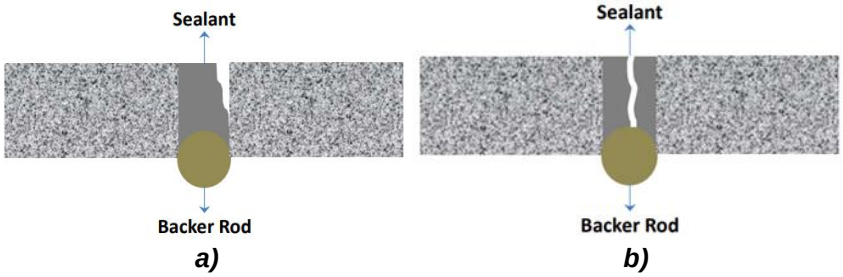

Figure 3. Joint sealant failure due to a) adhesion and b) cohesion (Choi et al., 2017).

Torn or missing sealant

The torn or missing sealant is expressed as the sealant failure due to the combination of adhesive and cohesive failures, which also involve the displacements of sealant from its position. This type of sealant failure is due to loss of sealant properties, improper surface preparation, and workmanship, poor sealant quality, and inadequate shape factors of the pavement joints (Choi et al., 2017).

Amount of incompressible material

The presence of incompressible materials, such as sand or rocks, into a poorly sealed pavement, result in blowups. During thermal expansion and contraction of concrete, a movement occurs which causes an

excessive blowup at the joints with incompressible solids, causing failure of the concrete pavement. The incompressible material itself does not cause the joint seal damage, rather, it is an expression of improper joint seal installation or the adhesion or cohesion damage to the sealant (Choi et al., 2017).

Joint faulting and pumping

Joint faulting refers to as the difference in elevations across the joint between adjacent slabs due to pumping from poor drainage and loss of fine materials at the jointed slabs, slab movement, and settlement, and slabs curling due to change in temperature and other causes. This is more prominent with jointed plain concrete pavement (JPCP), with the average faulting above 2.5 mm (Choi et al., 2017). The faulting degrades the ride quality and occurs either at the transverse or longitudinal joint. Likewise, the use of an unstabilized base or subbase or the absence of dowels could cause faulting even if the joint is sealed properly. Although the faulting is not necessarily caused by a failure in an adhesive or cohesive failure of sealant, the faulting problem could be highly exacerbated based on the performance of the joint seal. Furthermore, pumping occurs due to seeping or ejection of water from beneath the pavement through the pavement joint. In some cases, this damage is noticeable by deposits of fine sand mater on the pavement surface, which pumped (eroded) from underneath the pavement during traffic loading and leave a stain on the surface. When a larger amount of material is deposited, pumping becomes a huge problem leading to the unsupported slabs (Figure 4).

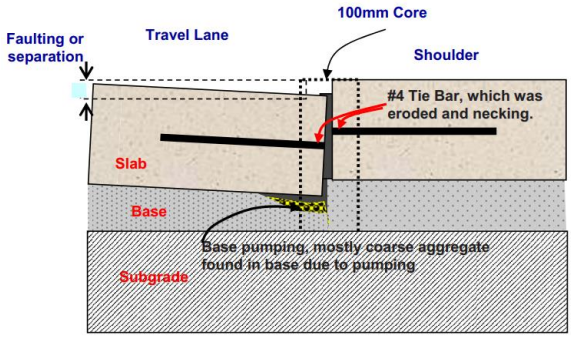

Figure 4. Schematic description of pumping and faulting at pavement joint (D.-H. Chen et al., 2009).

Effect of reservoir shape in joint sealing

The performance of any type of sealant (hot-poured, cold-applied, or preformed sealant) depends on the joint reservoir and the stress applied at these joints. The shape of the joint reservoir is controlled by the amount of joint movement. According to the state agencies, the joint width determination may be considered in conjunction with the estimated joint movement. The online application for joint movement as provided by ACPA (ACPA, 2018) considers the joint spacing, concrete coefficient of thermal expansion, drying shrinkage, sealing temperature, and base type to estimate the joint movement. The estimated values for joint movement range between 0.10 and 0.25 inches (2.5 to 6 mm) (ACPA, 2018).

Eacker & Bennett (2000) presented the estimated values of joint movement for different agencies. Once the joint movement is determined, the appropriate reservoir width can be developed with a perspective of the dimensions or deformability of the selected sealant material, as discussed below:

For hot-poured sealants or thermoplastic sealants, the ability for the sealant material to extend across a range of temperatures must be considered and measured. For instance, for a sealant type with an extensibility of 50%, a concrete pavement with an estimated joint movement of 0.25 inches requires a joint width of 0.5 inches or greater to provide sufficient deformation of the sealant type (FHWA, 2019). If a sealant with 200% extensibility was utilized for the same joint movement of 0.25 inches (6 mm), the joint width could instead be 0.125 inches (3 mm).

For cold-poured or thermosetting sealants, the recommended description by manufacturers should be followed to estimate the required width of the sealant provided with the estimated joint movement. However, the agency should evaluate the manufacturer's recommendations in light of their unique condition. Predictably, a silicone sealant with the estimated joint movement of 0.23 inches (6 mm) would require at least a joint width of 0.5 inches (13 mm).

For preformed sealants, the movement in the joints also influences the reservoir width. The manufacturer's standard and specification should also be followed by agencies for the selected compression seal with the estimated joint movement. Typically, performed sealants are to be installed so that the remaining seal compressed between 20 and 50% of their undeformed shape.

After the width of the reservoir has been evaluated, the shape factor is then employed to determine the depth required for the sealant (ACPA, 1995; ACPA, 2018a; Evans et al., 1999; FHWA, 2019). Pioneered by the work of Tons (1959), the stresses experienced by any sealant material are primarily a function of the sealant shape at the time it is poured to the joint (Tons, 1959). As shown in Figure 5, the poured sealant material is elongated (simulating the joint opening) and the sealant placed to a greater depth undergoes much greater stresses than the shallower sealant. As the sealant gets elongated, the "necking down" effect caused the higher stresses, resulting in adhesive failure. In this regard, the shape factor is employed to minimize this neck down and provides proper in-place sealant dimension. The shape factor is the ratio of the joint width to joint depth (W:D) as illustrated in Figure 6. A proper shape factor in joint sealing minimizes the stresses arising from the sealant-pavement interface and within the sealant itself. However, the selection depends greatly on the type of sealant to be employed.

The recommended shape factors from the literature are as described as follows (ACPA, 1995; ACPA, 2018a; Dispenza, 2014; Tons, 1959): For the asphalt sealants, a shape factor of 1:1 is recommended while a shape factor of 2:1 is recommended for silicone sealants. Thus, for the concrete joint with a width of 0.5 inches (13 mm), a hot-poured sealant would have a sealant depth as equals to the width which is 0.5 inches (13 mm), while a silicone sealant would require a sealant depth of 0.25 inches (6 mm). For the preformed sealants, the shape factor is influenced by the joint movement and the required depth to accommodate the compressed sealant. Typically, the minimum reservoir depths for compressed sealants varies between 1.5 to 2.0 inches (ACPA, 2018a). It is also essential to employ suitable backer rod materials not only to prevent the sealant from the bottom of the reservoir but most importantly to attain the desired shape factor and to secure an uncured sealant from running down into the cracks beneath the reservoir (Figure 6). The use of closed-cell, non-absorptive backer rods, as described in Table 1, are recommended and their compatibility with sealants should be confirmed before use. Because of the moisture-related problem, the open-celled materials should be avoided in joint sealant (ACPA, 2018a).

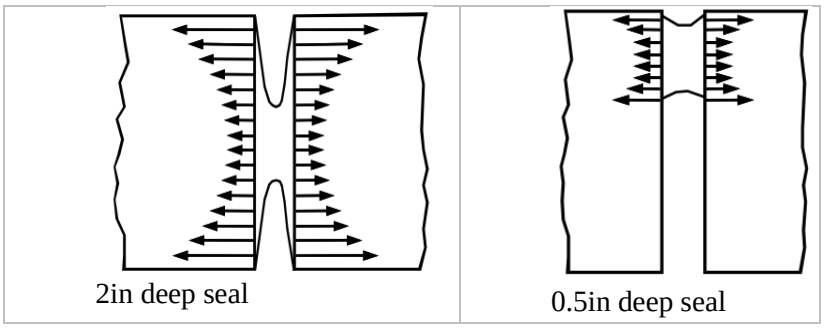

Figure 5. Schematic effect of shape factor on sealant stresses (Dispenza, 2014).

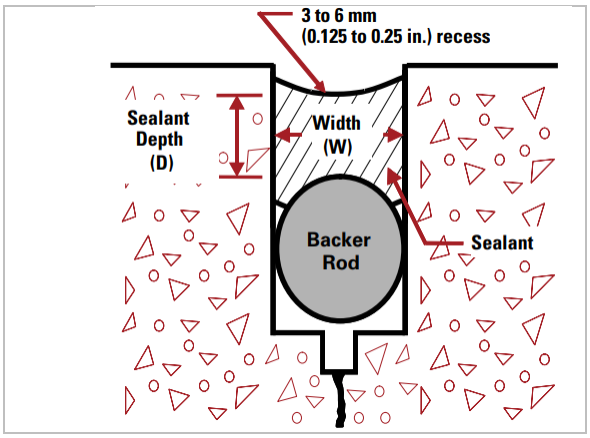

Figure 6. Schematic image of sealant shape factor and the effect of backer rod (Dispenza, 2014).

Durability measures of different sealants

During service life sealants are exposed to moisture, UV light, freeze-thaw cycles, motor oil, fuel, cyclic loading. Conventional construction sealants, including polysulfides, polyurethanes, epoxies, and acrylics are known to be sensitive to moisture. Water immersion has several adverse effects on the properties of the polymer sealants: plasticization, hydrolysis, and softening with swelling. swelling, changes in mechanical properties.

The mechanical properties of the polymer can degrade with moisture—hydrolysis lowers the sealant strength and can cause cohesive failure. In addition, the elastic modulus of polymeric sealants decreases as the water uptake of the material increases (Keshavaraj et al., 1994). Evaluating a sealant's performance following exposure to cold conditions assesses its capacity to retain elasticity and flexibility, enabling it to adapt to joint movements and prevent the formation of cracks or leaks. The stiffening of sealants at lower temperatures primarily arises from alterations in the material's rheological characteristics. Cold temperatures reduce the molecular mobility of the polymer chains within the sealant. In a more mobile or rubbery state, polymer chains can flow and deform easily, contributing to the sealant's flexibility. In colder environments, the constrained movement of polymer chains results in heightened stiffness. The long-term performance of a sealant greatly depends on its ability to withstand UV exposure, and humidity. Some effects of UV exposure include discoloration, reduced flexibility and adhesion.

Numerous laboratory test has been developed over the years to investigate the durability performance of various sealant materials used for concrete joint sealing. These test methods were carried out under different working conditions to accommodate the influence of different factors (e.g., traffic loading, thermal expansion, material type) on their performance. Many research studies have evaluated various durability properties such as aging resistance, corrosion resistance, high and low-temperature resistance, water resistance, and chemical stability (Liu et al., 2019).

Liu et al. (2003) and Liu & Wang (2008) compared and analyzed the durability performance of four different sealant materials (polysulfide, silicone, polyurethane, and acrylate) and concluded that the four sealant materials display different performance measures in which acrylate sealant has the lowest elastic recovery rate while the silicone joint sealant possesses poor oil resistance, and the polyurethane sealant has relatively optimal cost performance. Another study was carried out to investigate the tensile and shear fatigue properties of polyurethane and polysulfide joint sealants at room temperature and after freeze-thaw cycles (Liu and Wang, 2006). The results showed that the early performance of both sealants is significance affected by the degree of curing and the polysulfide joint sealant possesses better fatigue resistance and suitable for areas with a huge temperature difference all round year. Chen et al. (2004), also investigated the low-temperature tensile test on seven different normal-temperature construction sealants. The low-temperature tensile strength performance of each sealant corresponds to one another in combination with other relevant specification.

Shou et al. (2007) studied the bonding performance of joint sealant at different interface states (such as clean interface, wet interface, aging treatment interface, and cement slurry treatment interface). It was concluded that the debonding of sealant is easily caused by the wetting at the interface and also shows that the bonding strength can be improved by the bottom coating of the interface agent or by diluting sealant with solvent. Shou & Shang (2007) also performed a comparative study on the fatigue aging resistance of polyurethane and silicone sealants under cyclic loading of hot-pressing and cold-drawing. It was found that the silicone sealant shows better performance than polyurethane material due to the existence of silicone bonds in the silicone material and the presence of a higher adhesive strength retention rate of 95%.

Sun (2007) also conducted a systematic experiment on the durability performance of polyurethane sealant compound polymerized with petroleum asphalt. The other test procedures considered in this study are frost resistance, heat aging resistance, cohesiveness, and curing process effect, etc. It was shown that the sealant produces excellent performance compared to ordinary polyurethane materials and very beneficial for an actual field project in terms of cost-effectiveness. Furthermore, a study was conducted to evaluate the early deformation properties of various commercial sealants influenced by curing rate and curing degree. Results show that the double-component sealant shows a faster curing rate than one-component joint filler, and concluded that the lower the early curing degree of a joint sealant, the worse the performance in terms of elasticity of the material (Liu & Wang, 2008). Cai (2012) also conducted a series of experimental tests of a self-made double-component polyurethane sealant and compared with commonly used joint sealant, good performance with respective cost-effectiveness and the scope of application was reported. Li et al. (2014) also developed a new adhesive strength test method to evaluate the adhesive strength of self-leveling and non-self-leveling silicone sealants and proposed proper testing parameters. Lastly, a recent review on the durability performance was carried out, along with, requirements and research, the development status of

the existing silicone sealing compound. Additionally, an experimental test was conducted to improve adhesive deformation and durability (Li & Yi, 2015).

Polyurethane is one of the important materials of all sealant used from research due to the outstanding properties such as toughness, abrasion resistance, easy preparation, low price, etc. (Aguirresarobe et al., 2017; Shen et al., 2018). Recently a new polyurethane sealant has been modified with hydroxyl-terminated polydimethylsiloxane for sealing concrete joints. The new sealant shows better properties compare to the traditional sealant in terms of tensile strength, cohesion strength, and fatigue resistance (Xu et al., 2011). Also, Carbonell-Blasco et al. (2013) prepared a thermoplastic polyurethane made of rosin or rosin mixture and 1,4-butane diols in the chain extender. However, the presence of no shape memory performance and the difficulty to accommodate the working conditions in the concrete expansion joint associated with polyurethane has led to a decrease in their durability performance (Ahmad et al., 2011).

Another excellent material used for sealing pavement joint is the thermally induced shape memory polymers (SMPs) and above all SMPs, the shape memory polyurethane (SMPU) has been placed on high importance and has gained more attraction due to its scientific and technological significance (Gu & Mather, 2012; Li & Wang, 2016). SMPU is a block copolymer, with both soft and hard segments. This copolymer of SMPU makes them better performance for sealing application, the soft phase helps to maintain the temporary state of SMPU after deformation, and while the hard phase keeps the original state of SMPU (Babaahmadi et al., 2017; Xie, 2011).

Although SMPU shows an excellent performance in engineering applications, meanwhile, some limitations have been recently reported from literature such as thermal stability, smaller shape recovery force, lower tensile strength (Meng & Hu, 2009). However, the use of reinforcing phases such as fibers, particles, nanotube, graphene can improve the limitation associated with SMPU (Zhang et al., 2016). For instance, one common shortcoming of SMPU is the inability to meet performance measures when exposed to heat, oxygen, and UV light during service life. Jianjun et al. (2004) added anti-aging additives in the polymeric material to improve the photo-aging characteristics. Thus, it is crucial to select a suitable reinforcing phase to improve the mechanical and durability properties of SMPU. Of all reinforced materials developed from the literature, silica (SiO2), titanium dioxide (TiO_2), bauxite (Al_2O_3), and clay are the most common inorganic materials employed to bolster the SMPU sealant composites (Jancar et al., 2010). The presence of three crystalline phases (anatase, rutile, and brookite) in TiO_2 has made them to gain engineering attention recently (Seentrakoon et al., 2013; Zohrevand et al., 2014). The TiO_2 reinforced the application of SMPU sealants for expansion joint and also provide excellent characteristics such as non-toxic, low cost, corrosion resistance, increase tensile strength, aging resistance, UV radiation resistance, and chemical stability compared to other inorganic compounds (Lu et al., 2017; Zohrevand et al., 2014). Recent studies found that the employment of nanoparticles TiO_2 in SMPU improved both the mechanical and durability properties by uniformly filling the SMPU pores and wrapped by SMPU to form a compact skeleton structure (Chen et al., 2016; Li et al., 2015; Shen et al., 2018; Thakur & Karak, 2015; Wang & Zhang, 2014). Also, the SMPU/TiO_2 composite shows the presence of amorphous phases or microcrystal structures which improve the absorptivity and reflectivity of SMPU sealant to UV light and visible light, respectively. Finally, it was reported that 3% content of TiO_2 in SMPU improved the mechanical properties, aging resistance, and provide better performance in working conditions with transition temperatures (Shen et al., 2018). However, it is most important to tailor the shape-memory transition temperature (T_t) of sealant

according to its practical application environments (Zhan et al., 2013). This is because when the working temperature is close to the T_t of sealant, the premature shape recovery of sealant can be induced to accommodate the practical working conditions of expansion joints and also achieve the self-healing of damages (Zhan et al., 2013).

Test methods for joint sealants

The prediction and analysis of joint sealant performance in actual engineering field applications are often difficult to measure. The main reason for this complexity is because the current performance test of sealant materials is only limited to a few basic indicators as required in the specification. Based on the lack of significant laboratory experimental evaluation, it is quite challenging to accurately simulate the actual operating environment under working conditions. Some of these hard conditions to simulate during the laboratory test methods are the interminable changes in temperature, traffic loading, the exact expansion and contraction of concrete pavement joint, underlying condition at the joint, etc. However, some researchers across the field have investigated a series of the equivalent test procedures to simulate various working conditions.

Al-Qadi et al. (1999) proposed and developed a testing device capable of simulating the adverse effects of shrinkage, expansion of concrete pavement, and traffic loading in actual working conditions by applying both constant horizontal loading and cyclic loading to two types of cold poured sealants (silicone and polyurethane). The lab testing concluded that the performance of the sealant was affected quantitatively by joint width, joint expansion, aggregate type of concrete, and freezing and thawing cycles. Statistical models were developed to predict the number of loading cycles require for each sealant to fail. Also, it was found that the polyurethane sealant with concrete containing granite aggregates failed in the first 30 cycles of freezing and thawing. It was also recommended to employ a primer when silicone is used to seal concrete made with limestone, because of the incompatibility between the sealant and limestone concrete while silicone sealant is far better on granite concrete (Al-Qadi et al., 1999). Finally, it was concluded that, to optimize the stress resistance and improve the fatigue life of the sealant, the joint width should be kept at a reasonable size. A similar study was also conducted by Worms (Worms, 2005) to evaluate two types of hot-poured sealants using cyclic tension and compression test at three different temperatures.

Furthermore, Soliman et al. (2007) developed two laboratory tests to characterize the performance of hot-poured sealants in cold climates (Soliman et al., 2007). A cyclic compression and tension test at –30ºC were employed to test both the adhesion strength and cohesion strength of sealant and concrete pavement (Soliman et al., 2007). Also, the dynamic shear rheometer (DSR) test was utilized for evaluating the rheological properties of sealant at the temperature ranges of 5 ºC to 64 ºC. A good agreement was reported between the two laboratory test methods and a strong correlation between the laboratory evaluation criteria and two years of field evaluation. It was concluded that laboratory testing could replace the time consuming and costly field studies and provide the ability to test and evaluate the performance of new sealing materials. Similar DSR testing was also conducted by Lynch & Janssen, (1999) to characterize the viscoelastic properties of six silicone sealants at a temperature from -30 ºC to +50 ºC at different frequencies, and a master curve was generated that simulates the performance in the field. Masson (1999) and Al-Qadi et al. (2005) also used the bending beam rheometer test (BBR) to characterize the rheological properties of sealants at low temperatures; it was reported that the sealant rheology is influenced by the sealant stiffness and stress relaxation.

Furthermore, Lacasse et al. (1995) proposed and developed a cyclic fatigue test method to evaluate the high performance of different sealants under cyclic loading. These sealant materials used are silicone, polyurethane, and polysulfide which were compared with one another to assess the long-term performance of the sealant on-field application. White et al. (2012) also applied a stress relaxation test method to evaluate the nonlinear viscoelastic properties of sealant materials and reported that monitoring of apparent modulus changes with time. The result produced can be utilized as a precursor of joint sealant failure. Li et al. (2012) developed an accelerated testing device, the creep testing apparatus (CRETA), to determine the creep performance of two silicone joint sealants and studied their creep sensitivity to temperature changes between 0ºC to 60ºC, including freeze-thaw cycling. The result appears that the silicone sealant tested is a viscoelastic material and its creep response does not appear to be sensitive to the temperature changes. Likewise, an accelerated aging test device was also developed by White et al. (2013) to characterize joint sealants. The computer-controlled device was capable of independently controlling the ambient temperature, humidity, UV radiation, and stress deformation value of the joint sealant. The device could simulate the concrete joint as affected by both mechanical and environmental factors. It was concluded that the apparatus provides an excellent platform to study the long-term durability of constructing joint sealants.

Likewise, similar to the work of White et al. (2013), Li et al. (2014) developed a new testing method to accommodate the influence of temperature variation, humidity, and displacement change rate for characterizing the adhesive bonding strength performance of sealant materials. The variation of adhesive strength tests for two silicone sealants (self-leveling and non-self-leveling) under this different working conditions was measured by this new test. It was concluded that oven-aging reduced the adhesive strength for self-leveling sealant while the non-self-leveling silicone sealant was unaffected by the oven aging. However, the hot water aging and freeze/thaw aging were found to reduce the adhesive strength of both sealants. Wang (2012) also designed a series of both laboratory and field test methods capable of predicting the water sealing performance of sealant materials in the pavement joint.

Laboratory evaluation of a silicone sealant bonded to a different material such as asphalt, polymer concrete, and even steel was carried out (Malla et al., 2011). The test conducted where repair test, tension test, oven-aged bonding test, salt-water immersion test, and a cure (modulus over time) test. It was concluded that the silicone foam possesses the ability to bond to all material and can easily accommodate deformation typical of movement expansion joints (Malla et al., 2011). Previous studies on silicone foam also agreed with this findings (Malla et al., 2006, 2007, 2011).

One important study that presents a compressive test method for choosing an appropriate sealant and its performance for longer service life was proposed by Rogers et al. (1999). As shown in Figure 7, Rogers et al. developed laboratory testing procedures to characterize different types of sealant appropriate for joint under different working conditions. The protocol provides a step by step evaluation of choosing appropriate sealant to quantify the performance requirements under various working conditions (Rogers et al., 1999). These three test procedures are (1) the ASTM C794 adhesion-in-peel test to evaluate concrete/sealant adhesion; (2) dynamic mechanical analysis (DMA) to assess sealant flexibility by evaluating the glass transition temperature (T_g); and (3) the shear fatigue developed to analyze sealant performance when exposed to critical pavement expansion in addition with various traffic and environmental conditions.

Based on the review and analysis of the research status of different types of pavement joint sealants, a lot of research work has been conducted by various researcher, agencies, and DOTs on its preparation and related mechanical and durability properties. In general, there are still inadequacies in the current research studies of sealant materials and these could be implemented in future studies. In summary, future laboratory studies is suggested to be carried to evaluate polymer-based sealants and correlate with field performance conditions under various working conditions. From a literature review, it is quite difficult to evaluate the performance of sealant materials with short term studies. It is therefore crucial to develop a long-term study to make a conclusive result of sealant performance. It is best to propose a long-term procedure under the various working condition for the selection of the most compatible sealing system for any concrete joint by any state in any climatic region.

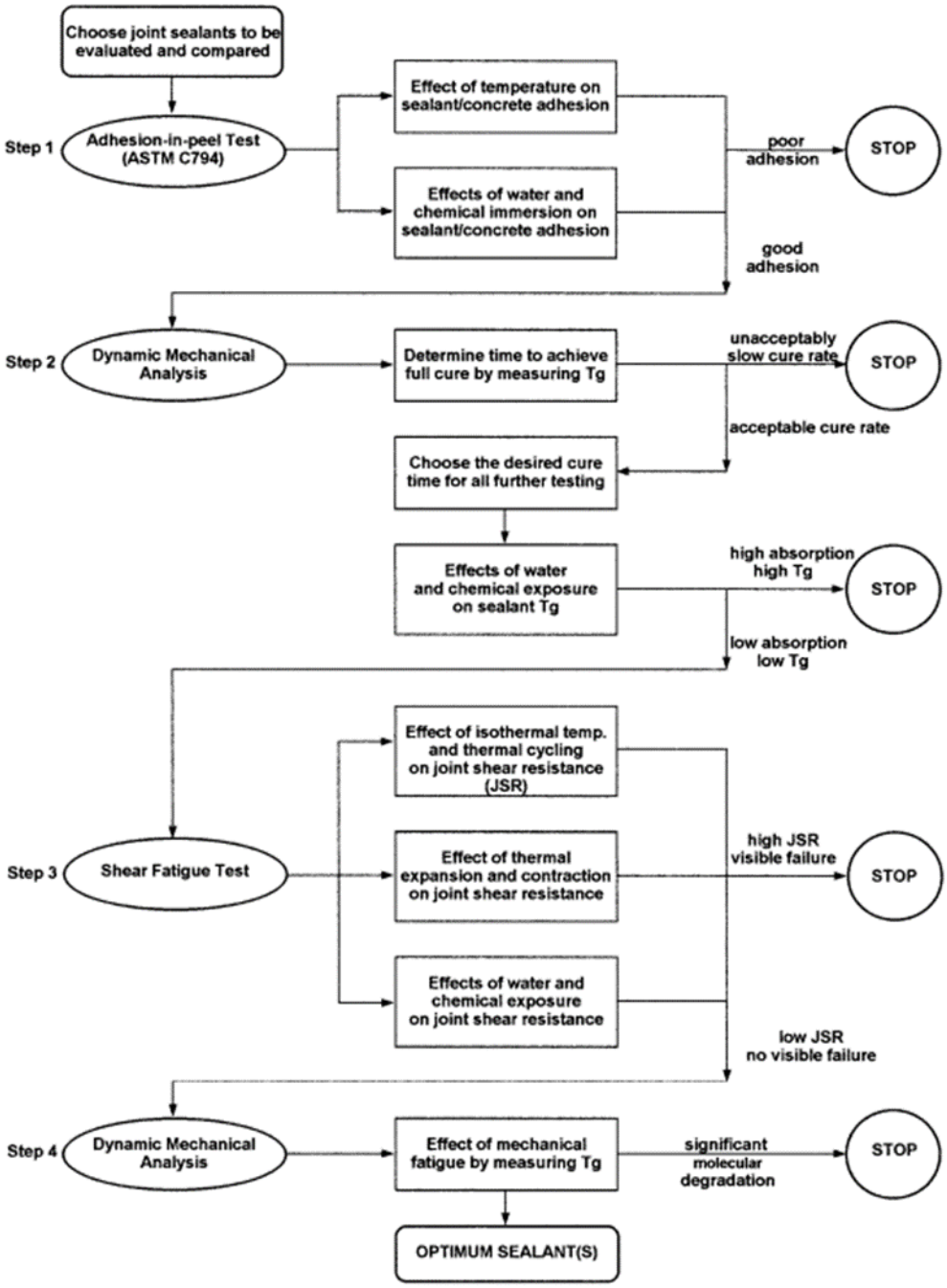

Figure 7. Schematic comprehensive testing method for evaluating a polymer joint sealant (Rogers et al., 1999)***.***

Self-healing of polymers

Self-healing refers to a material's ability to recover from physical damage. The idea of self-healing polymers was initially introduced in the 1950s. In the early 1980s, a theory of crack healing of polymer was first established by Wool & O'Connor, 1981) but the progress in the field of self-healing materials remained limited until the 21st century. The interest in polymeric materials exhibiting self-healing properties has significantly increased since 2000, leading to substantial advancements over the last two decades. Scientists have employed both physical and chemical methods to develop self-healing polymers. Chemical processes include the incorporation of covalent, free-radical, or supramolecular dynamic bonds. Some of the processes leading to physical self-healing include interchain diffusion, shape-memory effects, and the introduction of superparamagnetic nanoparticles (Wang & Urban, 2020). In many cases, these events are interrelated, but differentiation between the physical and chemical processes involved is not simple.

Diffusion

Molecular-level diffusion and local mobility are essential for self-healing (Wang & Urban, 2020). Chain mobility increases with the increase in free volume. When there is more free volume between polymer chains, there is typically more space for chains to move and slide, leading to enhanced diffusion. High diffusivity and flexibility are reflected in low glass transition temperature. In general, lowering the T_g enhances segmental chain mobility and diffusion but does not ensure self-healing.

The reptation model (de Gennes, 1971), describing chain diffusion within a tube, offers a molecular explanation for the time-dependent nature of self-healing of thermoplastics. This model implies that chains with lower molecular weight exhibit better repairing conditions, as they exhibit enhanced chain mobility and shorter repair times. Self-healing at a fractured interface is enabled by the presence of cleaved chains, untangled free chains, or dangling ends with one side anchored in the polymer network (Yang, 2015).

Dynamic Covalent Bonds

Dynamic covalent bonds refer to chemical bonds that can form and break under certain conditions. This ability to reform covalent bonds under specific conditions (like changes in pH, temperature, or the presence of catalysts), allows self-healing of polymers. Many bond exchange mechanisms have been explored in the last decade—transesterification (Zhang et al., 2017), transamination (Denissen et al., 2015), transcarbonation (Wu et al., 2020), disulfide exchange (Gao et al., 2021), imine bond exchange (Lv et al., 2019), siloxane, Figure 8. So far, the most extensive research has been done on esterification-based polymers. One of the reasons for its wide use is applicability to epoxy resins. The transesterification reaction is mainly divided into the dynamic transesterification of epoxy with acid anhydride and the dynamic exchange of polyurethane. However, fast bond rearrangement in esterification-based vitrimers is possible only at temperatures above 100 ℃ with a high catalyst loading (Denissen et al., 2015). Furthermore, ester bonds are sensitive to hydrolysis, which can negatively affect the long-term performance of esterification-based vitrimers (Denissen et al., 2015). Issues with the hydrolysis of imine bond are also an obstacle for applications of poly-imine networks (Denissen et al., 2015). Disulfide bond exchange is one of the mechanisms employed in many polymeric materials due to the commercial availability of disulfide compounds with some of them having the ability to exchange bonds at room temperature without using catalysts. Si-O bond is one of the less frequently used CANs. The Si-O bonds in siloxane are hydrophobic

which would be beneficial for application involving presence of water. Siloxane can exchange siloxane bonds in the presence of acid or base catalyst. Depending on the concentration of catalyst, the stress relaxation time of the siloxane bonds can be adjusted (Huang et al., 2020).

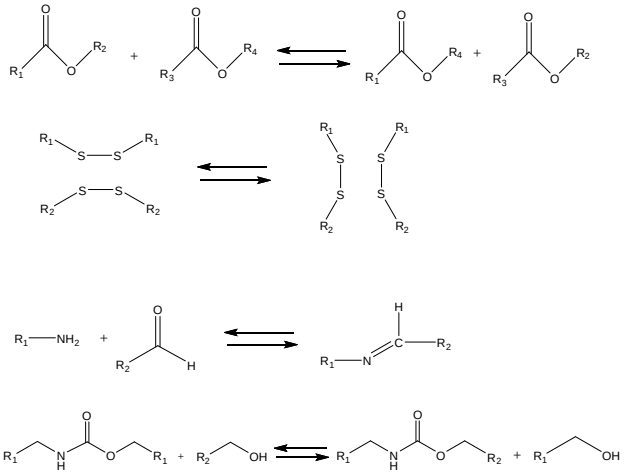

Figure 8. Examples of dynamic covalent bonds

Stimuli-responsive polymers

Factors such as the application of mechanical force on the healing interfaces, the increment of healing temperature, and external stimuli (e.g., UV light irradiation, visible light, and microwave), are important for fast self-healing.

Increasing the healing temperature is an effective method to improve the self-healing efficiency (Li et al.2020). Higher temperatures provide more thermal energy to the molecules within the material, increasing their kinetic energy and allowing them to move more freely. This enhanced mobility can aid in the reorganization of polymer chains or the realignment of molecular structures necessary for self-healing. Using temperature as a trigger for self-healing processes involves challenges related to achieving uniform heating of large surfaces (Kloxin & Bowman, 2013). For this reason, there has been interest in elastomers that can self-heal at room temperature due to convenience of the self-healing process. Some of the strategies to design elastomers that can heal at room temperature include introducing noncovalent hydrogen bonds into a covalent polymer network or dual-dynamic covalent system. Lv et al., (2019) designed a dual-dynamic polymer network by incorporating imine and aromatic disulfide bonds. Aromatic bonds can rearrange at room temperature due to their low bond energy. Imine bonds, i.e. exchange reaction between amines and aldehydes are responsive to pH and provide processability. Carbon nanotubes (CNTs) are added to improve the toughness and other mechanical properties of the elastomer. Without CNTs elastomer had a tensile strength of only 0.15 MPa. Adding 0.5% of CNTs increased strength to 0.4 MPa and elongation to 980%. It was shown that the toughness of the elastomer that was cut in half can completely recover after 12 h under ambient conditions.

Polymers can be designed with photoactive components that respond to visible light, allowing for controlled and precise initiation of healing reactions. Light-based healing facilitates the activation of healing mechanisms in hard-to-reach or inaccessible areas within a material or a structure. It enables precise

targeting and possesses the flexibility to tailor the light wavelength specific reaction conditions necessary for practical requirements (Xu et al., 2022). While UV light has been more commonly employed for initiating photoreactive processes due to its higher energy, recent advancements have extended the use of visible light in activating specific healing mechanisms. The advantage of using visible light is that it cannot cause damage to the polymer matrix. Visible light is suitable for covalent bonds with low bond energy (~240 kJ/ mol) which are used to design self-healing elastomers with longer healing times (>4 h), (Ji et al., 2015).

The ability of the damaged polymer's surfaces to come into contact can impact the subsequent self-healing, and determine the kinetics of the healing process. Pressure is often applied on the healing interfaces to facilitate the exchange of dynamic bonds within the polymer matrix. The compressive force lowers the activation energy barrier required for the dynamic bond exchanges. By doing so, it accelerates the rate at which these bond exchanges occur, effectively promoting the healing process (Kaiser et al., 2020)

Disulfide Exchange

Disulfide bond exchange reaction has been extensively studied and employed in many polymeric materials due to the commercial availability of disulfide compounds and ability to respond to external stimuli. The mechanism behind disulfide exchange has been described in the literature as a process of metathesis or radical-mediated mechanism. In disulfide metathesis, the exchange of disulfide bonds occurs through a rearrangement of sulfur atoms between different disulfide bonds. In the radical-mediated mechanisms, the process is initiated by the generation of radicals, often through the application of external stimuli such as heat, light, or specific chemicals. These radicals then attack the disulfide bonds, leading to their cleavage and the formation of thiyl radicals. Subsequently, these thiyl radicals can react with other disulfide bonds, initiating a chain reaction that results in the exchange of sulfur atoms between disulfide groups.

A recent study by Nevejans et al., (2016) aimed to determine the mechanism behind the disulfide bond exchange. The objective was to determine if the exchange occurs via a radical mechanism or through a thiol-disulfide exchange pathway. The model exchange reaction of 4-aminophenyl disulfide with diphenyl disulfide was followed for 12 h at 35 °C using NMR spectroscopy. Using 2,2,6,6-tetramethylpiperidine-1-oxyl (TEMPO) as a radical trap and 2,20-Azobis(4-methoxy-2,4-dimethyl valeronitrile (V-70) as radical source, it was shown that the mechanism behind the disulfide exchange happens due to radical formation and not via cleavage and recombination of the disulfide bond. According to this mechanism, formation of only a small amount of radicals is required to achieve extensive disulfide exchange. Considering that some disulfide compounds require use of a catalysts (triethylamine, TEA; tri-n-butylphosphine, TBP), NMR spectroscopy was conducted to determine effect of these catalysts on the exchange reaction. The study showed that the enhance in exchange reaction in the presence of TEA and TBP happens through formation of sulfur-based anions. Due to higher nucleophilicity of TBP compared to TEA, the faster product formation was observed, because a higher nucleophilicity enhances the fragmentation of disulfide bond to form thiolate anions.

Pepels et al., 2013 explored the impacts of chemical structure and catalysts affecting the process of disulfide bond exchange. The experiments were conducted using aliphatic compounds with disulfide bonds (dibutyl disulfide (DBDS) and dipropyl disulfide (DPDS) as model compounds. Gas chromatography-mass spectroscopy (GC-MS) was used to analyze the formation of products for different combinations of starting

polymers (Figure 9). It was shown that both the presence of thiols (PT) and base (DBU) was necessary to induce the exchange reaction (Figure 9a- $b^{1,dbu}$, $c^{1,dbu}$). When only one of them was present no disulfide exchange was observed. Based on this study it was concluded that thiol-disulfide exchange is faster than disulfide-disulfide exchange.

	1h at 20 ℃	1h at 20 ℃ + 1h at 60 ℃	1h at 20 ℃+ DBU	1h at 20 ℃ + 1h at 60 ℃ +DBU
DPDS+DBDS	a^1	a^2	$a^{1,dbu}$	$a^{2,dbu}$
DPDS+DBDS+1-PT	b^1	b^2	$b^{1,dbu}$	$b^{2,dbu}$
DPDS+DBDS+0.13% 1-PT	c^1	c^2	$c^{1,dbu}$	$c^{2,dbu}$

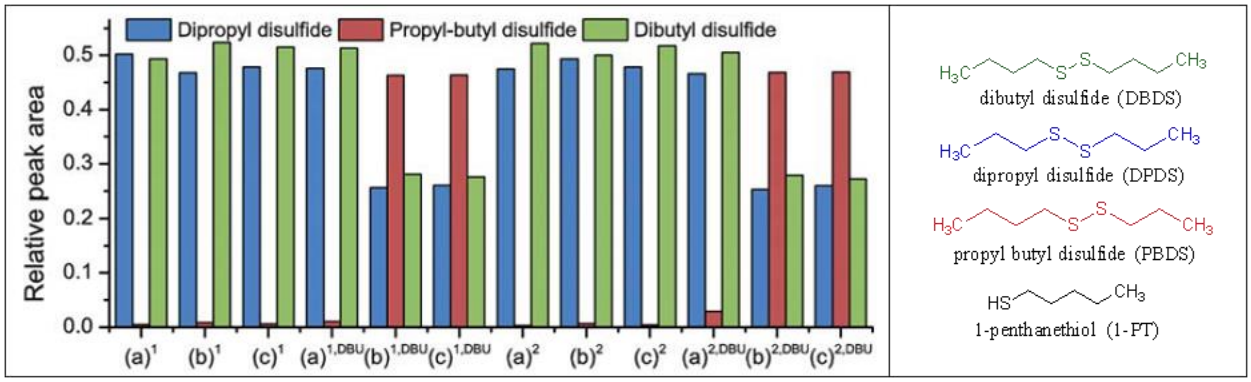

a) b)

Figure 9. a) Relative GC-MS peak intensities for disulfide exchange experiments, b) Chemical structures of the used model systems (Pepels et al., 2013)

The effect of the basicity of the tertiary amine on the thiol-disulfide exchange was also studied. Three different tertiary amines were tested: 4-dimethylaminopyridine (DMAP, pK_a=9.8), dimethylaminopropyl-amine (DMAPA, pK_a=10.38) and DBU (pK_a=12). They were added to the mixture of DPDS, DBDS and PT at 1% by total weight. Only DBU had a significant effect on the exchange reaction (Figure 10c), which indicates that the thiol-disulfide exchange depends on the basicity of the system. Further experiments showed that it also depends on the type of disulfide and the thiol used. When thiol terminated polysulfides were used, good exchange was observed even when DMAP and DMAPA were added as catalysts which was not the case with DPDS and DBDS. It was pointed out that the reaction rate of the thiol-disulfide exchange depends on the formation of thiolate anions which is determined by the stability of thiolate. Thiolate will be stable if the deprotonation rate is high but the rate of nucleophilic attack low. Another factor that increases the thiolate stability is higher the pH of the system.

	1h at 60 ℃	50% of DOx	1h at 60 ℃+ 50% DOx	18h at 60 ℃+ 50% DOx
DPDS+DBDS+1PT+1%DMAPA	a	d	e	f
DPDS+DBDS+1-PT+1%DMAP	b			
DPDS+DBDS+1-PT+DBU	c			

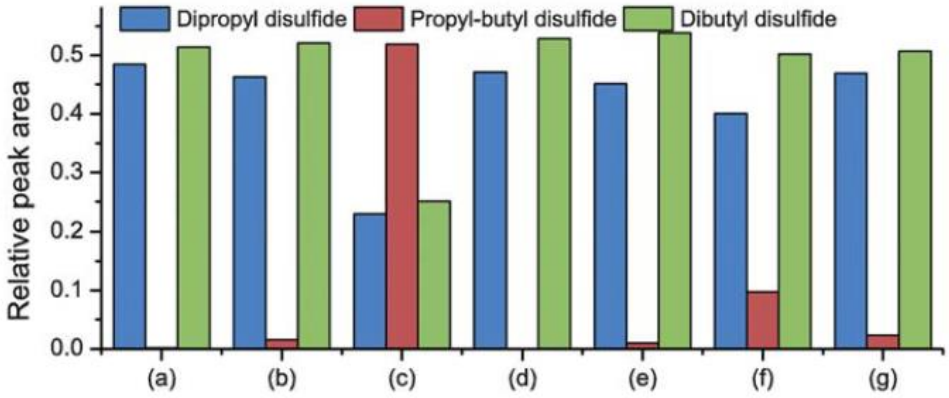

Figure 10 . Relative GC-MS peak intensities for dipropyl disulfide (DPDS), dibutyldisulfide (DBDS) and propyl-butyl disulfide (PBDS) for exchange experiments containing equimolar amounts of DPDS, DBDS and 1-pentanethiol (PT) (Pepels et al., 2013)

The second part of the paper is focused on the self-healing efficiency of a polymer prepared from polysulfide diglycidyl ether (Thioplast, T25) and thiol compounds: PTM1/PTM2 (pentaerythritol tetrakis(2-mercaptopropionate). 4,4-Methylenedianiline (MDA) was used as a control cross-linker because it does not contain dynamic bonds (Figure 11). The sample prepared using MDA, T25 and DMAPA had ultimate strain of 30% and strength of 250 kPa and low self-healing efficiency of 0.16. Samples prepared from PTM1 and PTM2 had similar elongation and strength but improved self-healing efficiencies of 0.81 and 0.99, respectively. When PTM2 and T25 were mixed at a molar ratio of 1.1, the ultimate elongation increased to 80%, while strength decreased to 140 kPa. Good self-healing efficiency of these polymers is based on the presence of thiol curing agent (PTM). The model experiments showed that there is exchange happening between PTM and Thioplast monomers, which means that the exchange had occurred during curing leading to different network topology with unreacted thiols. The presence of unreacted thiols is essential for the ability of the network to self-heal. It was also pointed out that after being stored in air, the samples strain decreased and strength increased. To determine if additional cross-linking occurs in presence of oxygen, a group of samples was tested after being stored for 1 day under nitrogen and compared to the samples stored under oxygen. The results revealed higher maximum stress in the samples stored in air. The additional cross-linking is likely a result of oxidative self-polymerization of thiol groups.

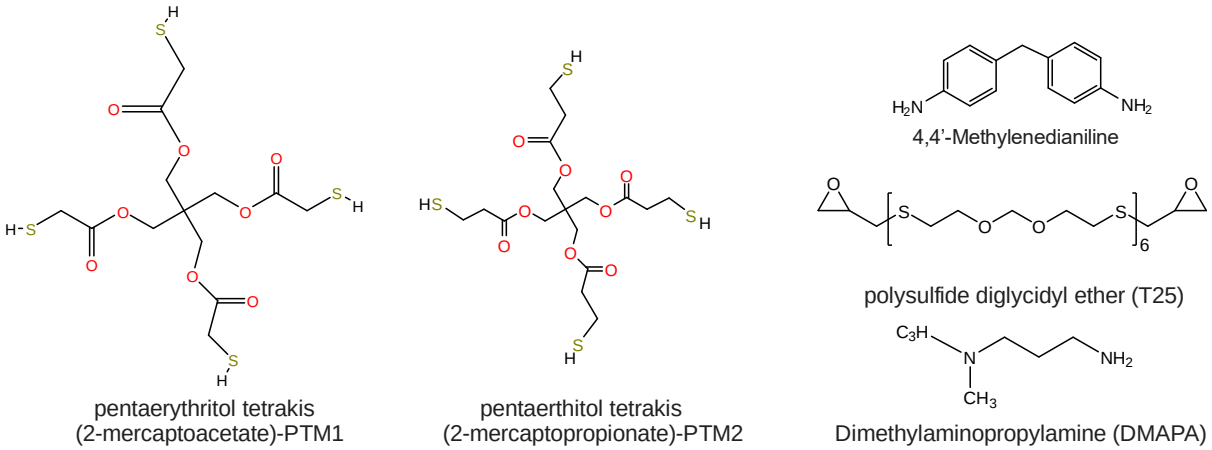

Figure 11. Chemical structure of the monomers used for the self-healing elastomer, Pepels et al., 2013

Self-healing elastomers with disulfide bonds

Several self-healing elastomers were developed in the last 10 years but many of them require tedious pre-syntheses to obtain building blocks that contain dynamic linkages. The review of published literature included below was focused on the synthetic procedures, type of monomers and prepolymers used in synthesis, mechanical and self-healing properties of self-healing elastomer with the objective to identify those that have the potential to be used as sealants in joints in concrete pavements.

Taking advantage of the strength inherent to polyurethanes and the potential of exchangeable disulfide bonds found in polysulfide oligomers, Gao et al., (2018) synthesized self-healing polysulfide-based polyurethanes (PSPU). The synthesis involved polysulfide oligomers (LP55) as the soft segment, alongside isophorone diisocyanate (IPDI) and 2,5-diamino-3,6-dimethylmercaptotoluene (DMTDA) as the hard segment (Figure 12). The effect of hard segment content (15, 20, and 25% of DMTDA) on mechanical strength, stress relaxation, and the effectiveness of the self-healing process was examined. For the purpose of creating control samples without dynamic bonds (PTPU), polyurethanes based on PTMG (Polytetramethylene ether glycol, Mn=3000 g/mol), were synthesized with hard segment ratios of 20% and 15%.

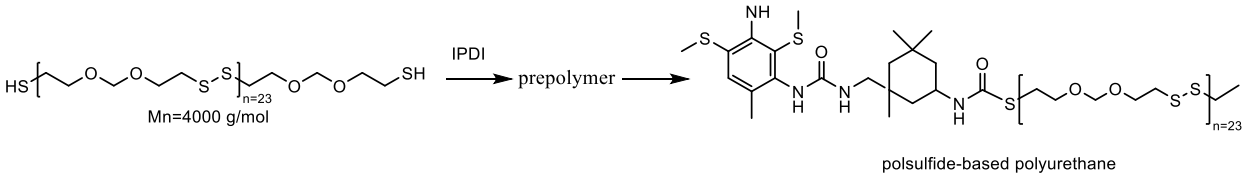

Figure 12. The typical synthesis route of polysulfide-based polyurethanes (Gao et al., 2018)

Increasing DMTDA content from 15% to 25% increased the tensile strength from 2.6 MPa to almost 6 MPa. Ultimate elongation was above 600% and was not affected by DMTDA content (Figure 13a). Self-healing efficiency was defined as the ratio of the tensile strength of the healed sample to the tensile strength of the original sample. The self-healing experiments were carried out at 75 °C for 48 h. The self-efficiency for PSPU which had the lowest content of DMTDA (15%) was 95%. Although the PTMG-based polyurethane network is more flexible (indicated by lower T_g), its self-healing efficiency was lower (49%) (Figure 13b). This is an evidence that the disulfide metathesis reaction significantly contributes to the healing process in polysulfide-based polyurethanes.

The stress relaxation path in the case of PSPU continuously declined to zero after the initial sharp decrease Figure 14. The observed pattern of stress relaxation suggests that the cross-linked network allows for complete stress relaxation through bond rearrangement. For comparison, in the case of PTPU the stress reached a plateau with time, like conventional materials.

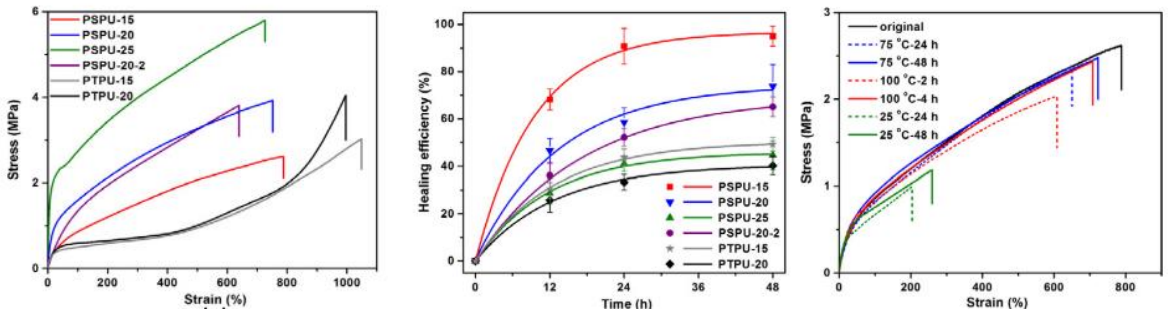

a) b) c)

Figure 13. a) Tensile stress-strain response of the polyurethanes. b) Healing efficiencies of the polyurethanes deduced from the tensile strength after healing at 75 °C for different times. c) Tensile stress-strain curves of PSPU-15 after healing at 25 °C , 75 °C , or 100 °C (Gao et al., 2018)

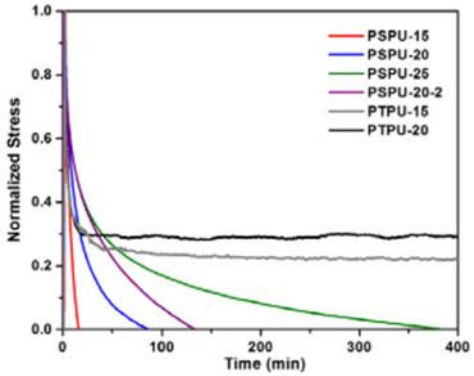

Figure 14. Stress relaxation curves (Gao et al., 2018)

Gao et al., (2017) prepared a self-healing sealant by mixing thiol-terminated polysulfide oligomers (LP3, LP23, LP2, LP32, LP55) with epoxy resin (Figure 15). The reaction was initiated with a tertiary amine (2, 4, 6-tris(dimethylaminomethyl)phenol, DMP). The molecular weight of polysulfide chains and the content of cross-linking agent were varied to determine their effect on mechanical and thermal properties and self-healing. Two different types of epoxy resin were also evaluated: bisphenol A and bisphenol F (less rigid molecule unit). Aromatic terminated polysulfide was designed and added to the mixture to improve self-healing at room temperature.

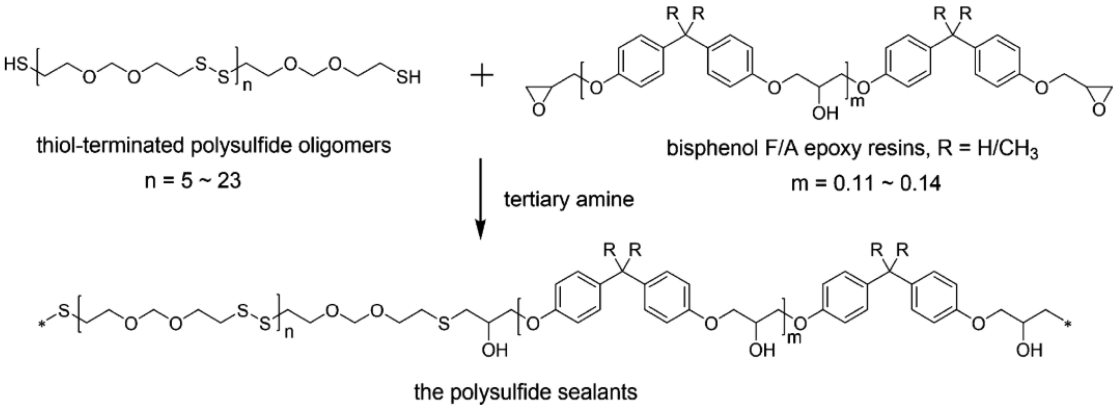

Figure 15. Schematic representation of the reaction between the polysulfide oligomer and epoxy resin (W. Gao et al., 2017)

The tensile strength of the sealants ranged from 0.7 MPa to 1.1 MPa, depending on the polymer's composition (Figure 16). Sealant samples containing LP3 (with an Mn of 1000 g/mol) polysulfides displayed a tensile strength of approximately 1 MPa. In contrast, samples prepared with LP55 (with an Mn of 4000 g/mol) polysulfides exhibited a tensile strength of roughly 0.75 MPa. Ultimate elongation varied from 157% in sealant formulations prepared with LP3 to 478% in sealant formulations prepared with LP55 and it was significantly affected by the amount of branching of polysulfide oligomers.

Self-healing efficiency was 90% after healing for 60 min at 75 ℃. When healing experiments were performed at room temperature only 49% of ultimate elongation was restored and 73% of their tensile strength. Modifying polymer composition by aromatic terminated polysulfides improved healing ability at room temperature: efficiency was 86% for ultimate elongation and 96% for tensile strength.

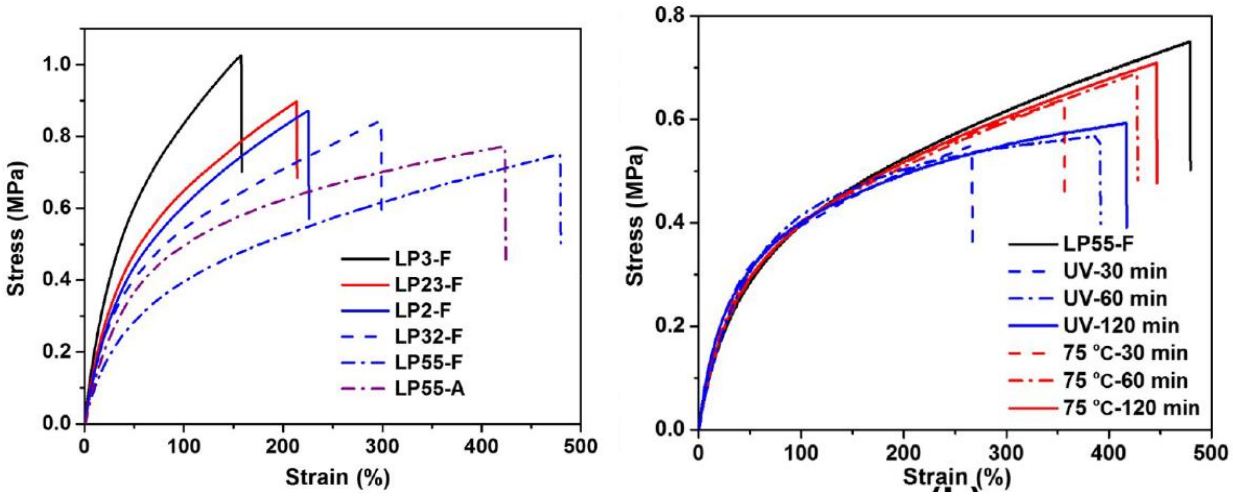

a) b)

Figure 16. a) Tensile stress−strain curves of the polysulfide sealants. b) Tensile stress−strain curves of LP55-F after healing at 75 °C or under UV light for different times (Gao et al. 2017)

It was shown that the degree of cross-linking had a weak effect on T_g. However, the molecular weight of polysulfides and the type of epoxy resin had a significant effect. Increasing the molecular weight of polysulfides from 1000 g/mol to 4000 g/mol, decreased T_g from -34 ℃ to -45 ℃. Relaxation tests showed that at 75 ℃ sealants behave more like viscoelastic liquid than viscoelastic solid.

Gao et al., (2021) explored the impact of fillers such as CB, SiO_2, and TiO_2 on both self-healing and mechanical properties of a sealant prepared through the reaction of polysulfide oligomers and MnO_2. Four different percentages of MnO_2 were tested: 1.75%, 2%, 2.5%, and 3%. The content of DMP-30 was 2% and was kept constant for different formulations. The curing procedure comprised 12 hours of curing at room temperature followed by an additional 72 hours at 75 °C.

Sealant elongation varied between 492% when 1.75 % of MnO_2 was used to 458 % when 3% of MnO_2 was used. The tensile strength was between 0.98 MPa and 1.23 MPa. Increasing the content of MnO2 increased the strength as cross-linking was increased. The self-healing experiments were conducted at 75 °C and self-healing efficiency measured at 12 h, 24 h, 48 h. After 48 h, the 59% of the strain was restored and 78% of the tensile strength. In the sample that was cured by reacting LP55 and MnO_2 stoichiometrically, there were

no unreacted thiols and the authors attribute self-healing to the disulfide exchange reaction. The sealants with residual thiols in the sealant had better self-healing behavior. The restored strain was up to 88%. It was pointed out that DMP-30 promotes the formation of thiolate anions which favors thiol-disulfide reaction. The self-healing process in polysulfides cured with MnO_2 is slower compared to those cured with epoxy. This is ascribed to the spatial hindrances created by the reduced MnO_2, impeding the exchange of disulfide bonds. The lowest self-healing efficiency was observed in the sealant with the highest MnO_2 content. It is possible that in this case MnO_2 acts as a filler and inhibits the disulfide exchange reaction.

Zhang et al. (2013) prepared elastomers from liquid polysulfide (PSF) oligomers (LP-3, LP-23, LP-980, LP-2, LP-32, LP-55) and bisphenol-A diacrylate resin (Mn = 510–600 g/mol). The reaction was catalyzed by DMP-30 at 2% by the total weight of monomers. The simplicity and efficiency of the reported procedure provides a fast approach for preparing polysulfide elastomers. The effect of PSF molecular weight on the curing behavior was studied using real-time infrared spectroscopy. It was observed that after 24 h, the conversion reached 98% in all samples. However, the reaction's initial rate was more rapid for the elastomer synthesized with LP-3 when compared to LP-2. In the former case, a 50% conversion was achieved after just 5 minutes, while the latter required 20 minutes to reach the same level of conversion. The faster initial conversion was attributed to higher thiol content and lower viscosity of LP3. High conversion of thiols was achieved despite of different molecular weight of the liquid polysulfide oligomers. All of the samples used in this study had gel fractions around 90 wt% except for Elastomer-LP-55. The effect of chain length on gel fraction was negligible.

Table 3. The main properties of liquid polysulfide oligomers

Liquid polysulfide oligomers	LP-3	LP-23	LP-980	LP-2	LP-32	LP-55
Average molecular weight	1000	2500	2500	4000	4000	4000
Cross-linking agent	2%	2%	0.5%	2%	0.5%	0.05%
Mercaptan fraction	5.8-7.7%	2.5-3.5%	2.5-3.5%	1.5-2%	1.5-2%	1.5-2%

Tensile strength ranged from 0.91 MPa when LP-3 was used to 0.76 MPa when LP-55 was used Figure 17. Elongation was between 126% and 412%. tensile strength of the samples was comparable to that of polysulfide polymer cured by metal oxide.

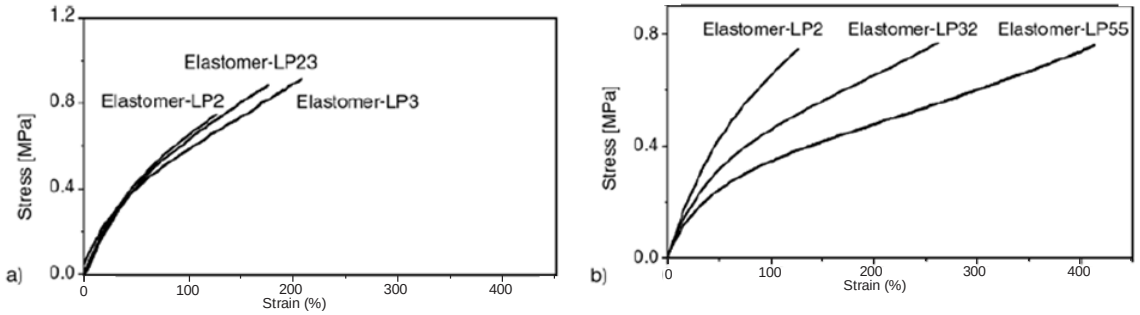

Figure 17. Strain-stress curves of polysulfide-based elastomers, Zhang et al., 2013

Gao et al., (2021) described the synthesis of a range of elastomers from acrylate and thiol-terminated polysulfide oligomers. The reaction between acrylates and thiols is commonly referred to as thiol-ene click reaction. Thiol-ene click reaction can be performed via a thiol-ene radical reaction) or via thiol-ene Michael addition under nucleophiles or strong bases. The thiol-ene click reactions are significantly influenced by

the type of initiator used. In this paper, different types of thiol-ene click reactions were explored and involved using: photo-initiator (DMPA), thermal-radical initiator (dilauroyl peroxide (LPO)) and bases (DBU and DMP-30). Thermal-radical initiators undergoes a process of thermal decomposition at elevated temperatures, which leads to the formation of radicals. In LPO, the weak oxygen-oxygen (O-O) bond is the primary bond that breaks at elevated temperatures to generate radicals. A photo-initiator is a compound that initiates a chemical reaction upon exposure to light, typically UV or visible light. The absorption of photons usually occurs in the conjugated systems of double bonds or aromatic rings present in molecules. In DMPA, the part that typically absorbs photons to initiate a photochemical reaction is the aromatic phenyl ring. The reaction kinetics of alkaline acrylates is dependent on the nucleophilicity of the catalyst, because the higher the nucleophilicity of the catalyst, the larger the number of active thiolate anion intermediates that can be generated.

Table 4. Different Initiators for thiol-ene reaction (Gao et al., 2021)

photo-initiated	thermo-initiated	alkali	
DMPA	LPO	DBU	DMP
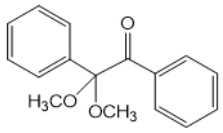	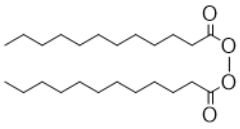	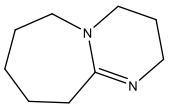	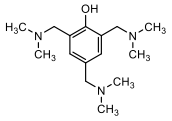

The synthesis involved mixing acrylate monomers and polysulfide oligomers at the same ratio of thiols in the polysulfide oligomers and double bonds in acrylate monomers. The amount of initiators used was 1% by weight. Based on the gel fractions studied the swelling behavior in toluene, the alkaline network had the highest gel fraction. The network with photo initiators had the lowest gel fraction. Acrylates with redox initiators (LPO+DBU or LPO+DMP) had lower gel fraction than networks with alkaline catalysts, indicating that they are less effective. The acrylates may be partially homopolymerized for redox-AE and photo-AE, resulting in excess polysulfide oligomers in the acrylate-based elastomers. Self-healing tests at 100 ℃ showed that alkaline acrylates had the best self-healing ability.

Aromatic disulfides exchange is one of the few dynamic covalent chemistries that has been reported to occur at room temperature using a tertiary amine as the catalyst. Rekondo et al., (2014) prepared a self-healing poly(urea)-urethane elastomer with a diamine crosslinker-bis(4-aminophenyl) disulfide. This material was able to heal at room temperature by a simple contact without external stimulus or a catalyst. Self-healing efficiency was quantified by measuring tensile strength. The tensile strength of the original sample was 0.8 MPa and the ultimate elongation 3100%. 97% of the strength was restored after 24 h. The self-healing is attributed to the metathesis reaction of aromatic disulfides and two urea groups, capable of forming a quadruple H-bond (Figure 18). To explore these two effects, the self-healing capability of a reference elastomer, lacking disulfide bonds was examined. The healing efficiency of the reference elastomer was 51%, which was attributed to the contribution of the H-bond between the urea groups. The authors used NMR to study the exchange reaction between two aromatic monomers with disulfide bonds as model compounds. When triethylamine (TEA) was used as a catalyst the reaction was complete after 1h. Without TEA, the exchange reaction reached equilibrium after 22 h. These experiments confirmed that the disulfide exchange is possible at room temperature without the use of catalyst.

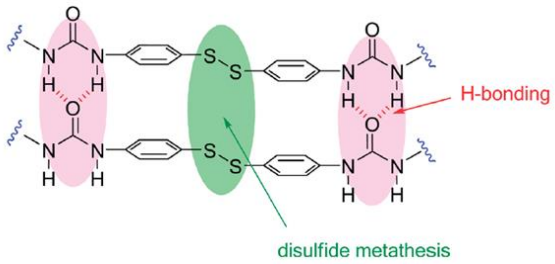

Figure 18. Proposed mechanism behind the self-healing process (Rekondo et al., 2014)

CHAPTER 2

Methodology

The primary objective in formulating the sealant was to design a flexible elastomer capable of self-healing under ambient conditions. The most important design considerations for sealants in rigid concrete pavement joints are related to providing: 1) sufficient elasticity to allow for thermal movements of the joint, 2) adhesion to concrete (initial and long-term), 3) low elastic modulus over a range of temperatures to limit the stresses at the concrete/sealant interface, 4) durability, i.e. ability to resist degradation when exposed to the environment; 5) glass transition temperature—lower than that of the service temperature ensures better low-temperature performance by improving flexibility. The focus in developing the self-healable sealant formulation was on its tensile behavior and self-healing efficiency, where the goal was to achieve stress, elongation, modulus, and adhesion to concrete comparable to other commercially available sealants.

In establishing performance requirements for the cold-applied polysulfide sealant, ASTM D5893 (2016) for cold poured silicone sealants was used as a reference considering the lack of up-to date specifications on two-component cold-poured sealants. Federal specification SS-S-200E (1992) for two-component cold-pour sealants has been inactive for new design since 2009. The ASTM D5893 standard provides requirements for various physical and mechanical properties including:

- The sealant must cure within 21 days.
- Extrusion rate should not be less than 20 mL/min (test method C1183).
- The sealant should be tack free, with no transfer to polyethylene when tested at 5 hours (test method C679).
- The sealant should not lose more than 10% of its original weight (test method C792).
- No cracks, separation, or other openings in the sealant or between the sealant and the concrete during non-immersed, water immersed and oven-aged conditions.
- When tested at SLC using a type 00 durometer the hardness should be above 30 (test method C661).
- No flow when tested at 93 ℃ for 72 h.
- Ultimate elongation should not be less than 600% (test method D412).
- Tensile stress at 150% elongation should not exceed 310 kPa (test method D412).

Due to time constraints and project specific objectives, we prioritized the following requirements during the material development: 1) the sealant shall cure within 21 days, 2) sealants should withstand elongation higher than 600%, 3) tensile strength should be limited to 0. 31 MPa at 150% strain to reduce the stress on the concrete/silicone bond, 4) specimens should not develop any cracks or separation between the concrete and the sealant when tested at -29 ℃ for five cycles of 100% extension each, 5) the hardness should not be less than 30 when tested at 23 ℃ using Type 00 durometer, 6) a sealant must be able to withstand exposure to UV. All requirements except the last one are specified by ASTM D 5893. However, this requirement

would be an important consideration for polysulfide sealants. The specified elongation requirement of 600% in ASTM D5893 is not coherent with the anticipated joint movements in concrete pavement. The elongation of 600% significantly exceeds joint movement expectation of 100% as reflected in the performance requirement for the water immersed bond at -29 ℃. Considering that poor adhesion to concrete is indicated as disadvantage of silicone sealants, specifying elongation of 600% does not contribute to the sealant's effectiveness and seems unnecessary. Search for studies supporting the adequacy of this requirement or any information about the initial development of the standard did not uncover any relevant studies. For this reason we have maintained the 600% elongation requirement but adjustments will be considered if new findings emerge.

It is important to note that two-component polysulfide sealants face challenges due to cost consideration and competition from silicone and polyurethane sealants. In the review of the selection of sealing systems published in 2006 (Odum-Ewuakye & Attoh-Okine, 2006b), none of the 22 states covered in the study did not report using polysulfide sealants. Eight-seven percent of the states in the wet-freeze region that use sealants reported use the three types of sealants: asphaltic, silicone and neoprene. However, it is likely that cold-applied polysulfide sealants may evolve in the future to meet industry need for enhanced sealant performance and durability.

Sealant development involved testing various formulations prepared from commercially available prepolymers. An elastomer prepared from epoxy resin and thiol-terminated polysulfides emerged as the most promising due to its capability for self-healing under ambient conditions. The influence of two different catalysts and their content on epoxy-thiol curing under ambient conditions and mechanical properties was analyzed. Techniques such as isothermal calorimetry, DMA, FTIR, swelling in toluene, and tensile testing were employed to understand curing processes, mechanical properties, and self-healing ability. From the five formulations, three were chosen for evaluation under conditions typical of joints in concrete pavements. This involved assessing adhesion (per ASTM D5893), fatigue, hardness, and exposure to UV light. Concrete joints were also tested based on ASTM C1135 as it allows testing until failure which was needed to evaluate self-healing efficiency of sealants in joints. The evaluation of self-healing under moisture effects was conducted using ASTM C1135. Additionally, we investigated the effects of compression on self-healing by applying controlled displacement—a consideration specific to joints in concrete pavements due to the expansion of concrete during temperature changes. Overall, the research aimed to provide a comprehensive understanding of sealant formulations, their mechanical properties, and self-healing capabilities under various conditions relevant to concrete pavement joints.

Materials

2,2'-Dithioldianiline (AFD, Mn=360 g/mol) was purchased from TCI America Inc., epoxy terminated polydimethylsiloxane (DMS-E09, Mn-246 g/mol) was obtained from Gelest Inc., poly(propylene glycol) diglycidyl ether (Mn=640 g/mol) from Sigma Aldrich, polysulfide oligomers (Thiokol, Mn=4000 g/mol) were supplied by Toray International America Inc., catalysts (TEA, DMP) were procured from Sigma Aldrich, bisphenol A diglycidyl ether (Mn=360 g/mol) from Hexion. Figure 19 shows the structure of the compounds.

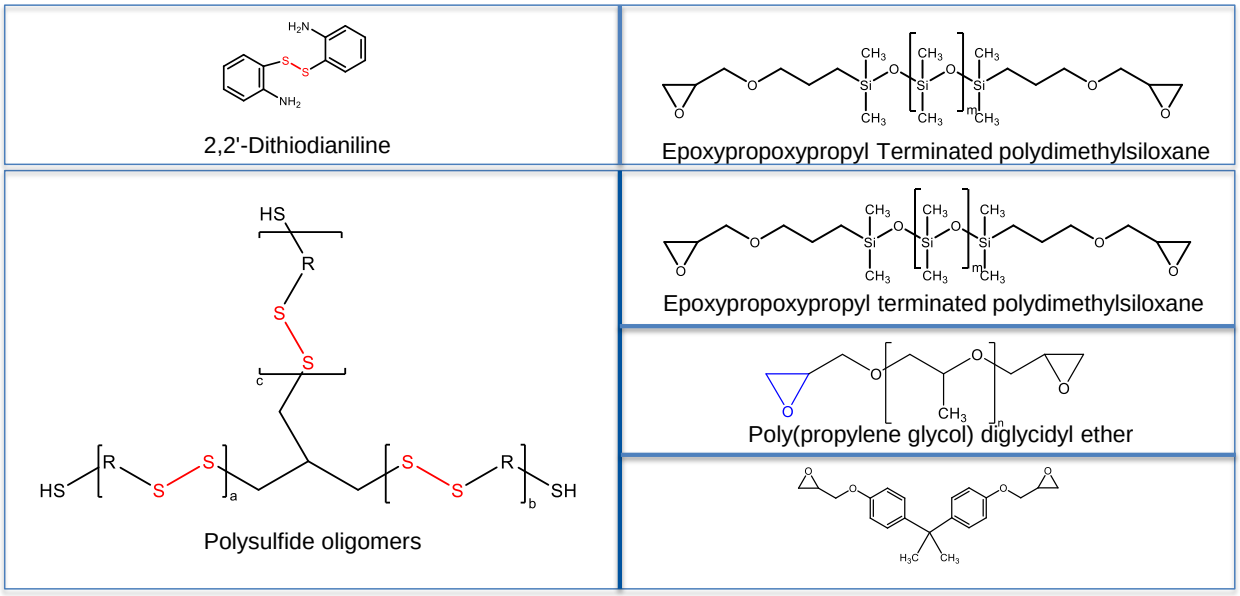

Figure 19. Chemical structure of the compounds used for sealant formulations

FTIR Spectroscopy

Fourier Transform Infrared (FTIR) spectroscopy was used to monitor the changes in thiol and epoxy absorption associated with the concentration of those reactive functionality. The disappearance of those peaks provides a quantitative measure of the extent of cure. Spectra were collected in transmission mode using Nicolet iS50 FTIR spectrometer in the near-IR spectral range, from 2000 cm^{-1} to 7000 cm^{-1}.

Swelling experiments

Swelling of the polymer networks in solvent was conducted to assess the presence of unreacted, potentially leachable, components. Sealant materials were cured for 21 days. The specimens were weighed in the dry state and then submerged in a vial of toluene. After 24-hours, the specimens were removed from the vial and excess toluene was blotted away. Subsequently, the swollen sealant materials were dried in an oven at 55 ℃ under vacuum to evaporate all the remaining toluene. Their final weight was measured and compared to the initial weight. In the swollen state, any unreacted leachable component can diffuse out of the polymer network. The final weight then represents only the crosslinked or 'gelled' portion of the polymer. The gel fraction percentage is calculated as: (Weight of dried sample after swelling / Initial weight of sample) x 100.

Dynamic Mechanical Analysis (DMA)

DMA was used to identify glass transition temperature (T_g), which we designate as the temperature at which the sealant transitions from a glassy to a rubbery state. The DMA was conducted using a DMA 8000 (Perkin Elmer, USA) by applying 1% strain at 1 Hz frequency and heating the sample from -60 °C to 60 °C at 3 °C/min heating rate. The rectangular samples, with dimensions of approximately 10 mm (length) × 5 mm (width) × 2 mm (thickness), were tested in tension to measure their storage and loss moduli and damping coefficient.

Tensile testing

Tensile strength and elongation of elastomers were measured on an MTS Exceed E42 universal testing machine equipped with a 50 N load cell. For each composition, five dogbone specimens (60 mm long with cross-sectional dimensions within the gauge length of 4 mm x 2 mm) were tested at a 50 mm/min displacement rate. The strain was calculated as a change in the crosshead position relative to the initial length, considering that the order of deformation values is measured in 10^2. Stress was calculated with respect to the initial cross-sectional area (i.e., engineering stress).

Self-healing experiments

In self-healing experiments, dogbone specimens were removed from the mold and cut in half using a straight razor blade. Samples were then realigned back into the molds, taking care that halves are in contact to allow healing for 24 hours under standard laboratory conditions (SLC, 21 ℃, RH 50%). Following the self-healing, samples were tested in tension. The healing efficiency for each sample was defined as the percentage of restored elongation of self-healed samples.

Adhesion to concrete

Assessment of sealants bonding strength to concrete substrates is critical as it directly influences the sealant's effectiveness and ensures long-term functionality. To demonstrate the applicability of the self-healing sealant in concrete pavement joints, joint specimens were made to evaluate adhesion to concrete. Specimens were prepared by pouring the sealant into a cavity (12. mm x 12 mm x 50 mm) formed between two identical concrete prisms separated by PTFE spacers. The concrete blocks were prepared according to (ASTM D1985, 2019) standard practice. The concrete with a water-to-cement (w/c) ratio of 0.49, was cast into 100 x 75 x 250 mm molds and then saw-cut into the required size (25 mm x 50 mm x 75 mm, Figure 20, Figure 21) after 14 days of curing. Saw-cutting the specimens to desired size allows the aggregate to be exposed, which simulates saw-cutting of control joints in the field. Monotonic tension was applied on the joint sealant (a critical cause of failure in the field), which simulates slab contraction at low temperatures. Specimens were loaded to failure by applying a controlled displacement of 50 mm/min. Commercially available silicone sealant approved for use in rigid pavement joints was chosen as a cold-pour sealant for comparison with the self-healing polysulfide sealant. The commercial silicone is used for sealing joints in portland cement concrete pavements. It is a one-part, ready-to-use sealant that can be directly dispensed into the joint. According to the product data sheet, after curing for 21 days at 25 °C and 50% RH, joint

movement capability is +100%/-50% after 10 cycles (ASTM C719), tensile stress at 150% is 193 kPa (max 310 kPa, ASTM D412), and ultimate elongation >1000%.

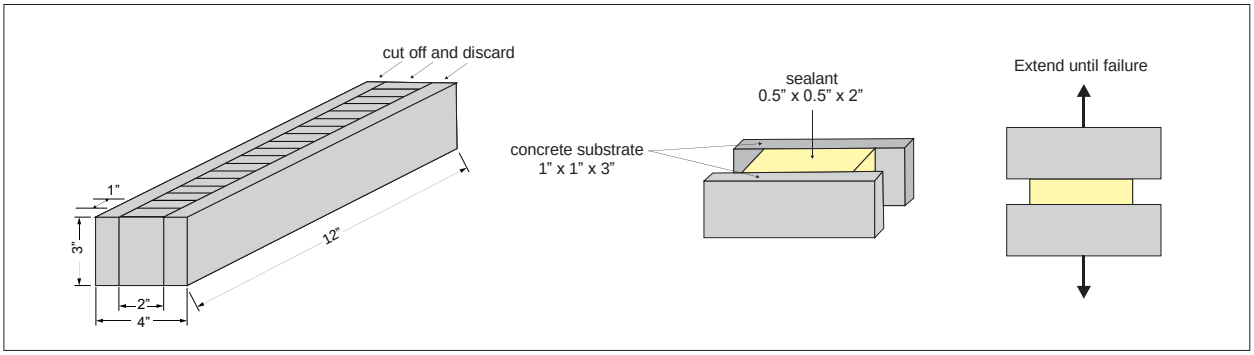

Figure 20. Illustration demonstrating the preparation of concrete joint sealants for testing according to ASTM C1135, 2005

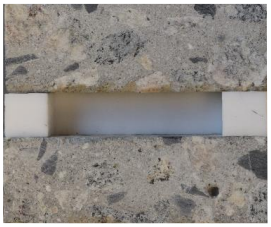

Figure 21. Concrete sealant joints

Exposure to cold (ASTM D5893, 2016)

To evaluate sealants adhesion to concrete in cold environment, specimens (Table 5) were first immersed in 500 mL of deionized water per specimen for 96 h and stored under SLC. At the end of a 96 h water-immersion period, the specimens were removed from the water and placed in an environmental chamber (Tenney) and kept there for 4 h at -29 ˚C. Immediately after exposure, specimens were tested in tension by applying controlled displacement of 3 mm/h until it reaches 12.7 mm (100% strain). Following the extension, the specimens were taken out of the testing machine and inspected for any detachment between the concrete and sealant, or any internal damage within the sealant. After inspection, the PTFE spacers were inserted and each specimen was recompressed. This was done by allowing the weight of the top block of the joint to recompress the sealant, Figure 22. The joint was subjected to five extension and recompression cycle after being exposed to cold temperatures.

Table 5. Joints exposed to moisture and cold temperatures (ASTM D 5893)

	Sample name	Procedure
Sealant joint	LP55-E-R1-DMP1*	The specimens were immersed in water for 4 day and cold temperature for 4 hours before testing in tension by applying 100 % strain at 3 mm/h strain rate.
	LP55-E-R1-TEA1	
	LP55-E-R1-DMP1-TEA1	

*Sample name: “LP55”-type of polysulfide, “E”-epoxy, “R1”-molar ratio of epoxy to polysulfide, “DMP” (TEA)-type of catalyst, “1”-catalyst content expressed as percent weight of epoxy and polysulfide

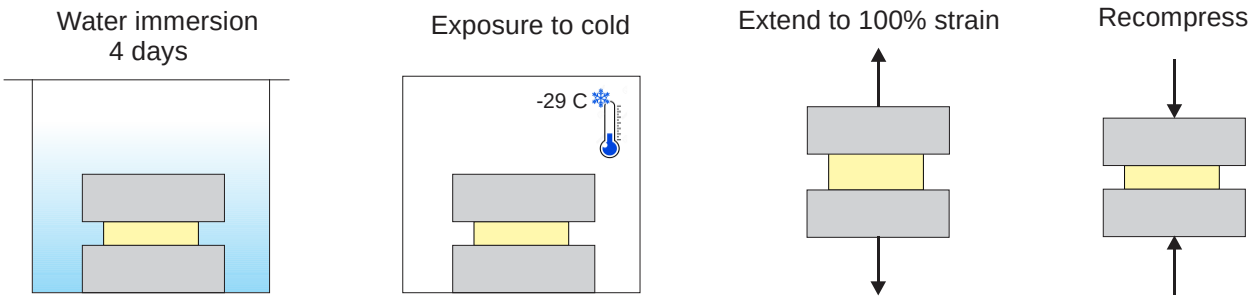

Figure 22. Illustration demonstrating the preparation of concrete joint sealants for testing joints exposed to cold temperatures

Exposure to UV and water spray

The sealants (Table 6) were allowed to cure for 21 days and then subjected to UV radiation and water spray using Q-SUN Xe-1 xenon test chamber (Figure 23). The test chamber can simulate outdoor sunlight, water spray and elevated temperature. Q-sun is equipped with light system with automatic irradiance control and black panel temperature control. The irradiance was set to 0.35 W/(m2 · nm) at 340 nm and temperature to 25 ℃. The exposure cycle was 102 min light only and 18 min light with water spray. The duration of exposure was 10 days.

Figure 23. Q-SUN Xe-1 xenon test chamber

Table 6. Specimens exposed to UV and water spray

	Sample name	Procedure
Sealant dogbones	LP55-E-R1-DMP1	10 specimens were placed into the test chamber and exposed to UV light/water spray. Five specimens were tested immediately after 10 days long exposure. The other five specimens were taken out of the chamber, cut and self-healed under standard conditions before testing in tension.
	LP55-E-R1-TEA1	
	LP55-E-R1-DMP1-TEA1	

Hardness

Durometer measurements were made using a handheld durometer. The instrument has an internal spring mechanism that pushes a small metallic tip to indent the sealants surface. The final shore hardness measurement is determined by the depth of indentation and is given as a dimensionless value between 0 and 100 with a high value of shore hardness indicating a high resistance to indentation. Shore hardness measurements were based on ASTM C661 - Standard Test Method for Indentation Hardness of Elastomeric-Type Sealants by Means of a Durometer ASTM C661-15, 2022. Specimens (25 mm x 50 mm x 12 mm) were cured at ambient temperature for 21 days. At the end of the curing period readings were taken using Shore 00 durometer. The durometer was pressed against the samples surface with a force of 1 kg.

Effects of mechanical forces on self-healing

In investigating the impact of compression on joint self-healing, controlled displacements of 10% and 20% of the joint width were applied. The preparation of the joint for self-healing involved pouring sealant into a 12mm-wide cavity, partitioned by a thin plastic sheet, Figure 24. Once the sealant cured, the plastic sheet was removed, allowing the two halves of the joint to come into contact and trigger the self-healing process. The compression was controlled by varying the thickness of PTFE spacers between concrete substrate during self-healing under ambient conditions (Figure 25).

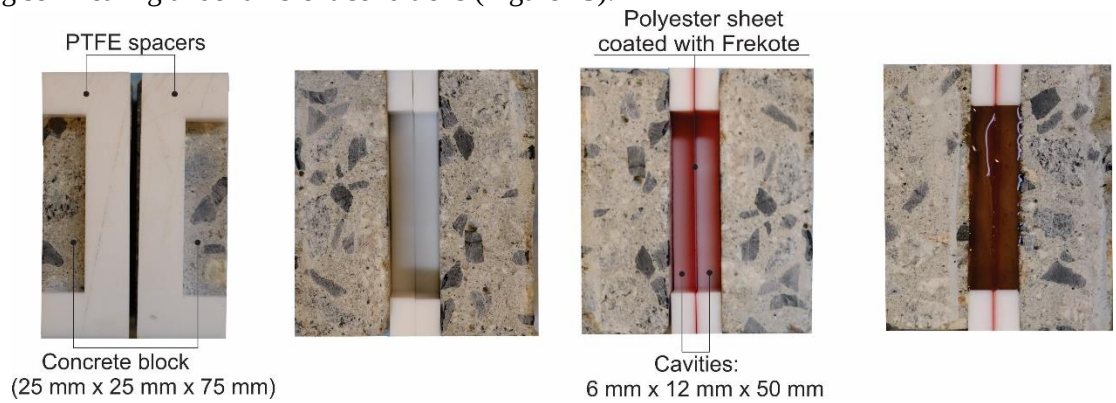

Figure 24. Effect of compression on self-healing of joints-test setup

Figure 25.Illustration of applying controlled displacement for self-healing of sealants in concrete joints under ambient conditions

Exposure to moisture

To evaluate sealants adhesion and self-healing under more realistic conditions, a set of joints was tested after being immersed in water. Three sets of specimens (three different sealant formulations, Table 7) were prepared and allowed to cure for three weeks in SLC. The testing involved evaluations of both joint specimens and dogbone specimens subjected to tension. After the curing period of 21 days, joint specimens were immersed in deionized water in a covered container and stored for four days under standard conditions. For each group of specimens, 6 replicates were prepared. Three specimens were tested immediately after exposure. The other three specimens were removed from the water, cut and self-healed under standard conditions before testing.

Table 7. Specimens exposed to water immersion

	Sample name	Procedure
Sealant dogbones	LP55-E-R1-DMP1	Ten specimens were immersed in water for 4 days. Afterwards, the surface moisture was removed and their tensile properties tested. Five specimens were tested immediately after exposure. The other five specimens were removed from the water, cut and self-healed under standard conditions before testing in tension.
	LP55-E-R1-TEA1	
	LP55-E-R1-DMP1-TEA1	

	Sample name	Procedure
Sealant joints	LP55-E-R1-DMP1	Six specimens were immersed in water for 4 days. Afterwards, the surface moisture was removed and their tensile properties tested. Three specimens were tested immediately after exposure. The other three specimens were removed from the water and self-healed for 24 h under standard conditions by applying 20% strain to the joint.
	LP55-E-R1-TEA1	
	LP55-E-R1-DMP1-TEA1	

Fatigue testing

This study simulates field deflections of joint sealants, normal deflections due to temperature variations, and shear deflections due to vehicle stresses using a custom fixture designed by Saad A. Abo-Qudais (Al-Qadi & Abo-Qudais, 1995); Al-Qadi et al., 1999). The fixture has two chambers for holding concrete specimens. To prevent the specimen from rotating during testing, each chamber has four (internal) adjustable plates. The fixture supports the specimen, which consists of sealant sandwiched between two 50 mm x 50 mm x 50 mm Portland cement mortar cubes, at various orientations. By holding the specimen at a specific angle, the in-line deflection applied by the testing equipment is transmitted to applied normal and shear deflections on the sealant. For this study, the original fixture is modified and then manufactured according to the test configuration and to allow its installation on MTS machine. The fixture is modified to hold the mortar cubes at an angle of 60º to the horizontal, subjecting the sealant sample to shear stress-to-normal stress ratio as 0.577.

Figure 26 shows the picture of fatigue test fixture. The two cubes of the specimen are confined inside steel boxes by adjustable plates that prevent specimen movement and secure the cubes. By altering the angle at

which the specimen is held, the fixture can be set to varied shear to normal deflection ratios. In order to simulate field conditions, specimens were subjected to cyclic deflection-controlled tensile loading. Through the specified fixture, a deflection was applied to a specimen using a MTS 800 Material Testing System. The sealants were evaluated under deflection-controlled conditions by programming the MTS 458.91 Micro-profiler to produce a sinusoidal response of 2.5 mm of maximum amplitude. The test fixture then converts the machine-applied in-line deflection into normal and shear deflections on the joint sealant. The normal deflection produced in the sealant specimen at this amplitude was 2.2 mm, which corresponds to the maximum expansion and contraction of a 18 m slab length caused by a change in temperature of 10℃. The shear deflection produced in the specimen was 1.2 mm, which represents the utmost deflection caused by a vehicle load.

This cyclic deflection of 2.4 mm was applied by the machine at the rate of 10 Hz and was tested upon at least four replicates of each sealant sample. For a particular measurement, the normal and shear deflections were held constant while the load change was recorded. The joint sealant is subsequently inspected for signs of debonding, such as adhesive or cohesive failure. If no failure was detected, deflection cycles of up to 1,000,000 were applied. The force required to generate the deflection was measured at the end of every ten cycles. Each test is conducted until failure or up to one hundred thousand cycles if failure does not occur.

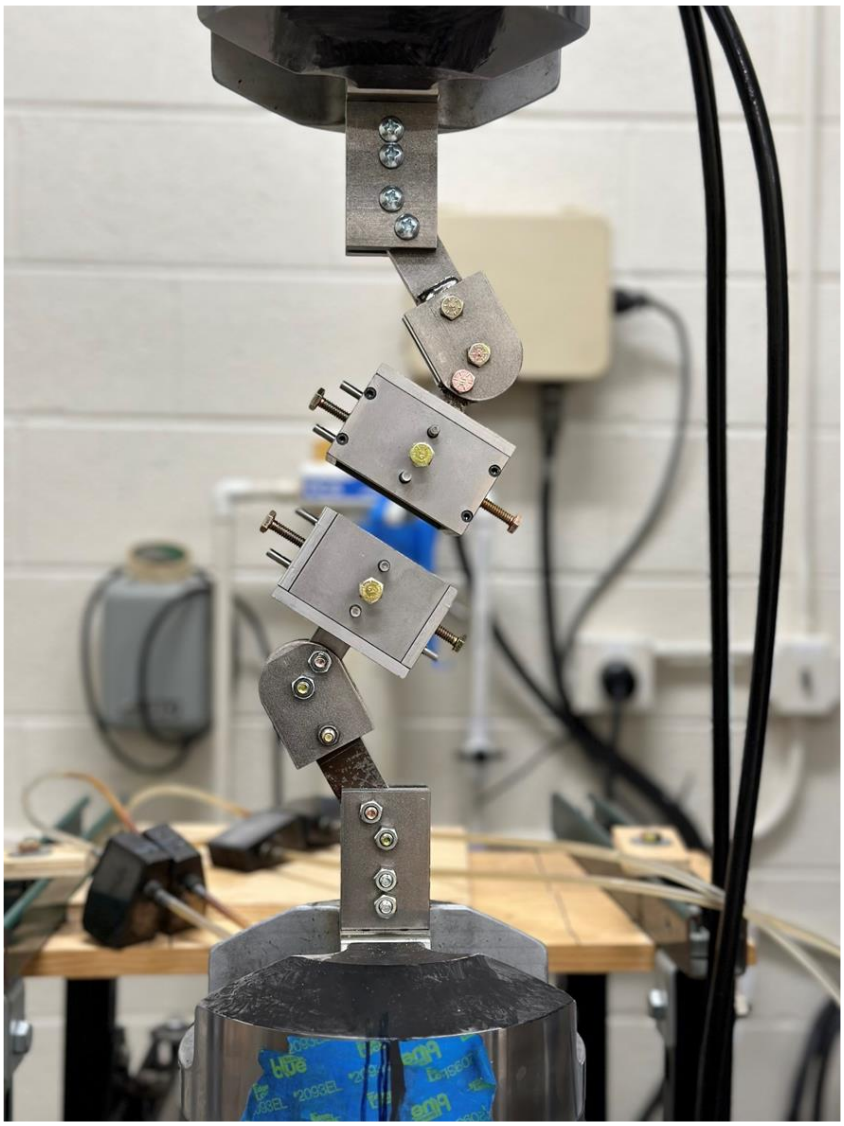

Figure 26. Fatigue test fixture

CHAPTER 3

Findings

Material development

Elastomer with aromatic disulfides

Aromatic disulfides are known for their ability to exchange bonds under ambient conditions, making them promising candidates for creating elastomers with self-healing properties. 2,2-dithioldianiline (AFD) is an aromatic compound with a -S-S- bond that has the potential for disulfide exchange (Krishnakumar et al., 2020) Lv et al., 2019), Recondo et al. (2013). Epoxy-terminated polydimethylsiloxane was used as a polymer backbone. PDMS is highly flexible and exhibits excellent elasticity.

The synthesis procedure involved heating epoxy-terminated PDMS to 60 ℃ in round bottom flask and later adding 2-AFD. The reaction mixture was continuously stirred at the same temperature for 5 min (Figure 27). Subsequently, the reaction mixture was poured into a mold and kept at 150 ℃ for 7 hours for curing. Finally, the specimens were used for tensile testing and self-healing.

The stress-strain response in tension is shown in Figure 28. A silicone sealant commonly used as sealants in joints is included as a reference. The modulus of DMS-AFD was ~1.5 MPa. The elongation was relatively low ~100% and the elastomer was not able to self-heal under ambient conditions.

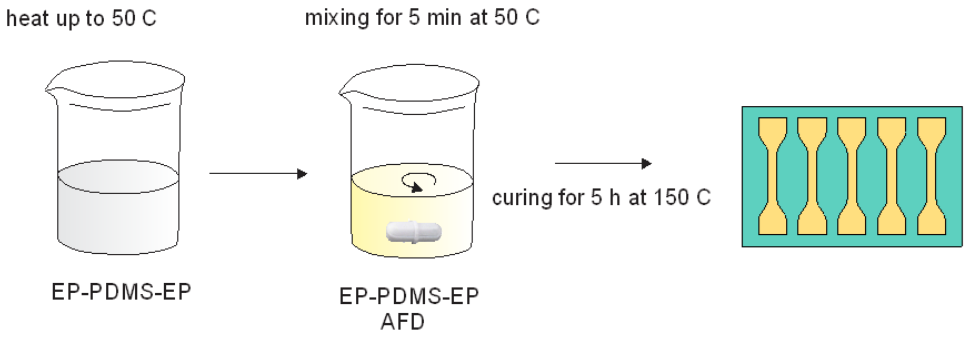

Figure 27. Illustration showing preparation procedure of the PDMS/AFD elastomer

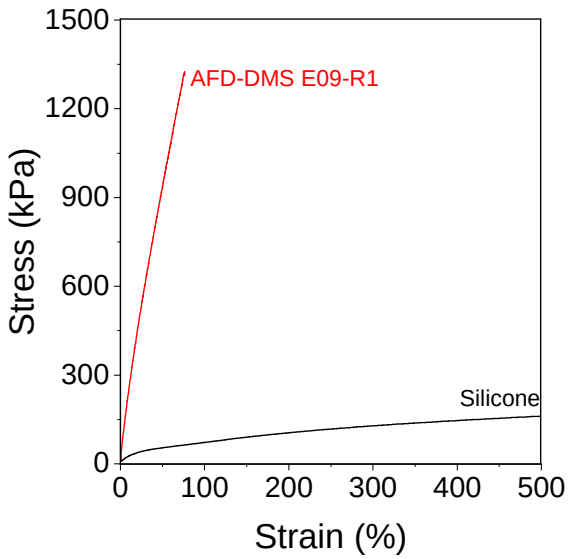

Figure 28. Stress-strain relationship of an elastomer prepared using epoxy-terminated polydimethylsiloxane and 2,2-dithioldianiline

Elastomer with aliphatic disulfides

To improve elongation, the formulation was modified by introducing polysulfide liquid oligomers (Thiokol) instead of AFD. Thiokols contain dynamic -S-S- bonds and are more flexible than the amino phenyl compound. Liquid polysulfides are polymers with two consecutive sulfur atoms in the polymer backbone, terminated by highly reactive thiol groups. Liquid polysulfide polymers are synthesized using sodium polysulfide and bis-(2-chloroethyl) formal. 1,2,3-Trichloropropane (TCP) is added to control the degree of branching of the polymer backbone. The most common types of polysulfides have molecular weights of 2,000-7,000 g/mol. The degree of branching of the liquid polysulfide, expressed as a percentage of trifunctional monomer, is not more than 2 mol%.

Challenges surfaced when attempting to make these two monomers (DMS-E09 and LP55, Figure 29a) react effectively. The primary issue originated from an uncertainty regarding the composition of polysulfide oligomers, which consist of both difunctional and trifunctional oligomers. Adjusting the stoichiometry of thiol and epoxy functional groups led to the successful production of an elastomeric material, with an ultimate elongation of 200% and tensile strength of 200 kPa, Figure 29c. However, this material still did not exhibit self-healing properties under SLC. Subsequently, similar experiments were conducted using poly(propylene glycol) diglycidyl ether in place of PDMS, but encountered similar results in terms of the material's inability to self-heal under SLC.

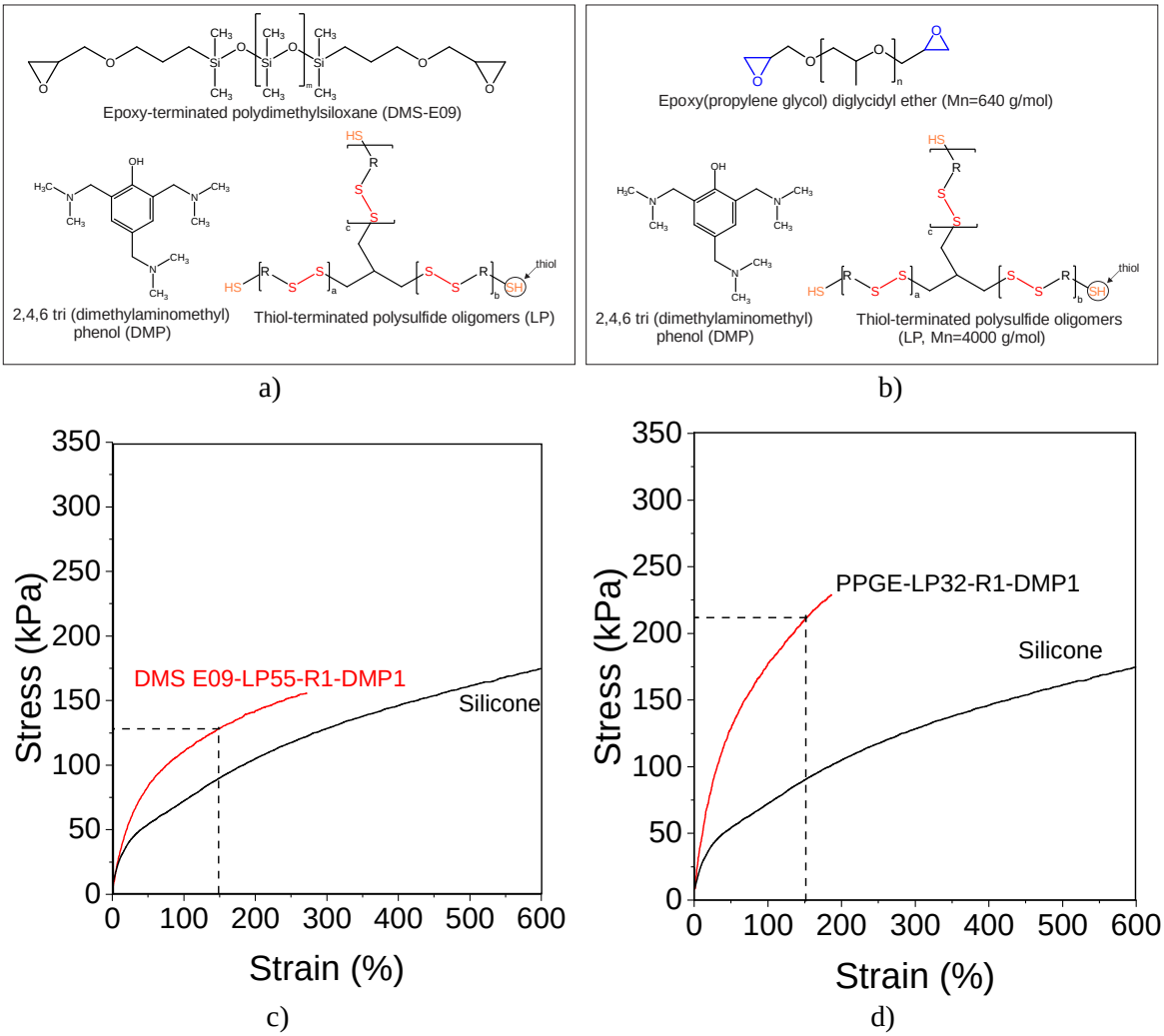

Figure 29. a,b) Chemical structure of the monomers, c)Stress-strain response of an elastomer prepared using epoxy-terminated polydimethylsiloxane and Thiokol, d) Stress-strain response of an elastomer prepared using epoxy terminated poly(propylene) glycol and Thiokol (silicone sample did not fail when the testing machine capacity was reached, the elongation of silicone was >1000%)

As a next step, sealant formulation was modified by using bisphenol-A epoxy as a crosslinker for thiol terminated polysulfides, (Figure 30). Several self-healing elastomers were developed in the last 10 years using thiol terminated polysulfides and epoxy. The benefit of introducing epoxy is a reduced compression set of polysulfide-based sealants (J. Zhang et al., 2012) and excellent adhesive properties. The reaction between epoxy and thiols, also called epoxy-thiol click reaction is commonly initiated by amine base catalysts. Thiol-epoxy curing with tertiary amines is fast and can take place at a convenient rate even at room temperature. In the following experiments, the reaction of the epoxy and polysulfide was initiated by using 1% (of the total weight of epoxy and polysulfides) of 2,4,6-tris(dimethylaminomethyl)phenol (DMP) which has been previously reported as an efficient initiator for epoxy-thiol reaction (Gao et al., 2017). Unlike prior research that used elevated temperature for curing (75 ℃ for 24 h), our samples were cured at room temperature over a period of three weeks.

Experiments included testing three different sealant formulations with varying amounts of branched polysulfide oligomers (as indicated by the percentage of 1,2,3trichloropropane, TCP, used during synthesis of polysulfide oligomers): LP2, LP32, and LP55 (Table 8). The synthesis procedure involved combining all compounds in a plastic cup and mixing in a high-speed mixer at 2000 rpm for 2 min (Figure 31). The mixture was poured into a silicone mold and cured in SLC for 21 days. These sealant formulations were prepared by mixing epoxy and polysulfides at r=1. As expected, LP2 had the lowest elongation (~150%), followed by LP32 (346%) and LP55 (386%), Figure 32. All of them had the ability to self-heal under ambient conditions, Figure 33. Based on its tensile properties (elongation, strength), it was concluded that LP55 has the most potential as a sealant for concrete pavement joints, so further tests were conducted on it.

Table 8. Properties of thiol-terminated polysulfide oligomers

	LP2	LP32	LP55
n (number of repeating units)	23	23	23
Average molecular weight (g/mol)	4000	4000	4000
SH-content (mol/kg) (Robinson, 1992)	0.6	0.53	N/A
Cross-linking agent (mol%)	2	0.5	0.05

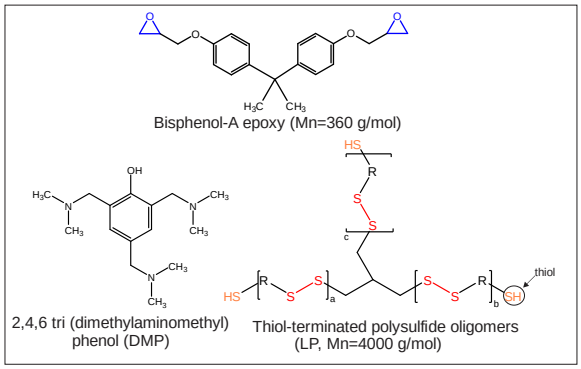

Figure 30. Chemical structure of BADGE, thiol-terminated polysulfide and DMP

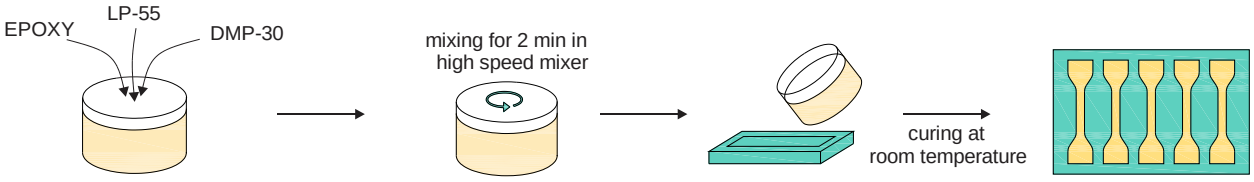

Figure 31. Illustration for preparation of the epoxy/Thiokol elastomers at ambient temperature

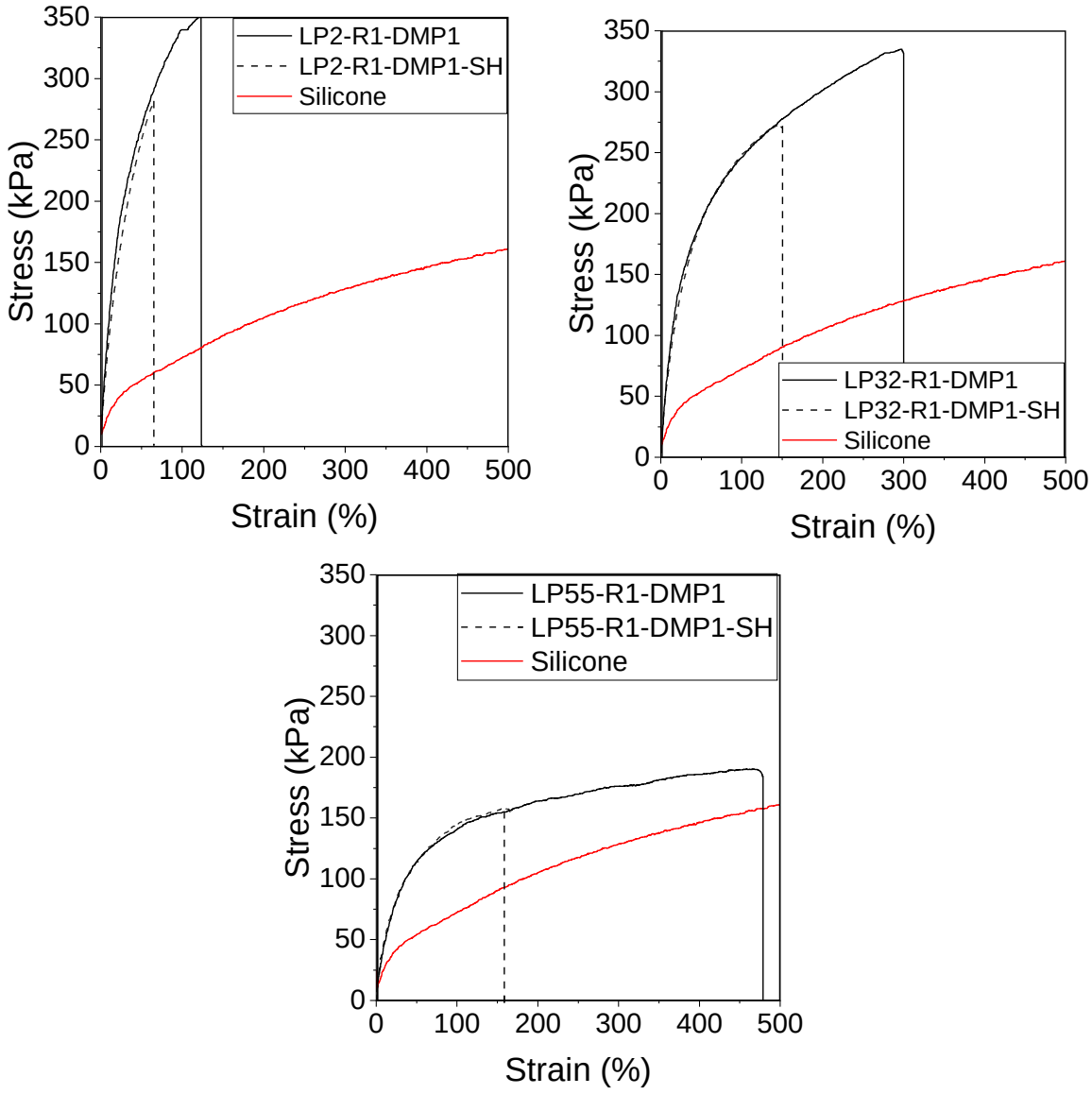

Figure 32. Comparison of strain-stress behavior of three sealants prepared using thiol terminated polysulfide oligomers with different amount of branching. Silicone sealant is included as a reference (silicone sample did not fail when the testing machine capacity was reached, the elongation of silicone was >1000%)

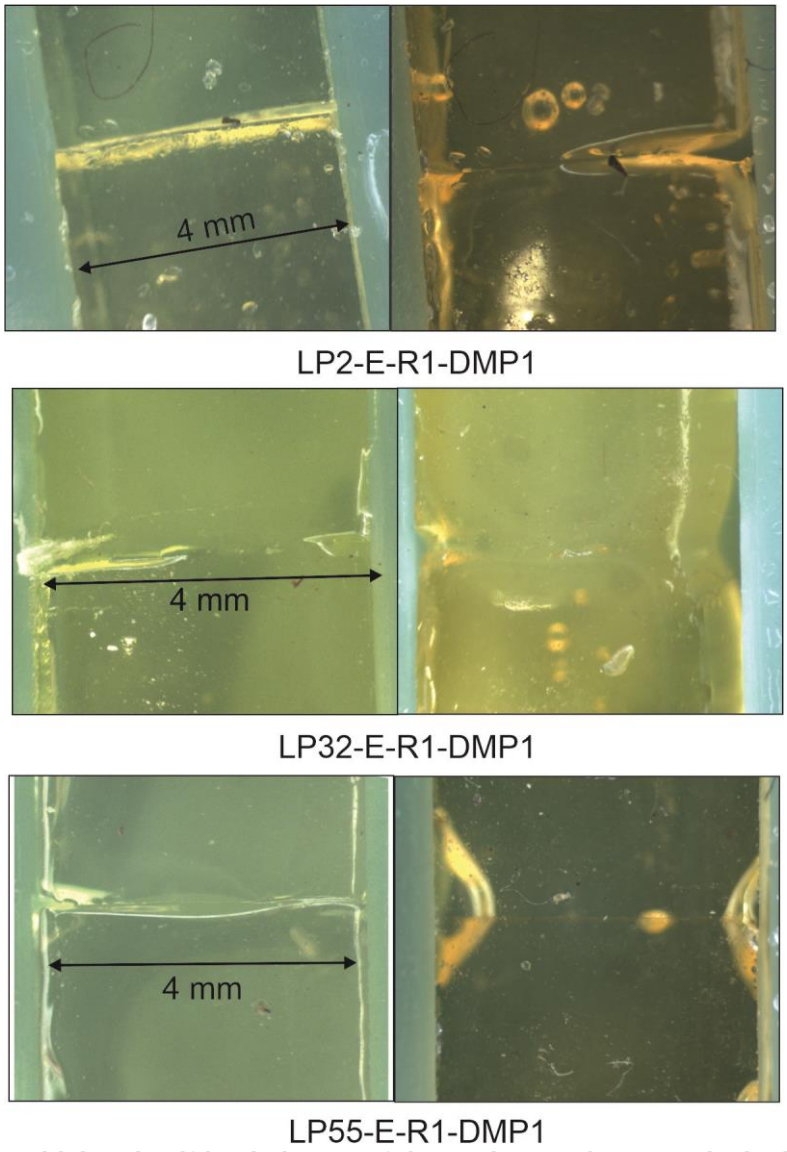

Figure 33. Initial and self-healed state of the sealant under an optical microscope

Influence of initiator type on epoxy-polysulfide network formation

Different initiators can lead to variations in the reaction rate and influence the network formation which ultimately determines the material properties and self-healing. As shown above, DMP was successfully used as initiator for the epoxy-thiol reaction. In the effort to improve self-healing efficiency of the sealant, triethylamine (TEA) was also tested as an initiator. There has been interest in TEA as an effective catalyst for disulfide exchange or thiol-disulfide exchange which would improve self-healing efficiency (Rekondo et al., 2014).The addition of TEA at 0.1 by mol accelerates the disulfide exchange between aromatic disulfide compounds (Nevejans et al., 2016).

Triethylamine generally has higher basicity compared to 2,4,6-Tris(dimethylaminomethyl)phenol. The pKa values of DMP are pKa1 = 8.41; pKa2 = 9.12; pKa3 = 9.75 for amines; and pKa4 = 10.4 for hydroxyl (ECHEMI,2024). The pKa of triethylamine is 10.78, (PubChem, 2024). The catalyst's basicity

can significantly influence the epoxy-thiol reaction mechanism and subsequently impact the resulting mechanical and physical properties of the material (Geng et al., 2021).

The composition of the elastomers synthesized using two different catalysts to initiate epoxy-thiol reaction is shown in Table 9. Three different formulations were tested: 1) with only DMP, 2) with only TEA, and 3) combination of DMP and TEA. The amount of catalyst in the first two cases was 1% by weight of epoxy and polysulfide. When expressed as the molar content of the catalyst per epoxy, TEA was at 0.213 mol/EE and DMP at 0.083. Experimental trials involved reducing TEA content to 0.5% by weight, but this adjustment did not lead to curing of epoxy-thiol.

One of the challenges during the synthesis procedure was related to the functionality of polysulfide oligomers. The characteristics of the polymer network and its formation vary extensively based on the proportion of epoxy to thiol. When the ratio of reactive groups (r) is 1, the system is stoichiometric and the crosslinking density can reach its maximum when the system achieves full conversion. The number average functionality (f_n) of liquid Thiokols depends on the molecular weight and the quantity of branching agent 1,2,3-Trichloropropane (TCP). Based on the available literature, content of TCP in LP55 is 0.05% by mol, which means that certain content of branched polymers is present. In the sample nomenclature the R1 indicates a molar stoichiometry between the epoxy and polysulfide. The information regarding the average number-average functionality (f_n) was not available for LP55 in the literature. For LP32, which has higher content of the branching agent than LP55, the f_n is 2.1 (Robinson, 2001). This implies that the f_n of LP55 is between 2 and 2.1. Consequently, when the molar ratio of epoxy to thiols is 1, there exists some excess of thiols.

To better interpret the experimental results, the curing mechanisms for the epoxy-thiol reaction are discussed. The curing mechanism of thiol–epoxy reactions catalyzed by tertiary amines involves a number of reaction steps. One of the accepted reaction mechanisms is based on the reaction between the tertiary amine and thiol to produce a thiolate anion that then reacts with the epoxy ring, Figure 35 (Jin et al., 2015). It was shown that this mechanism describes epoxy-thiol curing in the presence of strong bases. However, if the basicity of the tertiary amine is low, then the proton exchange between the thiol and tertiary amine is unlikely (Fernández-Francos et al., 2016). In this case, the reaction starts with the reaction between the tertiary amine and the epoxy ring, Figure 36.

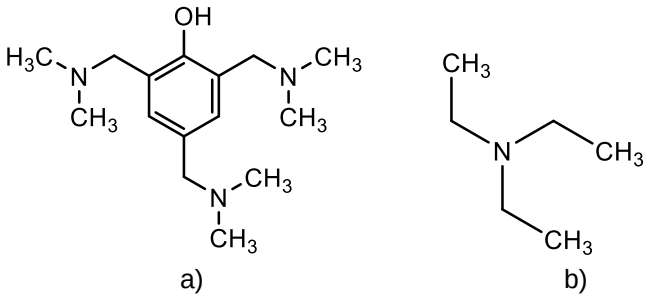

Figure 34. Base catalysts for epoxy-thiol reaction: a) DMP, b) TEA

1) Base catalyzed deprotonation of thiols to generate thiolate anions

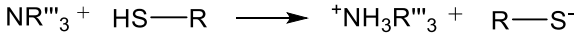

2) Nucleophilic reaction of thiolate anion with epoxide functional group to form alkoxide anions.

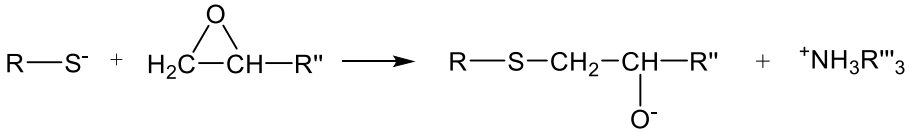

3) Protonation of the alkoxide via the base catalyst (or thiol)

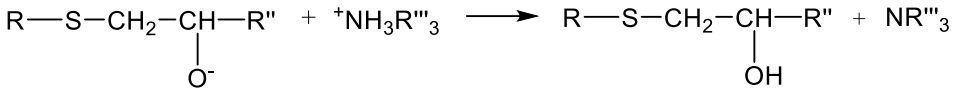

Figure 35. Reaction mechanism of the thiol-epoxy reaction catalyzed by tertiary amine, Jin et al., 2015

1) Nucleophilic attack of the tertiary amine on the epoxy ring

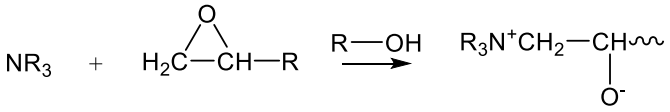

2) Proton exchange between the thiol and the alkoxide

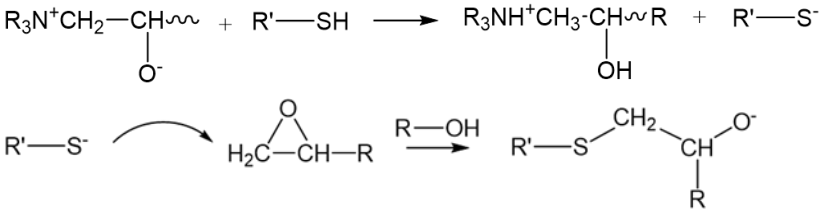

3) Ring opening of the epoxide

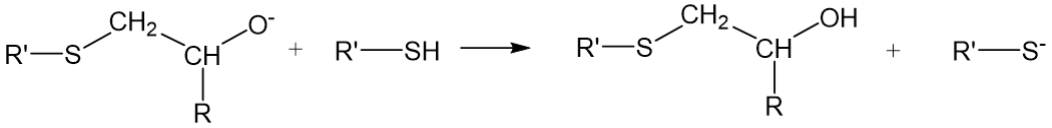

4) Alkoxide/thiol proton exchange

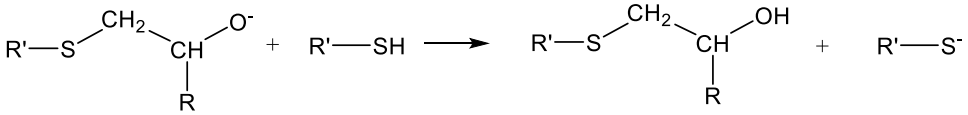

Figure 36. Reaction mechanism of the thiol-epoxy reaction catalyzed by amine, (Fernández-Francos et al., 2016)

Table 9. Sealant composition: catalyst type

Sample	LP55	Epoxy	DMP (g)	TEA (g)	DMP/EE	TEA/EE
LP55-E-R1-TEA1	10	0.9	0	0.109	0	0.213
LP55-E-R1-DMP1	10	0.9	0.109	0	0.083	0
LP55-E-R1-DMP1-TEA1	10	0.9	0.109	0.109	0.083	0.213

Curing under ambient conditions. Understanding the curing process and extent of curing under ambient conditions is important not only because it determines the sealant properties (mechanical, physical, durability) but also self-healing ability. The extent of conversion can affect self-healing in two ways: A lower degree of curing can lead to increased chain mobility. Higher chain mobility and flexibility of the network can facilitate self-healing. The lower extent of curing results in a higher concentration of unreacted thiols in the elastomer. Thiol groups are essential for the ability of the network to rearrange. When damage occurs, these unreacted thiols (Pepels et al., 2013) can react with disulfide bonds, promoting bond reformation and healing of the material. An elastomer that undergoes a more complete curing process possesses fewer available thiols for the healing mechanism.

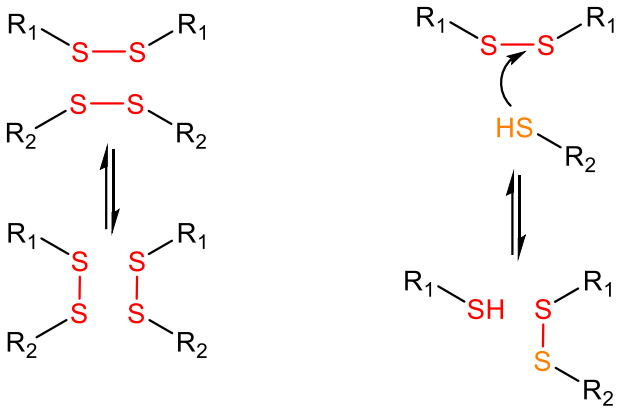

Figure 37. Disulfide-disulfide bond exchange (left), thiol-disulfide exchange (right)

To determine the extent of curing, the thiol peak in the FTIR spectra at 2530 cm^{-1} and epoxy peak at 4530 cm^{-1} were monitored over 24 h. In the sample with TEA, SH and epoxy peaks disappeared after 17 h. In the sample with DMP, both unreacted thiols and epoxy were present after 24 h of curing under ambient conditions, Figure 38. Based on the FTIR data there is no evidence that unreacted thiols are present in any of the samples after 21 days of curing. Tested samples were prepared with an excess of thiols, and for this reason, it was expected that there would be some unreacted thiols at the end of the reaction, but this was not the case.

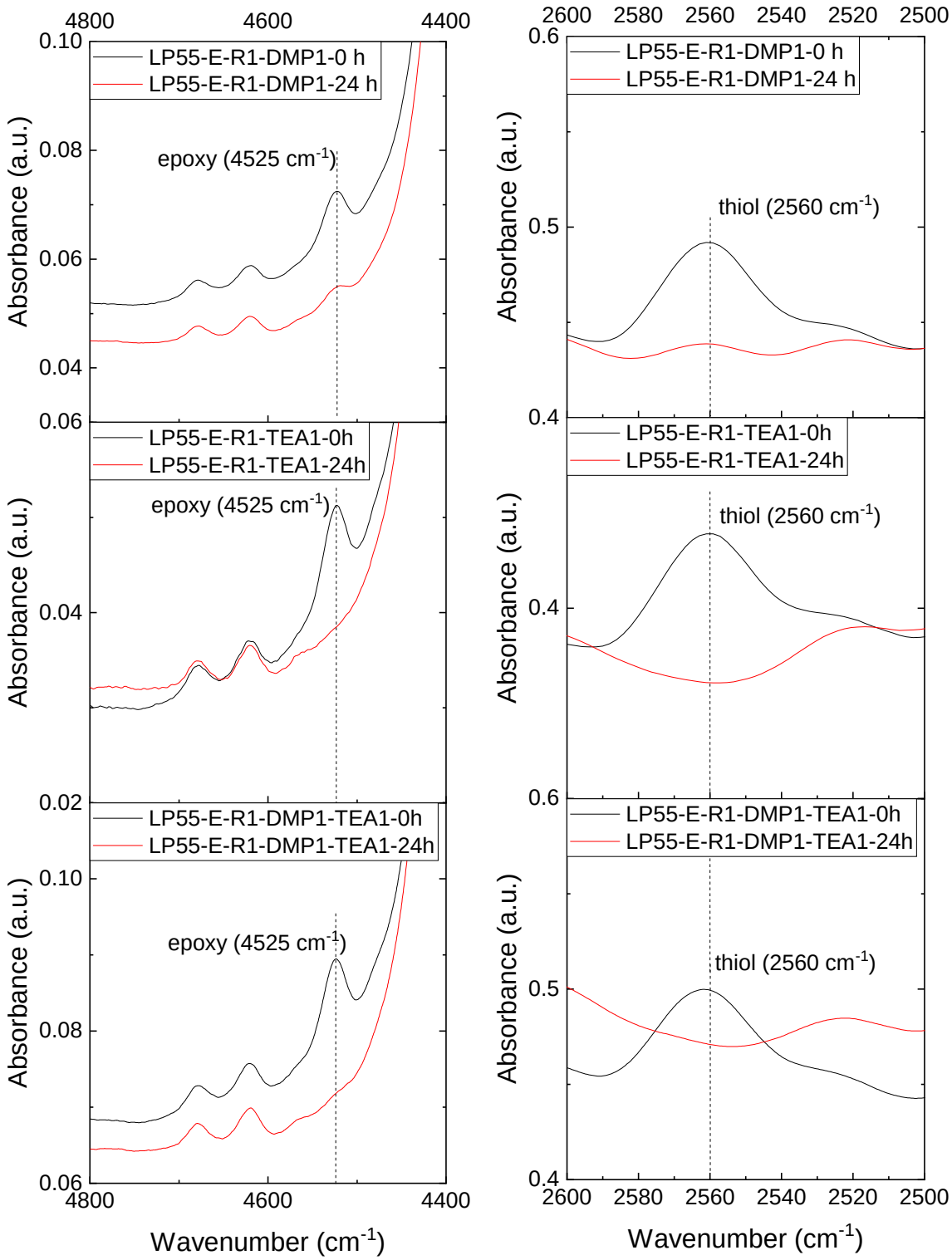

Figure 38. Impact of catalyst type in sealant formulation on epoxy-thiol conversion measured by FTIR

It is possible that the FTIR sensitivity was unable to resolve the unreacted functional groups, owing to convolution with other functional group and/or low molar absorptivity. To potentially address this limitation, isothermal calorimetry was used to directly measure the heat generated during the reaction. The

use of isothermal calorimetry aims to uncover information inaccessible by FTIR, offering a secondary method to monitor the reaction's progress and ultimate completion. Differences in the heat released or absorbed during the reaction when using different catalysts can signal variations in the rate and extent of curing. A lower released heat suggests incomplete curing, where fewer bonds form, leading to incomplete network formation and reduced material strength and durability.

The isothermal calorimetry runs were performed at 25 °C. The detectable heat released during curing was determined by integrating the heat flow evolved within the polymerization time (Figure 39). In the first 12 h of curing only 10% conversion was observed for both cases. When TEA was used as an initiator 60% conversion was reached after 12 h. More basic catalysts tend to facilitate faster reaction rates by effectively abstracting protons from thiol groups, promoting the activation of the thiol and initiating the ring-opening of the epoxy. This can lead to the formation of different intermediates compared to less basic catalysts, potentially affecting the final structure and properties of the cured material. Triethylamine is a tertiary amine with three ethyl groups attached to the nitrogen atom, making it more basic due to the availability of the pair of electrons on the nitrogen that can accept a proton. The presence of the bulky phenyl ring attached to the nitrogen atoms in DMP can create spatial hindrance making it more difficult for other molecules to access the reactive site. Consequently, this hindrance can influence the reactivity and kinetics of chemical reactions.

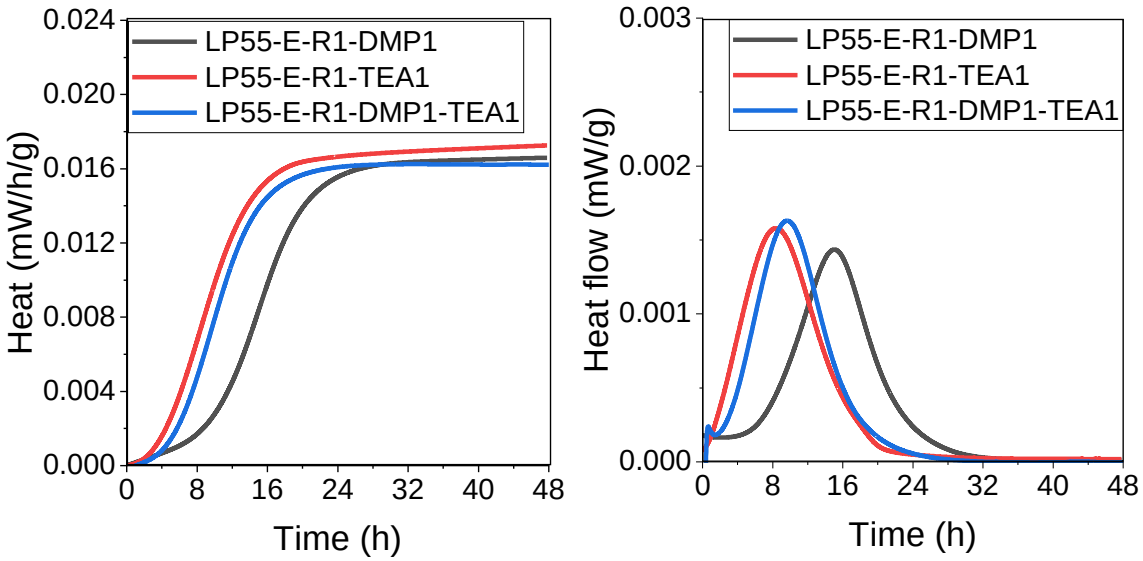

Figure 39. Isothermal calorimetry-effect of different catalysts

Gel fraction. Gel fractions of 90 and 75% (Table 10) corresponding to samples prepared with DMP and TEA, respectively, indicate that unreacted components are present in both samples. The gel fraction for the sample that contained both DMP and TEA was similar as in the sample with DMP only (90%). Regarding the sample prepared with TEA, the swelling ratio of 140% implies the existence of a more dense network structure compared to the sample with DMP with higher swelling ratio of 230%. The cross-linking density is strongly correlated to the degree of swelling the lower the chain network density, the higher their capacity to accommodate more solvent molecules. Lower gel fraction in the sample with TEA compared with the sample with DMP indicates higher content on unreacted components or presence of soluble content.

Presence of unreacted components indicate incomplete curing process, a factor that has significant influence on mechanical and physical properties.

Table 10. Gel fraction and swelling ratio (after 3 weeks of curing at room temperature)

Sample	Gel fraction (w%)	Swelling ratio (%)
LP55-E-R1-DMP1	90	228
LP55-E-R1-TEA1	76	144
LP55-E-R1-DMP1-TEA1	91	230

Mechanical properties. The comparison of the mechanical properties in tension of the three sealants is shown in Figure 40. The sample prepared with TEA exhibited lower elongation of ~300% compared to the sample prepared with DMP (~450%). The tensile strength was more than 2 times higher in the sample with TEA compared to the sample with DMP. The sample that contained both catalysts had elongation and strength similar to the simple with DMP. In reference to defined performance criteria, samples LP55-E-R1-DMP1 and LP55-E-R1-DMP1-TEA1 met the tensile stress at 150% strain criteria that is limited to 310 kPa, but did not meet the elongation requirement of 600%.

The stress-strain behavior of samples that were cut in half and self-healed at room temperature for 24 h is shown for comparison in the same figure with control samples (Figure 41). The self-healing efficiency of samples that contained either DMP or TEA was relatively low (41% and 20%, respectively) compared to the sample that contained both DMP and TEA which had self-healing efficiency of 78%. To determine which factors that had the most important effect on the mechanical and self-healing properties, additional experiments were conducted to understand polymer network formation when different catalysts were used.

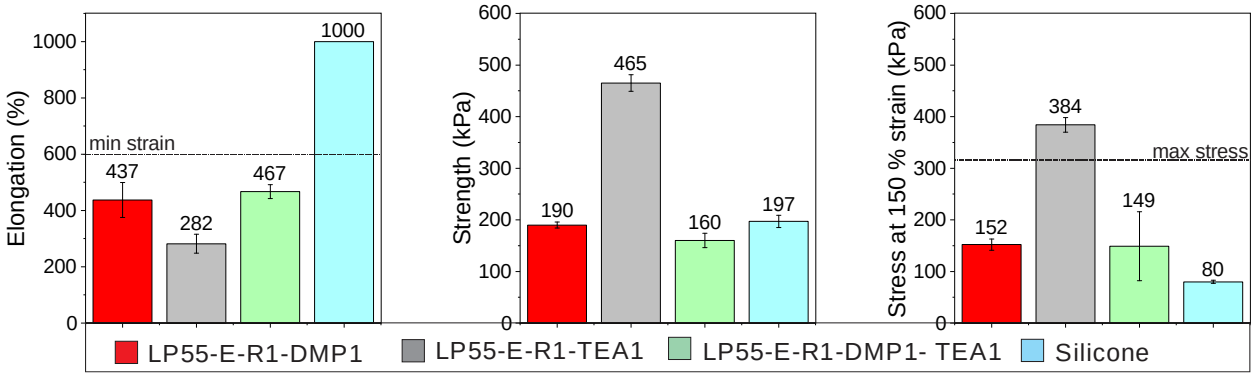

Figure 40. Comparison of elongation and strength among different sealant formulations

The stress-strain response in tension was nonlinear. The sealant shows a transition from essentially elastic behavior to plastic behavior at about 50% strain. Identifying the "yield" point is important because it can be used as a basis to establish design strain limits and minimize residual deformation. Upon unloading, the material exhibits permanent deformation in the range 10-15%, Figure 42. The reported residual deformation was measured after 3 weeks. This is important to note as the strain recovery occurs after a period of time. The value of residual deformation depends on many parameters: applied strain rate, temperature, imposed extension. All these parameters need to be analyzed in order to establish conditions under which sealant can completely recover from the applied strain.

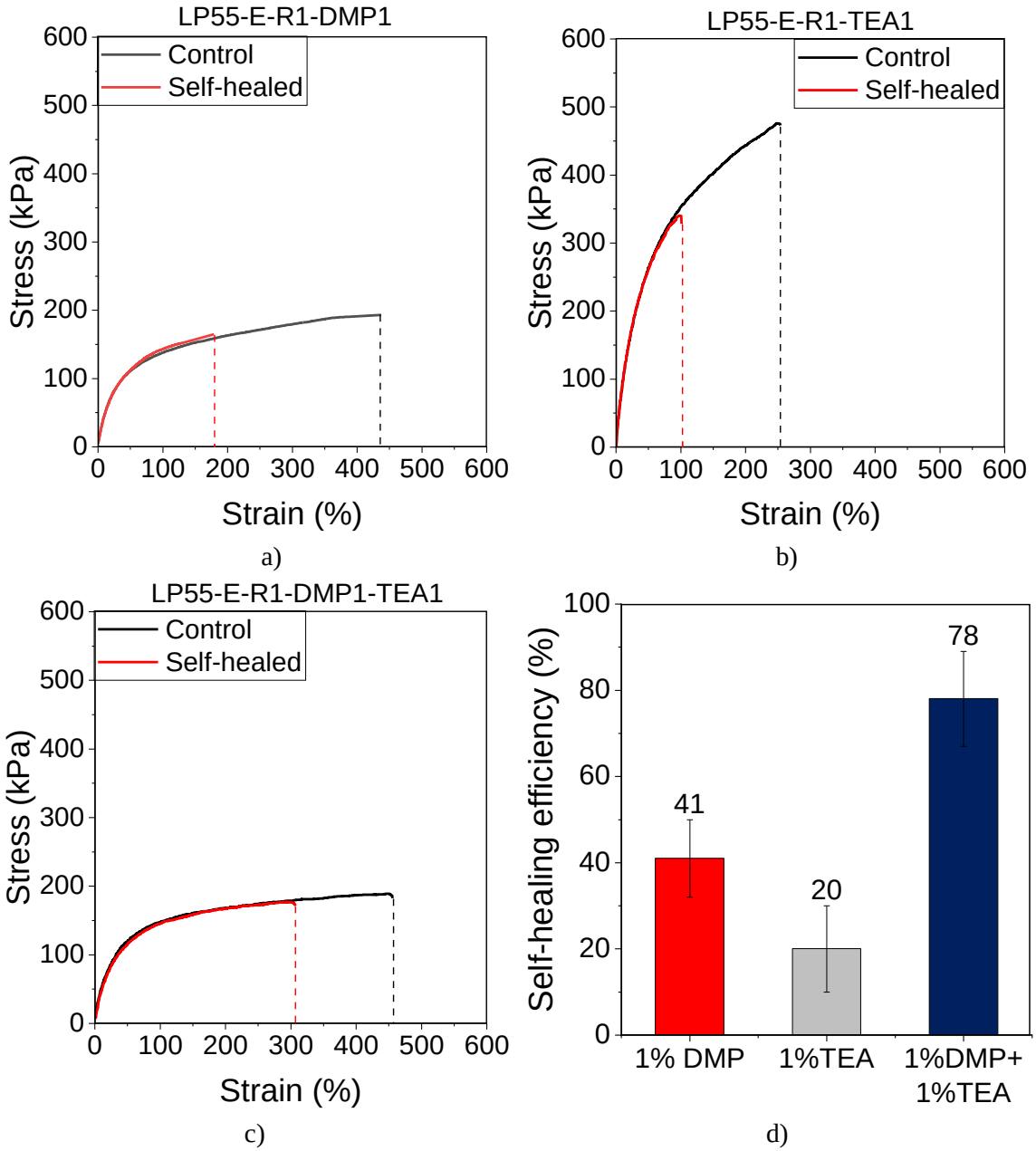

Figure 41. a,b,c) Comparison of strain-stress response of control and self-healed samples (only representative data was plotted here, all data is provided in the Appendix), d) Self-healing efficiency

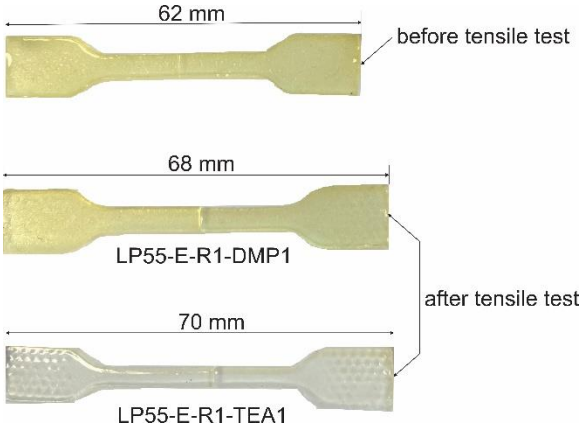

Figure 42. Residual deformation after applying displacement at 50mm/min rate until failure

Analysis of network formation. The analysis of the effect of catalyst type on the polymerization was conducted by monitoring conversion of epoxy and thiols in real time over 24 h (Figure 43). During the first 12 h, ~10% conversion was observed in the LP55-E-R1-DMP1 sample. After this induction period, the reaction took place at a fast rate following an autocatalytic mechanism. This autocatalytic behavior in thiol-epoxy reactions is caused by an autocatalysis effect of hydroxyls formed during the curing reaction. Consistent with observations of isothermal calorimetry experiments, the increase in conversion was faster when TEA was used, after 12 h the conversion of thiols was 60%.

FTIR data indicate that in the first 24 h, there is a difference in the rate of consumption of epoxy and thiol groups, with thiol groups being consumed at a faster rate than epoxy. Tested samples were prepared with an excess of thiols, and for this reason, it was expected that there would be some unreacted thiols at the end of the reaction, but this was not the case. Thiol peak disappeared after ~16 h when TEA was used as a catalyst and ~24 h when DMP was used as a catalyst/initiator. There could be side reactions where reactants participate in reactions other than the intended one. This can affect the overall conversion rate of epoxy/thiols compared to the primary reaction.

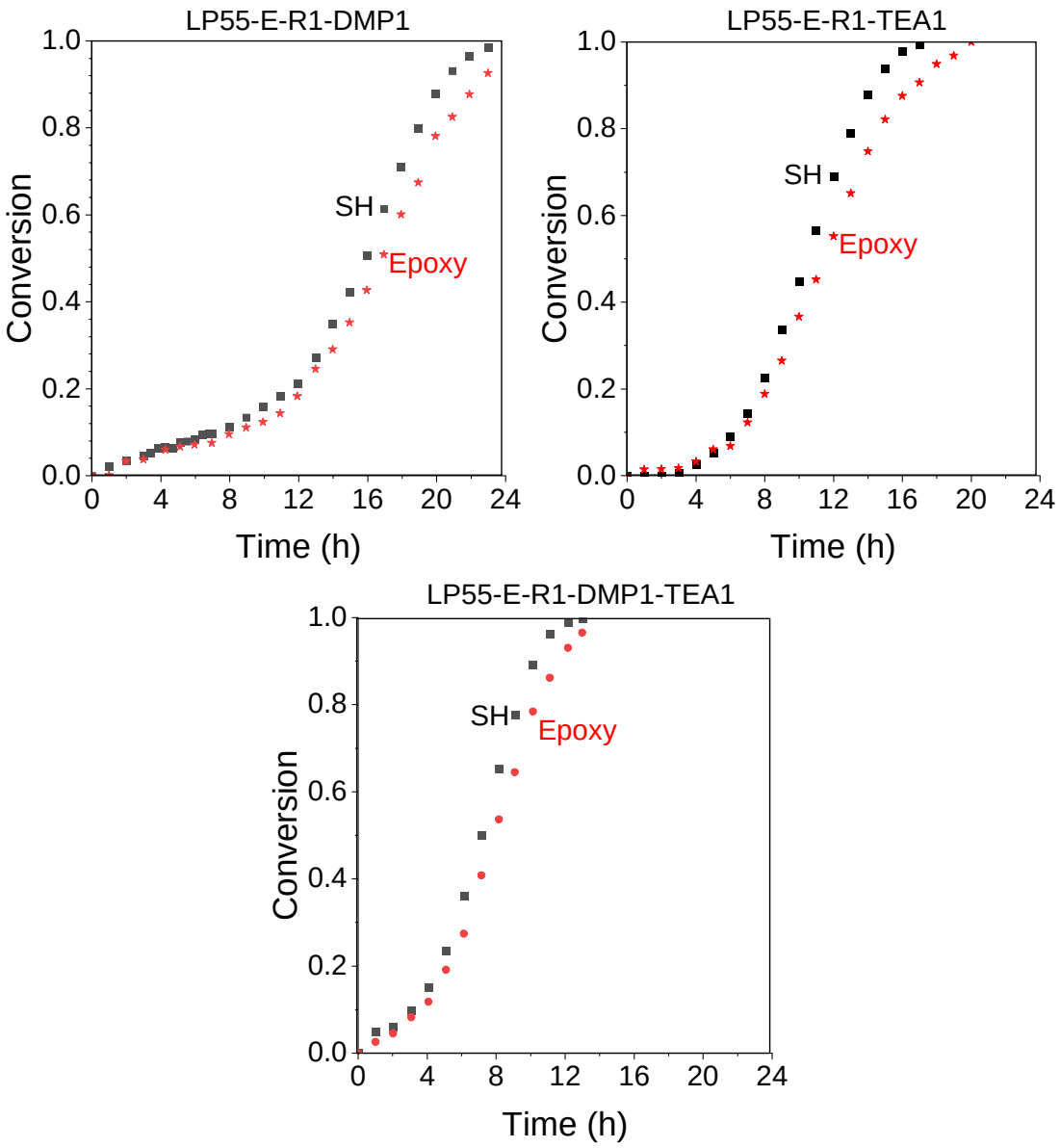

Figure 43. Conversion of epoxy and thiol—effect of catalyst

In the context of epoxy-thiol reaction, the presence of hydroxyl group in DMP is an important consideration. Hydroxyl group can affect the epoxy-thiol reaction by participating in side reaction and formation of intermediates or network formations that eventually can affect mechanical properties. The epoxy group can react with the hydroxyl group. The product of this reaction will contain new hydroxyl groups that can react with other epoxy rings, Figure 44.

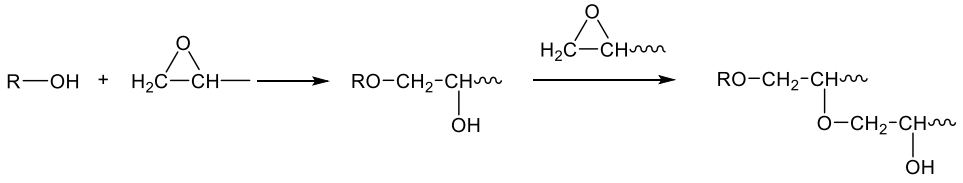

Figure 44. The epoxy–hydroxyl reaction (Brydson, 1999)

The effect of DMP and TEA on epoxy was analyzed by preparing mixtures of only epoxy and catalyst (either DMP or TEA) and cured at room temperature. The catalyst content per epoxy (Table 11) in these samples was the same as the catalyst content in corresponding samples prepared with LP55 and EPOXY.

Table 11. Composition of mixtures with only epoxy and catalyst (either DMP or TEA)

Sample	Epoxy (g)	Catalyst (g)	Catalyst/EE
E-DMP1	5	0.6	0.081
E-TEA1	5	0.6	0.213

Both catalysts proved as effective for epoxy polymerization (Figure 45). The reaction was faster when DMP was used. After 4 h, when the conversion of epoxies reached 40%, the reaction slowed down. The effect of TEA was different. In the first 12 h, only 5% of epoxies have reacted and after that, the rate of reaction increased Figure 45.

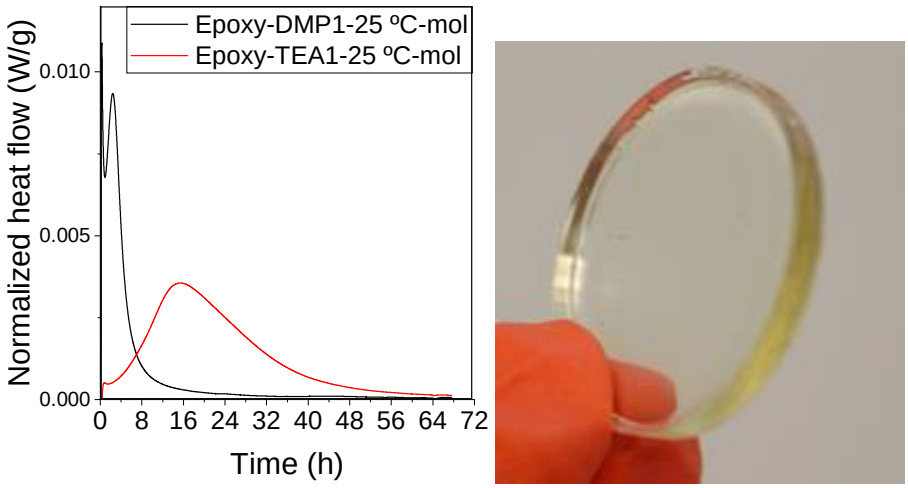

a) b)

Figure 45. a) Isothermal calorimetry–epoxy polymerization initiated by tertiary amines, b) Polymer obtained by epoxy homopolymerization in presence of DMP

Anionic polymerization of epoxy is commonly initiated by tertiary amines. The assumed mechanism is shown in Figure 46. It involves the formation of an alkoxide, which then reacts with an epoxy monomer while regenerating another alkoxide and so on.

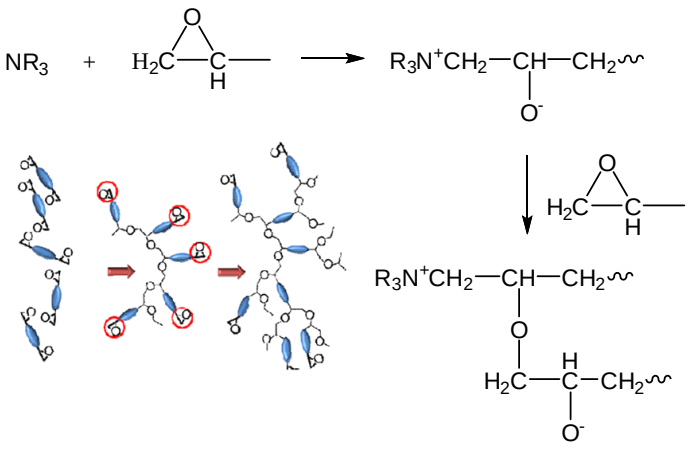

Figure 46. Anionic polymerization of epoxide initiated by a tertiary amine in the presence of an alcohol (Vidil et al., 2016)

Epoxy and hydroxyl conversion profiles in Figure 47 show that all hydroxyls in the sample with DMP disappear after ~2 h. The epoxy consumption continues at a slower rate than hydroxyl and after 24 h is approximately 50% in the sample with DMP. The epoxy consumption in the sample prepared with TEA occurs at a slower rate-after 24 h epoxy conversion is about 25%. In this sample the peak corresponding to hydroxyl groups decreased by 50% in the first 8 h of the reaction. The hydroxyl peak at 3500 cm^{-1} corresponds to hydroxyl groups in the epoxy resin, Figure 48. These hydroxyls are present as impurities due to the precursor compounds used in its synthesis of the epoxy resin (bisphenol A contains hydroxyl groups). Decrease in this peak can be the result of hydrogen bonding between the OH group in DMP and hydroxyl groups in the epoxy resin. It is also possible that the reason for DMP being more effective in epoxy homopolymerization reaction is presence of OH.

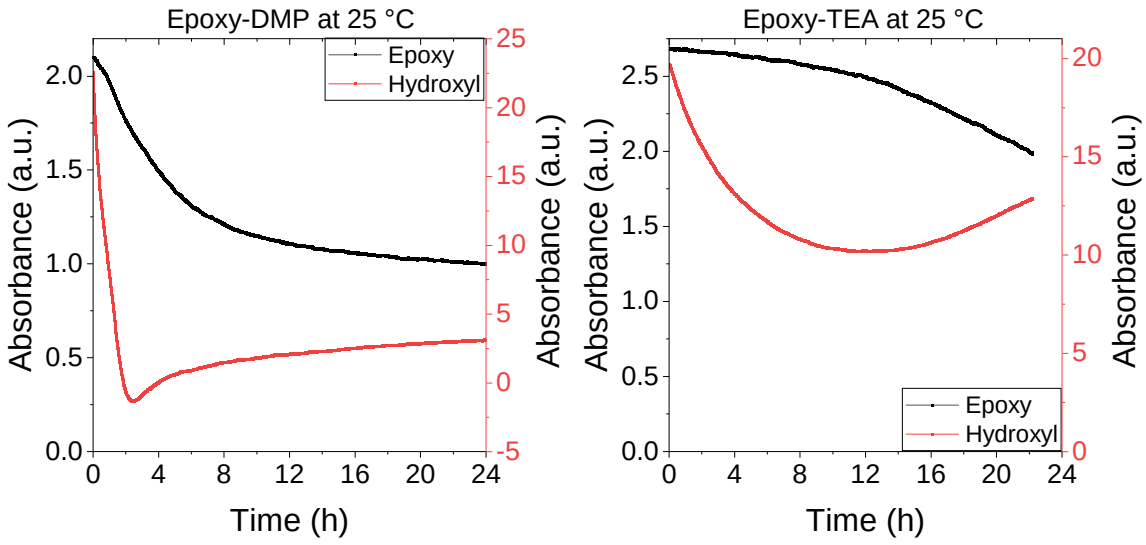

Figure 47. Conversion of epoxy in presence of: a) DMP, b) TEA

Although both initiations proved to be efficient in producing epoxy homopolymerization reaction, it is not clear if this reaction would occur in presence of thiols. Loureiro et al., (2015) observed epoxy homopolymerization during the epoxy-thiol reaction initiated by tertiary amine. Specifically, authors used benzyl dimethylamine as an initiator for the reaction between 3-mercaptopropionate and phenyl glycidyl

ether (PGE) mixed at a stoichiometric ratio to analyze the reaction taking place during the induction period. The analysis showed that homopolymerization took place in the presence of BDMA at 20 ℃. This study supports the argument that the epoxy homopolymerization in the LP55-E-R1-DMP1 could be a reason for the differences compared to the tensile properties measured in the LP55-E-R1-TEA1.

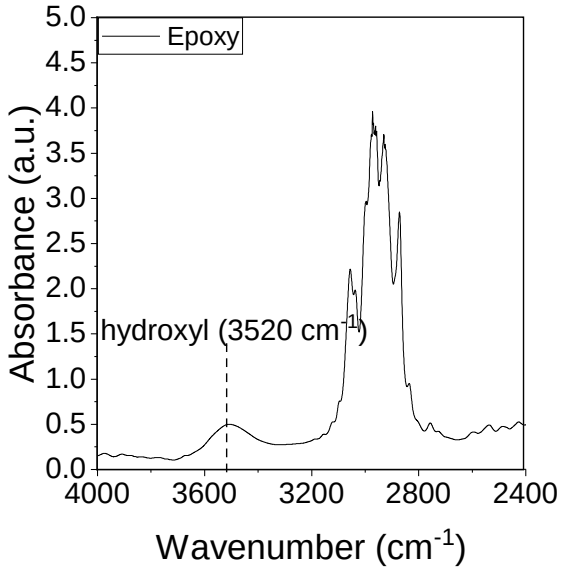

a)

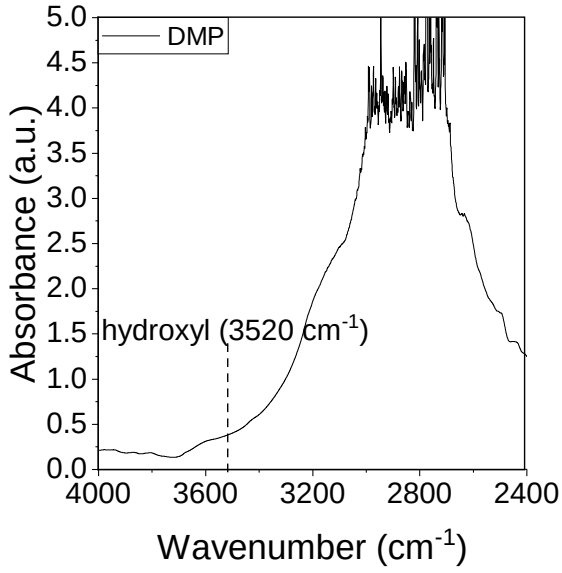

b)

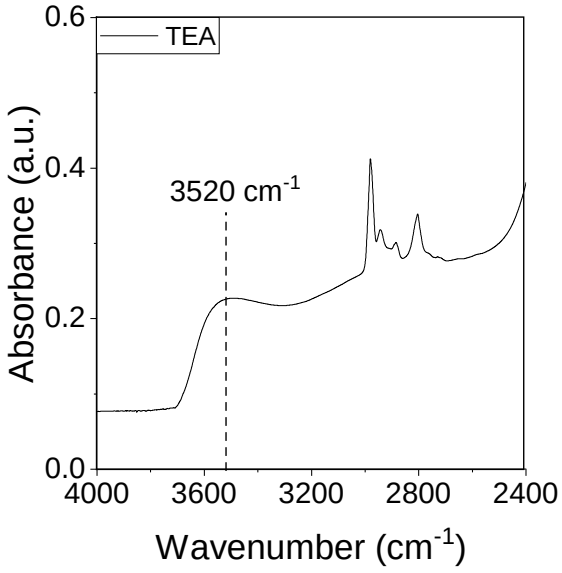

c)

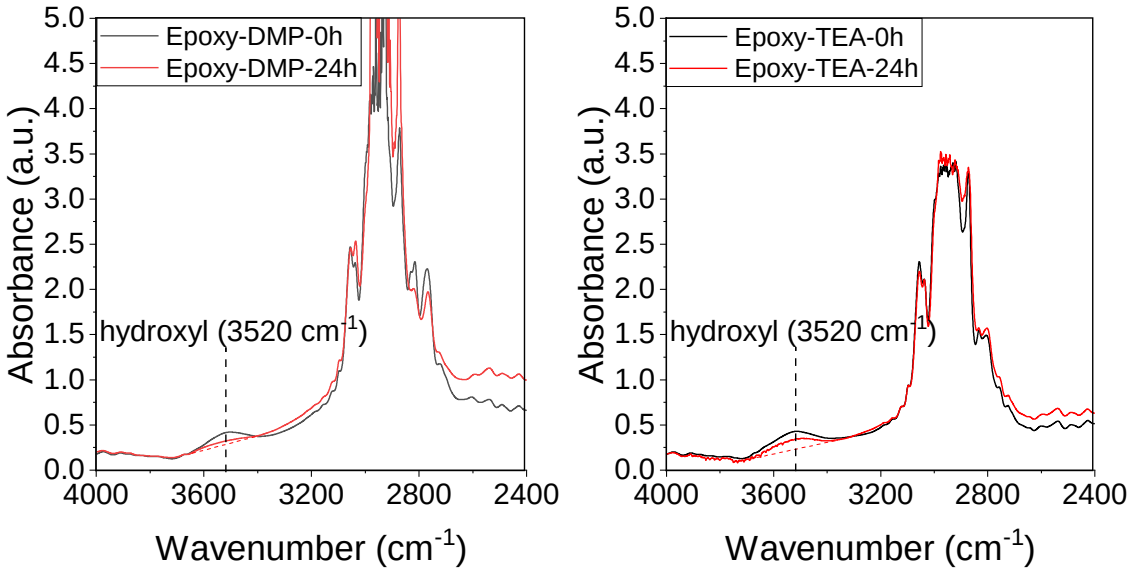

Figure 48. a,b,c) FTIR spectra of DMP, TEA, and epoxy resin. Hydroxyl groups are present as impurities in epoxy resin at 3520 cm^{-1} d,e) FTIR spectra of Epoxy/catalyst mixture before and after curing at room temperature for 24 h showing change in hydroxyl peak area

In general, epoxy homopolymerization in mixtures with excess of epoxy results in increased cross-linking and strength /modulus in epoxy-amine and-epoxy anhydride formulations (Fernández-Francos et al., 2016). To determine what would be the effect of epoxy homopolymerization during the induction period of the epoxy-thiol reaction on the mechanical properties of the sealant additional testing was conducted. The experiment involved mixing epoxy and DMP and adding LP55 after 1.5 h. After 21 days of curing under ambient conditions specimens were tested in tension. In addition to this, small pieces were swelled in toluene. Stress-strain data show that after reaching 55 kPa, the stress started to decrease, Figure 49. This often occurs due to the rearrangement of polymer chains within the elastomer. During this phase, the polymer chains might align or slide past each other, allowing for extensive deformation without a considerable increase in stress. The observed behavior is probably due to incomplete curing and the presence of unreacted polymer chains. After 24 h in toluene, the specimen was almost completely dissolved.

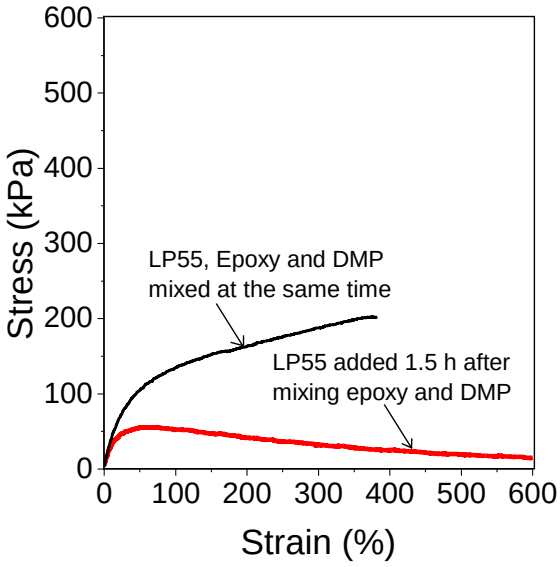

Figure 49. Stress-strain behavior for formulations prepared by adding LP55 after mixing DMP and epoxy resin. The experiment intends to simulate effects of epoxy homopolymerization during induction phase of epoxy-thiol reaction under ambient conditions

One potential side-reaction is the oxidative polymerization of polysulfide oligomers. Pepels et al., (2013) observed that samples prepared with thiol-terminated polysulfides stored in air had higher strength and lower elongation than samples stored in nitrogen. Authors concluded that this is likely the result of oxidative coupling of thiol groups forming additional cross-links.

It was hypothesized that the exposure of thiol-terminated polysulfide samples to oxygen may induce oxidative polymerization and formation of additional cross-links increasing the tensile strength. To determine the effect of oxygen on curing reaction, specimens were prepared and cured under nitrogen and compared to the specimens cured in air. The comparison of tensile testing results is shown in Figure 50 and Figure 51. Contrary to the initial hypothesis and the observation by other authors, the experimental results show that the tensile strength in the sample with TEA decreased when thiol-terminated polysulfides were cured in air (650 kPa to 465 kPa). It is possible that the reason for this decrease is that LP55 consists of mostly linear chains; that is, oxidation of thiols could have resulted in the formation of longer polymer chains leaving unreacted epoxy monomers in the network. In the sample with DMP the strength increased from 170 kPa (cured in N2) to 190 kPa (cured in O2), which indicates that different processes are occurring between the two groups. It is interesting that the gel fraction (Table 12) was the lowest (60%) in the sample with TEA cured under nitrogen (the sample that had the highest strength). Additional experiments are needed to understand the interaction between oxygen and catalysts on network formation.

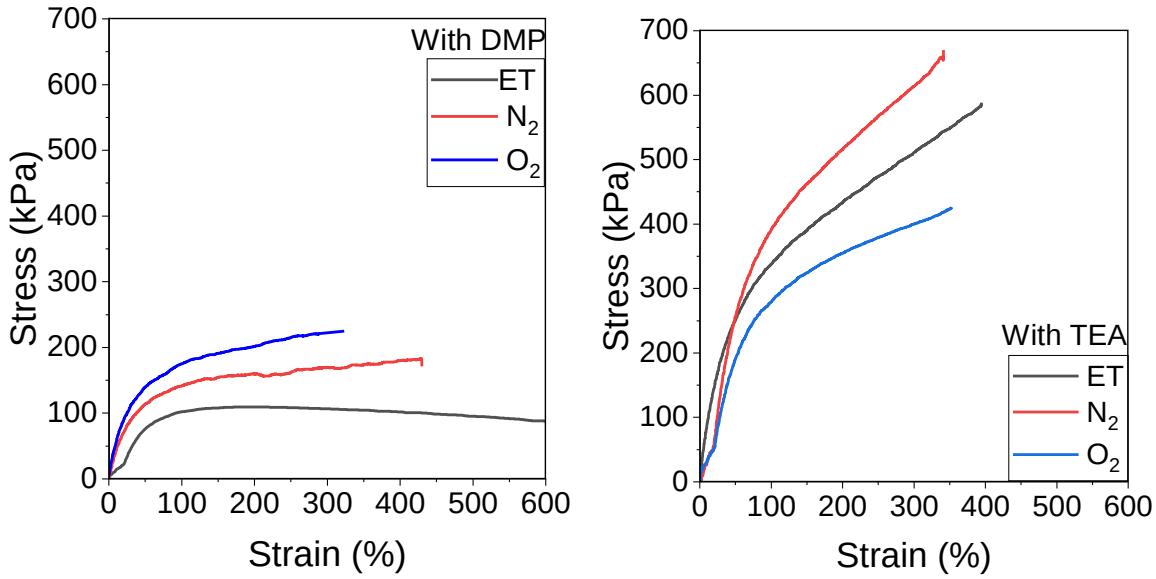

Figure 50. Tensile stress-strain behavior for samples cured in air under room temperature, air at elevated temperature and in nitrogen at room temperature (O_2 indicates that the sample was cured at room temperature in presence of oxygen, N_2 was curing under nitrogen at room temperature, and ET was curing at elevated temperature in the presence of oxygen)

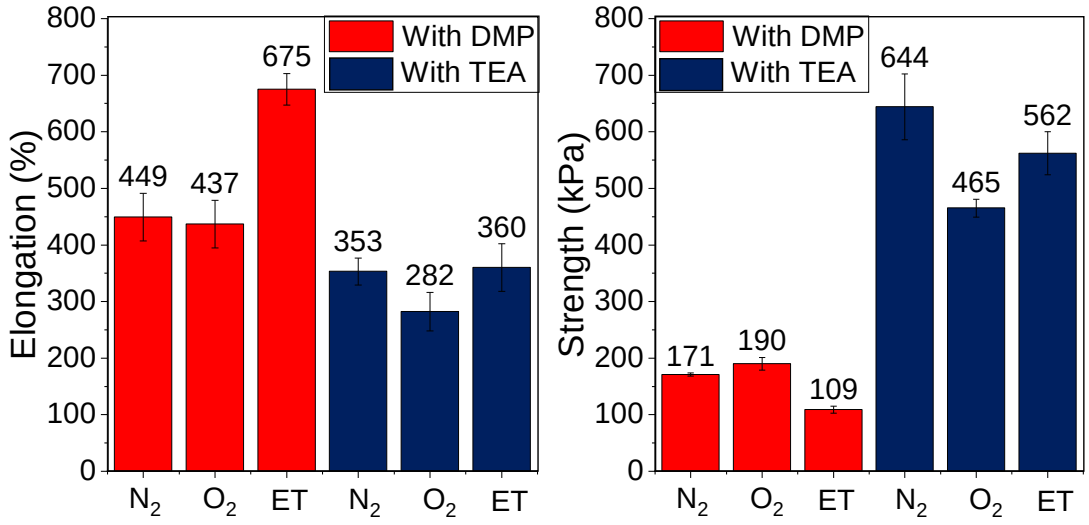

Figure 51. Comparison of sealants mechanical properties—curing under different conditions

Table 12. Gel fraction of samples cured under different conditions

Sample	Gel fraction (w%)			Swelling ratio (%)		
	AIR	OVEN	N2	AIR	OVEN	NITROGEN
LP55-E-R1-DMP1	90	90	/	228	252	227
LP55-E-R1-TEA1	76	95	60	144	219	154

Influence of initiator content on epoxy-polysulfide network formation

Figure 52 and Figure 53 show that the reaction starts earlier when the content of TEA increases from 1% to 1.5%. Increasing DMP content to 1.5% slightly accelerated the reaction initiation. When the DMP content was increased to 1.5% the tensile strength decreased from 180 kPa to 100 kPa, Figure 54. It is possible that DMP promotes epoxy homopolymerization or acts as a plasticizer decreasing the strength and modulus. When DMP content was increased to 2% by weight, the epoxy and polysulfide did not cure. Increasing content on TEA deceased curing time by 30%. The effect on tensile properties was not significant.

Table 13. Sealant composition: effect of catalyst content

Sample	LP55	Epoxy	DMP/EE	TEA/EE
LP55-E-R1-TEA1.5	10	0.9	0	0.323
LP55-E-R1-DMP1.5	10	0.9	0.123	0

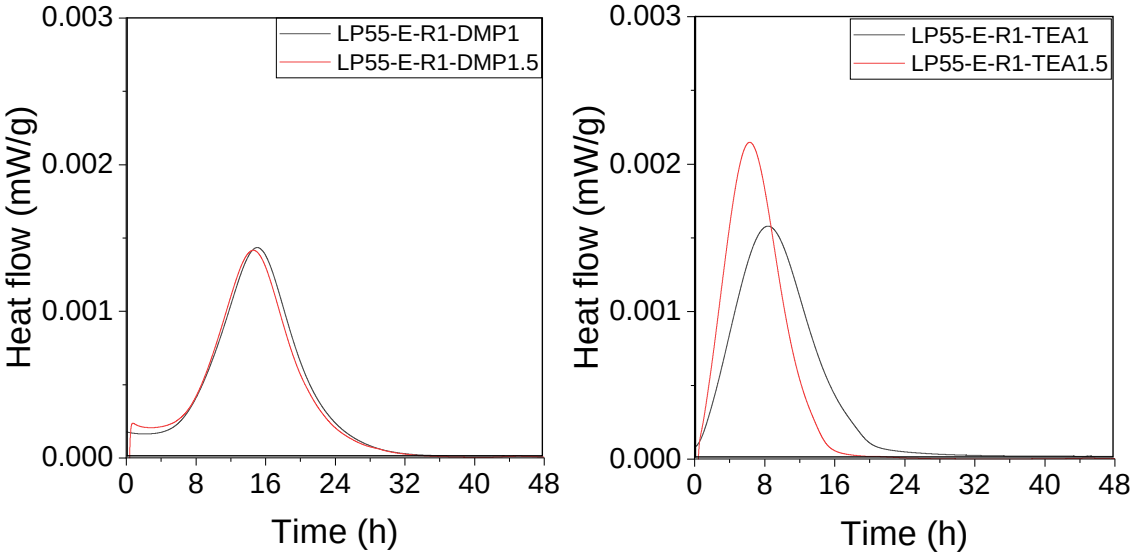

Figure 52. Impact of catalyst concentration in sealant formulation on the epoxy-thiol reaction heat flow measured by isothermal calorimetry

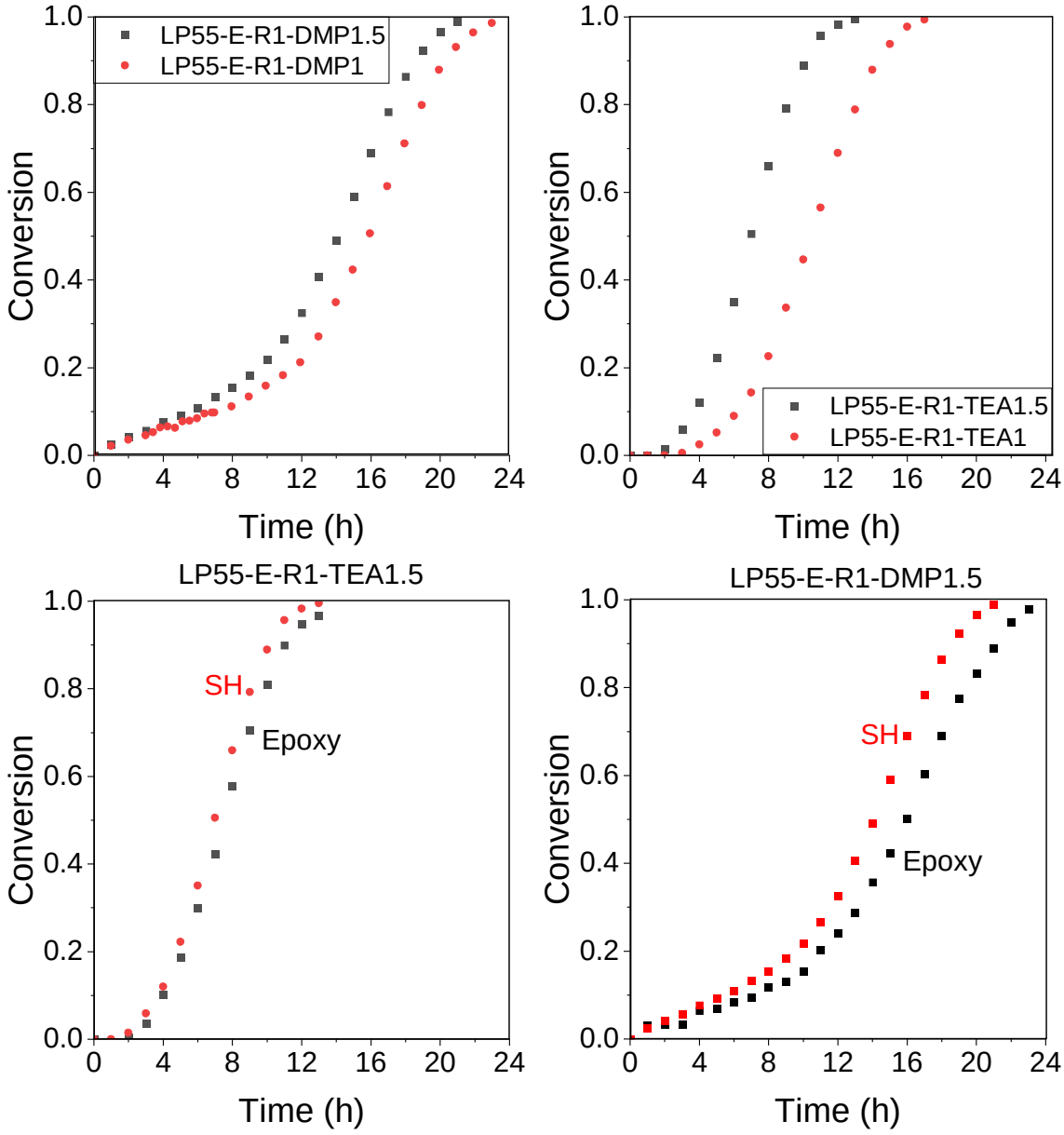

Figure 53. Impact of catalyst concentration in sealant formulation on epoxy-thiol conversion measured by FTIR over 24 hours

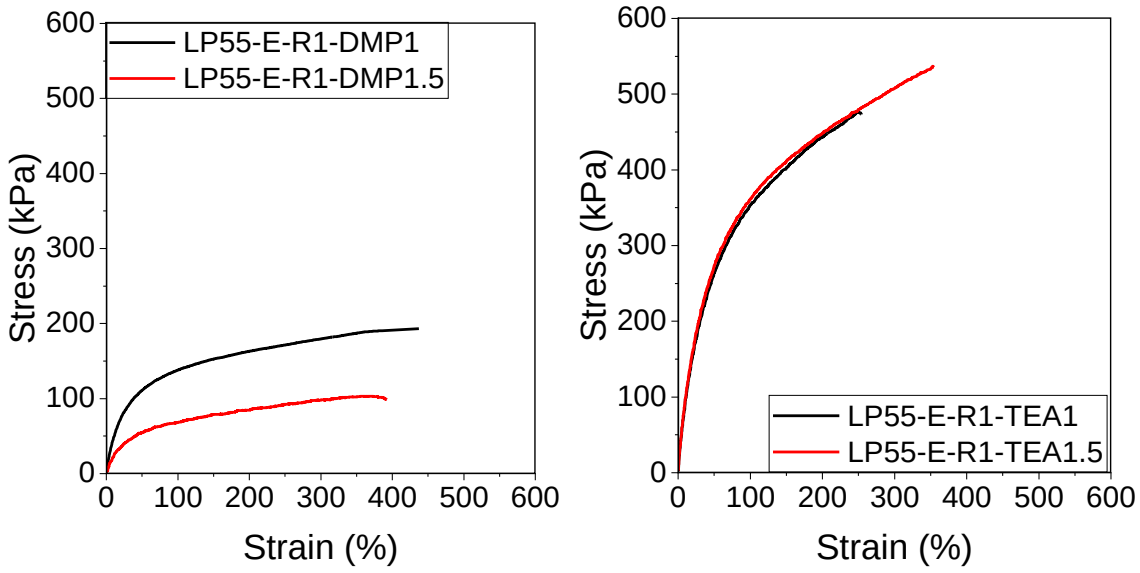

Figure 54. Effect of catalyst content of the tensile behavior of the sealant

Self-healing efficiency

The detailed values of control and healed tensile stress and strain are shown in Table 14. The self-healing efficiency measured as the percentage of restored elongation is plotted in Figure 55.

Table 14.Self-healing efficiency

Sample	Elongation %		Stress at 150% strain (kPa)	
	Control	Self-healed at ambient temperature	Control	Self-healed at ambient temperature
LP55-E-R1-DMP1	437	179	152	119
LP55-E-R1-TEA1	282	56	384	0
LP55-E-R1-DMP1.5	432	375	78	75
LP55-E-R1-TEA1.5	336	61	399	0
LP55-E-R1-DMP1-TEA1	467	367	160	167

Tensile and self-healing test show that the self-healing efficiency is higher when DMP is used as a catalyst. The best self-healing efficiency was observed in the LP55-E-R1-DMP1.5 sample. Increasing the content of DMP from 1% to 1.5% increased self-healing efficiency from 35% to 86%. As pointed out above, there is a possibility that DMP participates in side reactions at room temperature, which leads to incomplete curing. Lower degree of curing leads to increased chain mobility. This allows the chains to move more easily and deform under stress. Higher chain mobility and flexibility of the network enhances diffusion of broken chains and can facilitate self-healing. Another implication of incomplete curing is the presence of unreacted thiols. When damage occurs, these unreacted thiols can react with disulfide bonds, promoting bond reformation and healing of the material. An elastomer that undergoes a more complete curing process possesses fewer available thiols for the healing mechanism. Samples prepared with TEA had low self-healing efficiency of approximately 15%. In a rigid polymer network, the mobility of polymer chains decreases which makes self-healing more challenging.

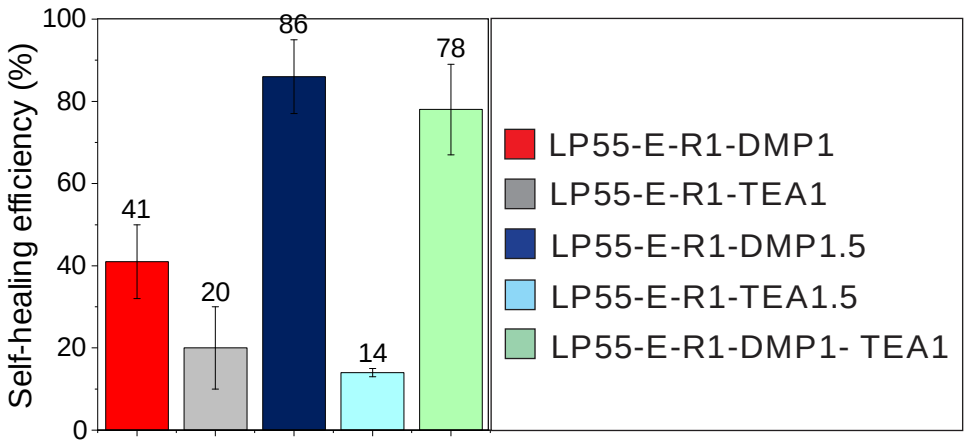

Figure 55. Self-healing efficiency

Although glass transition temperature, as an indication of the polymer network mobility did not vary among samples, differences in the storage modulus in the rubbery region were noticeable, Figure 56 a,b. The storage modulus, observed over the temperature range of 0 °C to 60 °C, consistently exhibits a noticeable decrease in all tested elastomers, with varying degrees of decline among them. Not only that the sample with 1.5% of DMP had the lowest storage modulus (Figure 57), it also exhibited a higher decrease of storage modulus with increasing the temperature. When a polymer has a higher cross-linking density, it tends to exhibit a slower rate of decline in the storage modulus within the rubbery regime. As a result, the material can retain its stiffness and elastic behavior over a wider temperature range. Although the sample that contained 1.5% of DMP had the best self-healing efficiency, from a viewpoint of practical application it is less suitable, since the decline of storage modulus with temperature was larger compared to other samples. The sample that contained both DMP and TEA had similar values of storage modulus in the rubbery region as the sample that contained only 1% of DMP. However, LP55-E-R1-DMP1-TEA1 had better self-healing efficiency than the sample with only DMP.

The experimental results which involved testing different monomers, catalysts and catalyst content have provided valuable insights into the performance of these sealants. Based on the testing results, three distinct sealant formulations were selected for further evaluation and additional testing. With these three chosen formulations, the objective was to capture the impact of various catalysts and ensure that the materials possessed mechanical properties comparable to other commercially available sealants. Considering that the choice of catalyst plays an important role in determining the material's performance, each of the three sealants were formulated to contain different types of catalyst: DMP, TEA and combination of DMP and TEA.

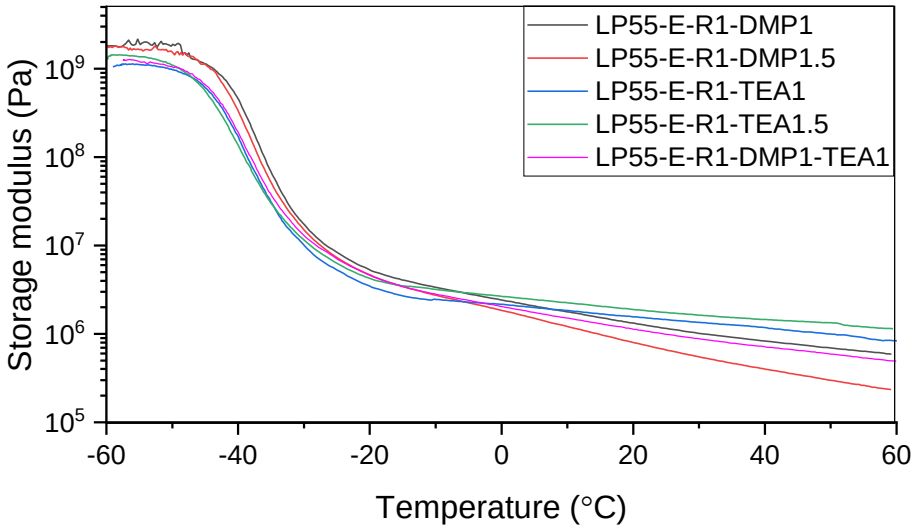

a)

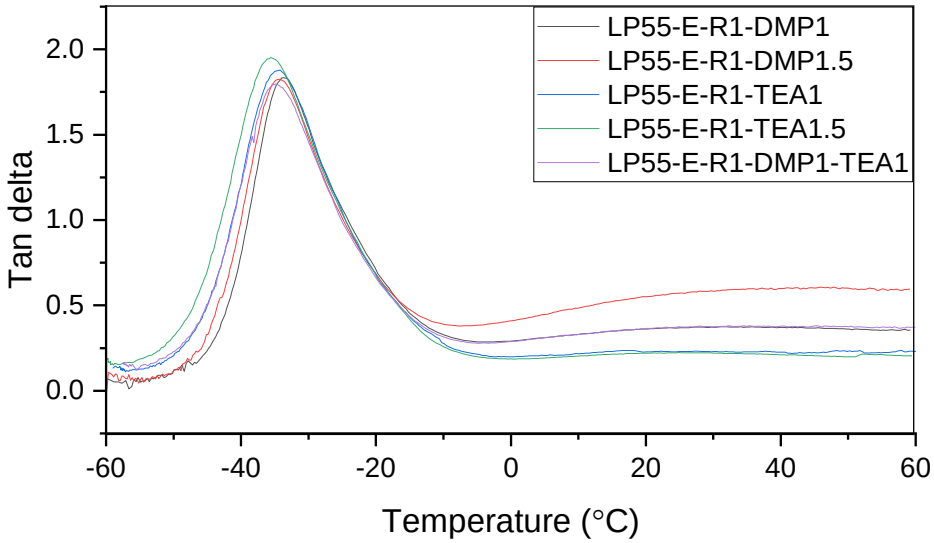

b)

Figure 56. DMA curves for a) storage modulus, b) damping coefficient (tan delta)

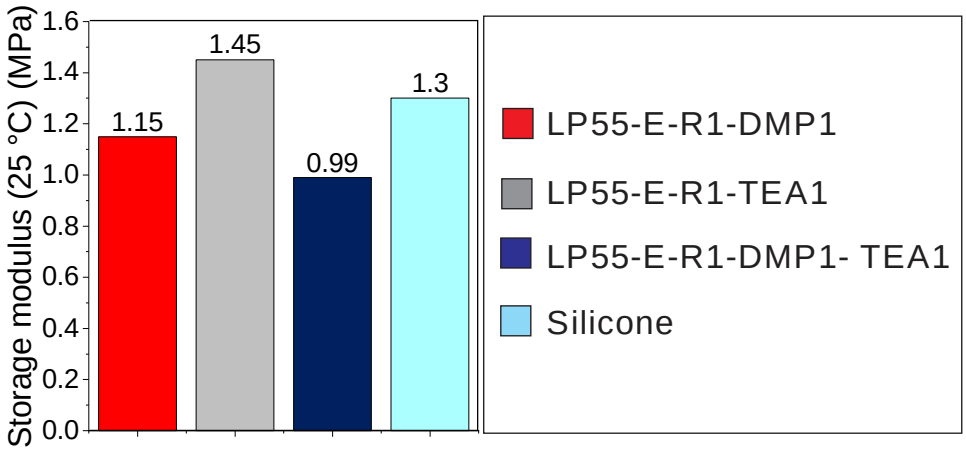

Figure 57. Storage modulus in the rubbery region (at 25 ℃) for different sealant formulations

Adhesion to concrete (ASTM C1135)

The results of joint adhesiom tests based on ASTM C1135 for the control silicone and self-healing polysulfide sealants are shown in Figure 58. The peak stress of the silicone sealant joints was on average 120 kPa, and the maximum elongation was 350%. The peak stress of self-healable polysulfide sealants was between 70 kPa and 270 kPa, while the ultimate elongation was above 1000% (Figure 58). On one hand, all silicone joints failed adhesively (Figure 59); the crack firstly appeared at the joint edge due to stress concentration at these locations before it propagated along the interface. On the other hand, the self-healing sealant joints exhibited cohesive failure after reaching relatively high elongation due to its low modulus.

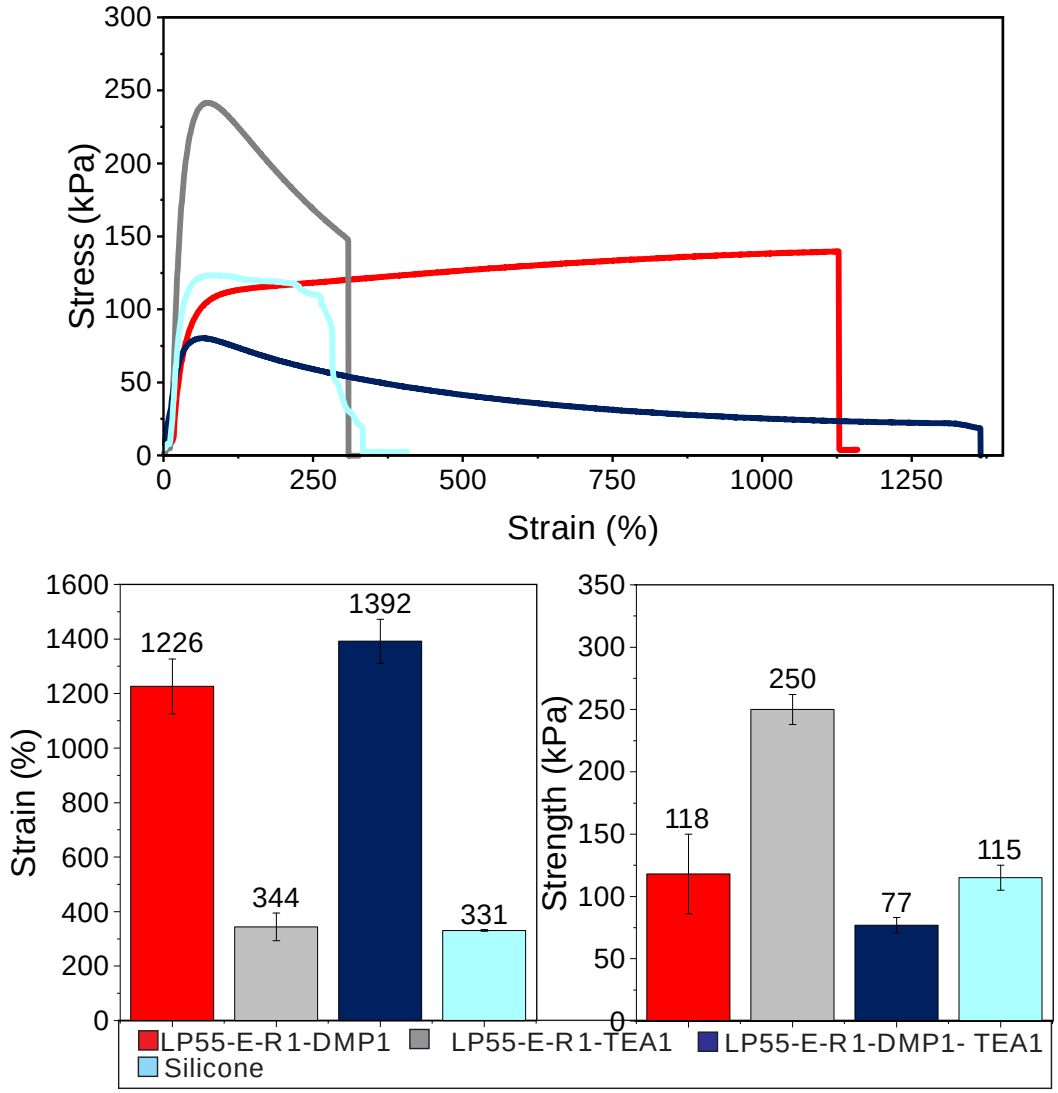

Figure 58. a) Comparative test results showing stress-strain behavior of different sealant joints subjected to tension, b) Elongation and strength of various sealants in concrete joints

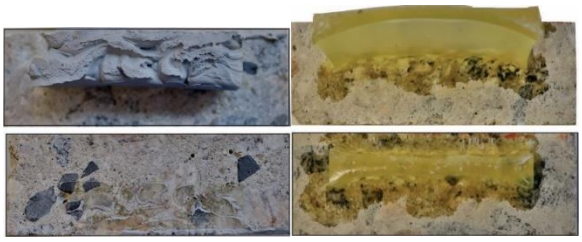

Figure 59. Failure modes of sealant joints: adhesive failure in silicone sealant vs. cohesive failure in self-healable sealant

As a reference, some sealant specifications define minimum cohesive strength for joints; for example, Joint Materials Section of the Virginia 2020 Road and Bridge Specification specifies that the adhesive bond to concrete mortar should be at least 241 kPa (measured by VTM-90) without an adhesive or cohesive failure after 10 cycles at -17 ℃. Although self-healable sealant formulations tested here exhibited relatively good adhesive behavior, it should be noted that SLC ae not representative of service conditions in rigid concrete pavements, which include presence of moisture, freeze-thaw cycles, motor oil, and fuel.

Exposure to cold (ASTM D5893)

The study aimed to assess the adhesion of self-healable sealants to concrete per ASTM D5893 standard. Results indicated that sealants prepared with DMP exhibited no failure, maintaining adhesion to the concrete surface after the specified exposure conditions (Figure 60). However, the sealant prepared with TEA showed signs of damage: one replicate experienced debonding, and another failed after the water exposure period (Figure 61). The observed debonding/failure after water exposure suggests potential weaknesses in adhesion or durability for the sample prepared with TEA. These results might indicate that the TEA formulation is less effective in maintaining adhesion under extreme conditions, impacting its reliability for concrete joint sealing applications.

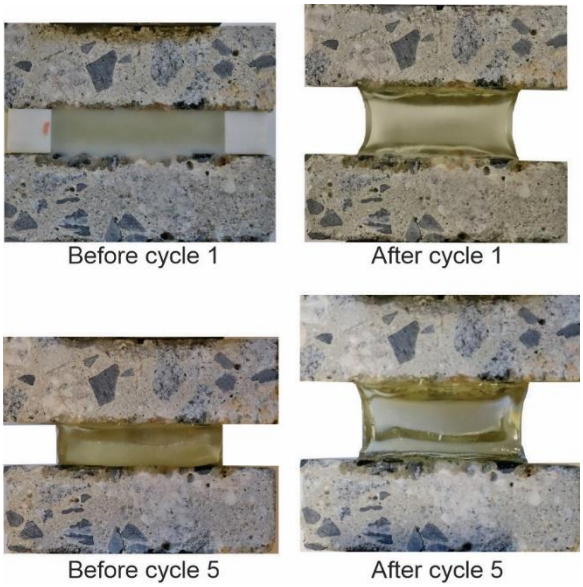

Figure 60. Visual evaluation of joint condition following cold temperature exposure: no damage after 5 extension/compression cycles LP55-E-R1-DMP1

In the tensile test, applying a slow strain rate of 3mm/h resulted in residual deformation after removing the load following a 100% extension (Figure 62). Residual deformation could be attributed to the viscoelastic

nature of the material. The strain rate, plays a significant role in how materials behave under stress. At lower strain rates viscoelastic materials display more pronounced viscous behavior. A low strain rate allows more time for the molecular rearrangement within the elastomer causing stresses to relax.

Figure 61: Visual evaluation of joint condition following cold temperature: presence of debonding after exposure in LP55-E-R1-TEA1

Figure 62: Residual deformation after applying 100% at 3 mm/h displacement rate

Exposure to UV and water spray

After exposure to UV light and water spray, the sealants degraded significantly. The results of tensile testing of samples are compared to the specimens that were kept in SLC, Figure 63. The measured strength decreased by more than 50% in the samples with DMP and elongation by 75%. The exposed surface was cracked, in some cases the cracks extended to 1mm of the 2mm thick cross-section (Figure 64). The observed deterioration is due to absence of UV blockers in the sealant formulation. The self-healing experiments were not performed on these specimens due to substantial degradation.

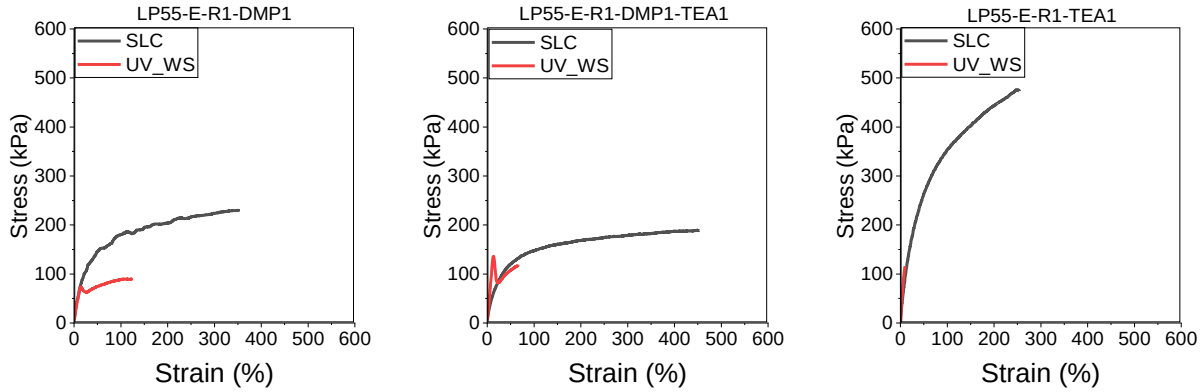

Figure 63. Stress strain behavior of the sealant before and after exposure to UV light and water spray

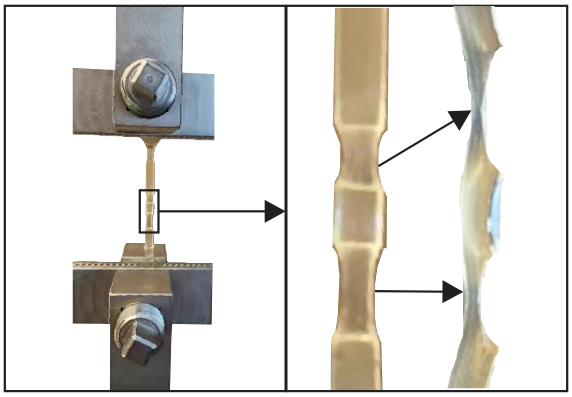

Figure 64. Cracking after exposure to UV and water spray

Hardness

The hardness of the three sealants are shown in Table 15. The results indicate that the minimum hardness requirement of 30 specified in ASTM D5893 for testing at 23 ℃ is satisfied. It is important to note that the reported readings were instantaneous indentations. Considering the susceptibility of the polysulfide to creep, these values could decrease depending on the duration of applied stress.

Table 15. Durometer 00 shore hardness

Sample name	Instantaneous indentation
LP55-E-R1-DMP1	70
LP55-E-R1-TEA1	70
LP55-E-R1-DMP1-TEA1	70

Exposure to moisture

Adhesion to concrete and self-healing in joints

The results of testing joints in tension after water immersion are shown in Table 16 and Figure 65. The ultimate stress for the sealant varied from 90 kPa to 220 kPa. The failure mode of joints immersed in water was predominantly adhesive (Figure 66). Only LP55-E-R1-DMP1-TEA1 exhibited cohesive failure mode. All self-healed joints failed cohesively (Figure 66). In sealant formulations prepared with DMP, self-healing efficiency after water immersion was above 100%. It was concluded that exposure to water does not negatively affect the self-healing process in joints, most probably due to the plasticization effects of water. The presence of hydroxyl groups in epoxy-polysulfide network allows for hydrogen bonding with water molecules. Hydrogen bonding between hydroxyl groups and water molecules enables the material to retain water or, in some cases, increase its water absorption capacity. Polymeric materials with a higher concentration of hydroxyl groups are often more prone to absorbing water. In some cases, water absorption due to hydroxyl groups can facilitate the mobility of polymer chains. When damage occurs, such as micro-cracks or breaks in the material, the absorbed water might help in the reorganization or re-alignment of polymer chains, aiding the healing process. Water can act as a plasticizer, making the polymer more flexible which is beneficial for slef-healing.

Table 16. Self-healing of joints (water immersed)

Sample name	Strain Control (%)	Strength-Control (kPa)	Strain-Self-healed (%)	Strength Self-healed (kPa)
LP55-E-R1-DMP1	445	126	620	102
LP55-E-R1-TEA1	90	221	64	188
LP55-E-R1-DMP1-TEA1	1001	87	1011	90

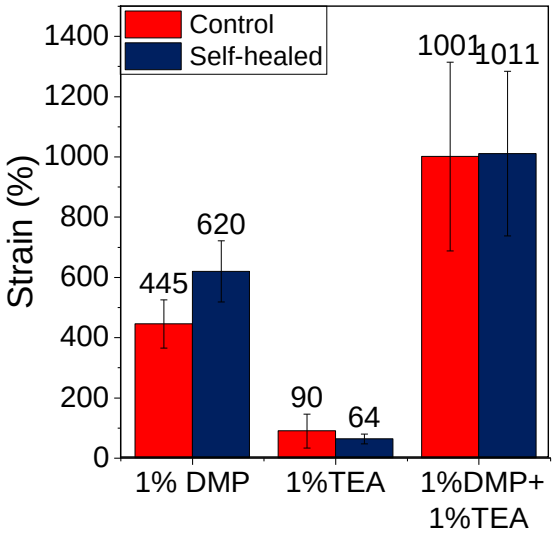

Figure 65. Effect of water immersion on self-healing of sealant joints

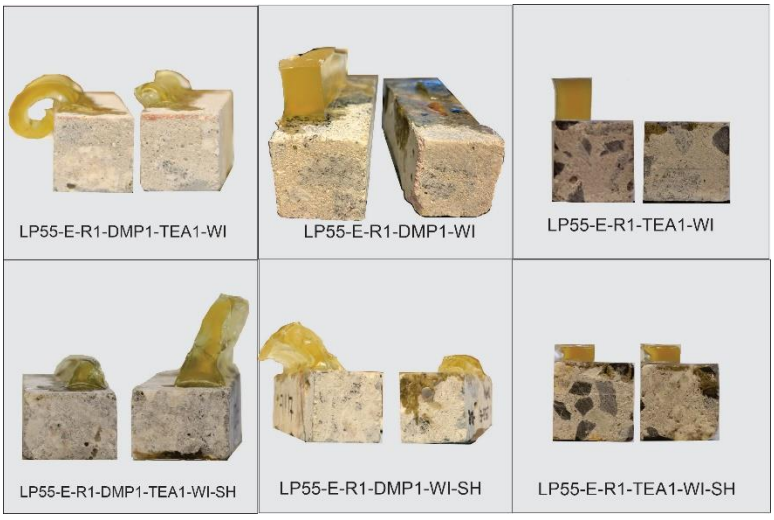

Figure 66. Failure modes of sealant joints after water exposure (WI-SH is short for water immersed and self-healed)

Sealants cohesive strength and self-healing

In the evaluation of three sealant formulations after water immersion, the control samples with DMP and a combination of DMP and TEA demonstrated similar elongation properties and strength- approximately

350% elongation and 160 kPa stress at 150% strain. However, there was a notable difference in their self-healing efficiency, with the sample containing DMP and TEA had a significantly higher efficiency of 91%, compared to 59% for the sample with DMP only, Figure 67. Considering that the content of catalysts in the combination of DMP and TEA was 2% by weight of the sealant, while in the case of DMP alone it was 1%,

The self-healing efficiency tested on dogbone specimens under tension was lower when compared to the self-healing efficiency of the sealant in joints. The reason for this is that the joints were self-healed by applying controlled displacement, while the dogbone specimens were self-healed by bringing two halves into contact with minimum pressure on the interface. The limitation in applying controlled compression on the interface of the dogbone specimens was due to the size of their cross-section.

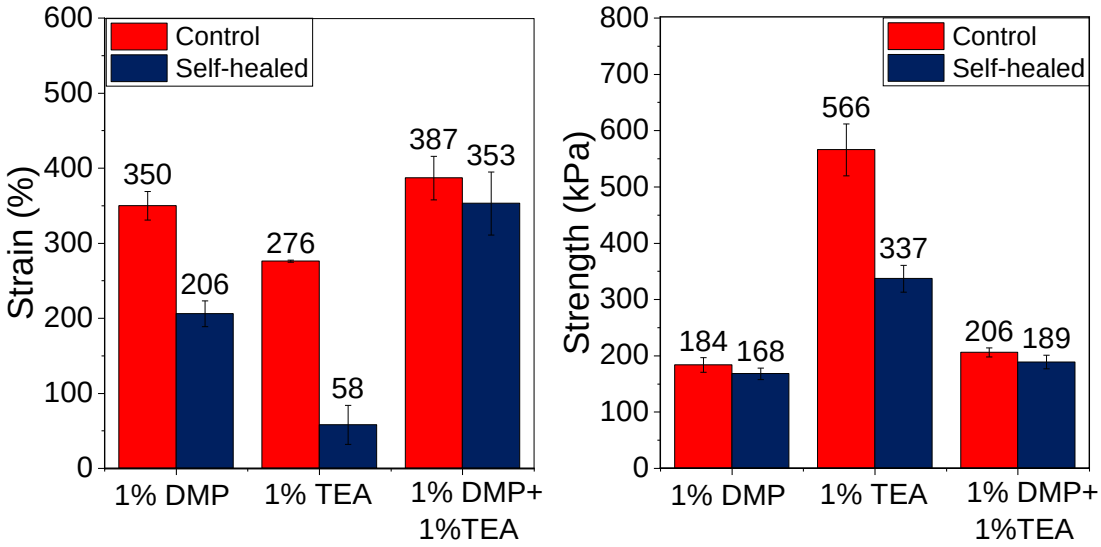

Figure 67. Effect of water immersion on sealants self-healing

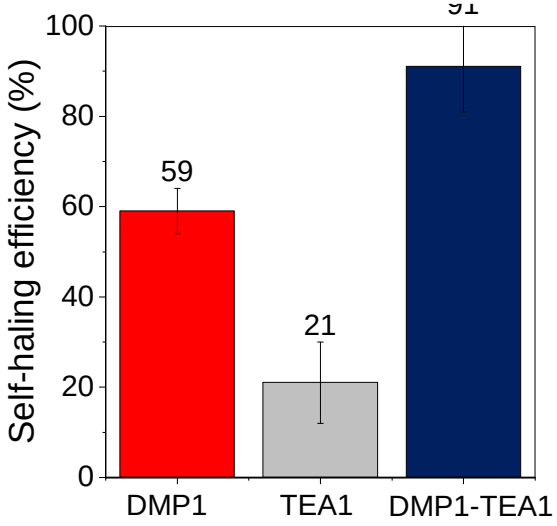

Figure 68. Effect of water immersion on sealants self-healing

Effect of mechanical forces on self-healing

The results showed that by increasing the applied displacement from 10% to 20% (percentage of the joint's width) the restored strain increased by at least 100% in samples with DMP (***Figure 69***). In The sealant that contained only TEA there was no increase in self-healing efficiency when the compressive force was increased. It is important to mention that in these experiments, specimens were not self-healed after being cut in half (like dogbones specimens). Instead, two halves were cured in a mold, forming two rectangular pieces that were later compressed. The absence of dissociated disulfides on the surface limits the self-healing mechanism primarily to physical processes such as diffusion and entanglement of polymer chains. Additionally, potential self-healing reactions may involve the reaction between unreacted thiols and disulfides in the polymer. Given that the compressive force had substantial effect on self-healing in the samples with DMP, the main healing mechanism is attributed to physical, rather than chemical, processes. Limited chain mobility in LP55-E-R1-TEA1 may have restricted healing even under increased compressive force.

The approach of making two pieces in a mold and then compressing them is not reflective of real-world scenarios. The ideal scenario where interfaces are brought into contact immediately after the fracture is not realistic in practical applications. For the sealants we designed and tested, this contact is facilitated by a temperature change causing expansion of the concrete. It is crucial to consider the aging effect, as over time, the number of dissociated groups within the broken interface decreases. This decrease in dissociated groups results in a reduction in self-healing efficiency, as there are fewer non-associated groups on the fracture surfaces available for the self-healing process. Understanding this aging effect and challenges associated with realistic damage scenarios is important for effective application of the sealant. Additional research is needed to address these challenges.

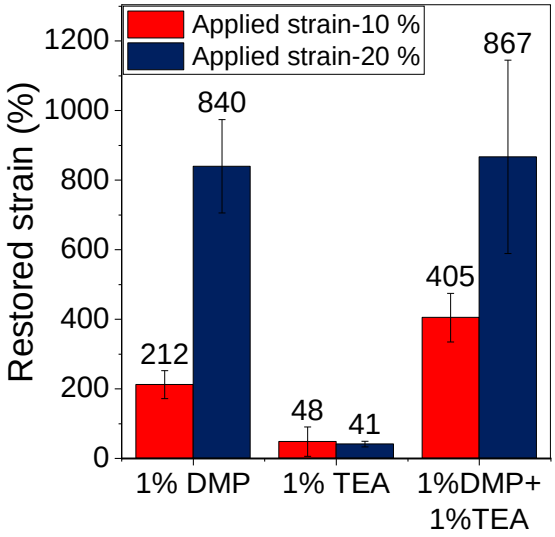

Figure 69. Effect of compressive forces on self-healing of sealants

Fatigue testing

The main objective of this study was to assess the performance of a pavement joint sealant that can simulate the dimensional movements observed in real field conditions. To achieve this goal, two types of joint sealants commonly used in rigid pavement joints were subjected to cyclic tensile loading and evaluated. A deflection-controlled cyclic tensile load was applied at a frequency of 10 Hz to four replicates of each type of sealant, referred to as Sealant 1 and Sealant 2. Each specimen was carefully examined for any indications of debonding or failure, and the normal stress in the sealant was recorded against the number of cycles.

Table 17 displays a summary of the test results. With roughly 309,000 cycles and an average normal stress of 28 kPa, specimen 1 of Sealant 1 failed relatively quickly compared to the other three specimens, according to Table 17. Sealant 1 specimens 2 and 3 failed after approximately 650,000 cycles. The specimen 4 of sealant 1 failed at roughly 750,000 cycles. Sealant 2 demonstrated significant variation in the test results, with specimen 1 failing after averaging about 641,890 cycles and 27 kPa of stress. Approximately 909,500 and 953,000 cycles later, specimens 2 and 3 of Sealant 2 failed, and they experienced 49 kPa and 33 kPa of average normal stress. On the other hand, specimen 4 showed failure after approximately 957,000 cycles at an average stress of 20 kPa. The test results revealed that all four specimens of Sealant 1 and Sealant 2 exhibited adhesive failure.

Table 17. Fatigue test results

Sealant Type	Sample no.	No. of cycles to failure	Average normal stress (kPa)
Sealant 1	Sample 1	308,850	27
	Sample 2	665,390	30
	Sample 3	644,840	30
	Sample 4	747,370	32
Sealant 2	Sample 1	641,890	27
	Sample 2	909,430	49
	Sample 3	953,680	33
	Sample 4	956,840	20

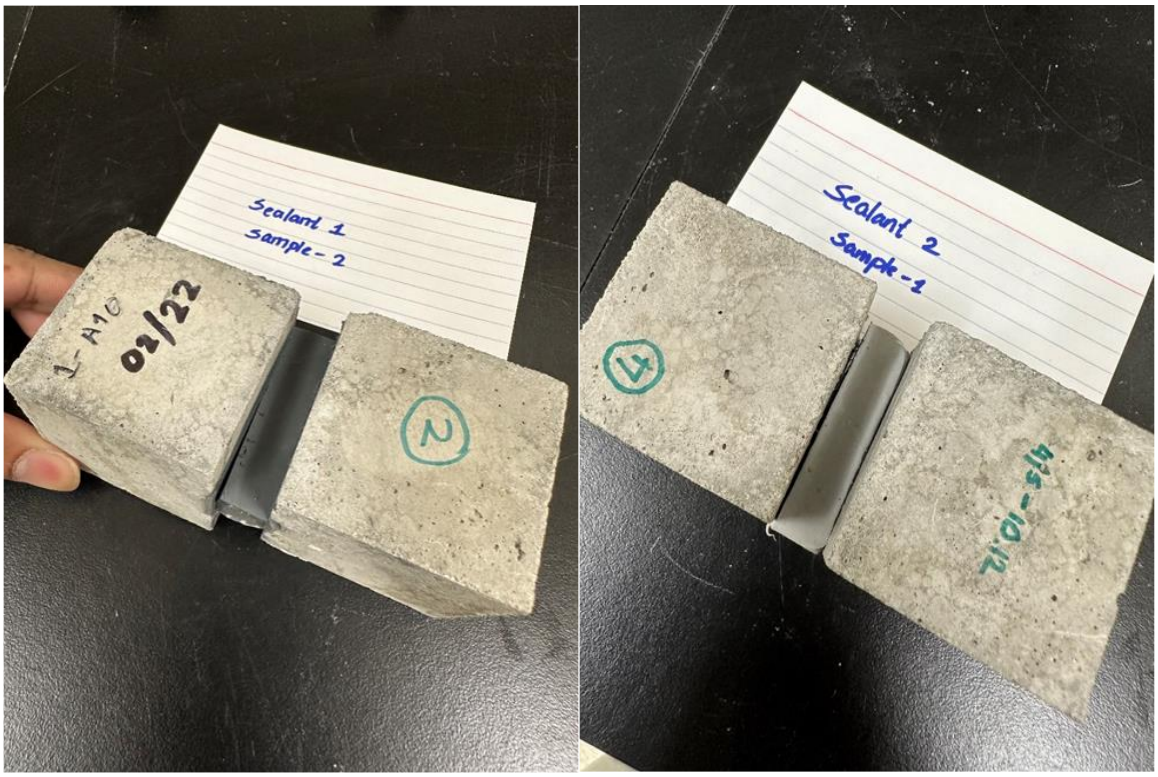

Figure 70. Typical failure modes for the commercial sealants after fatigue load

The average normal stress experienced by self-healing sealants was 80 kPa and 120 kPa for LP55-E-R1-DMP1 and LP55-E-R1-DMP1-TEA1, respectively, (Figure 73). LP55-E-R1-DMP1 failed after approximately 820,000 cycles. The LP55-E-R1-DMP1-TEA1 failed at 850,000 cycles.

Upon comparative analysis of the results obtained from the self-healing sealants with those of the commercial sealants (sealant 1 and sealant 2, Figure 71, Figure 72), it can be concluded that the self-healing sealant fatigue performance was comparable to the commercial sealants which failed after less than 1,000,000.

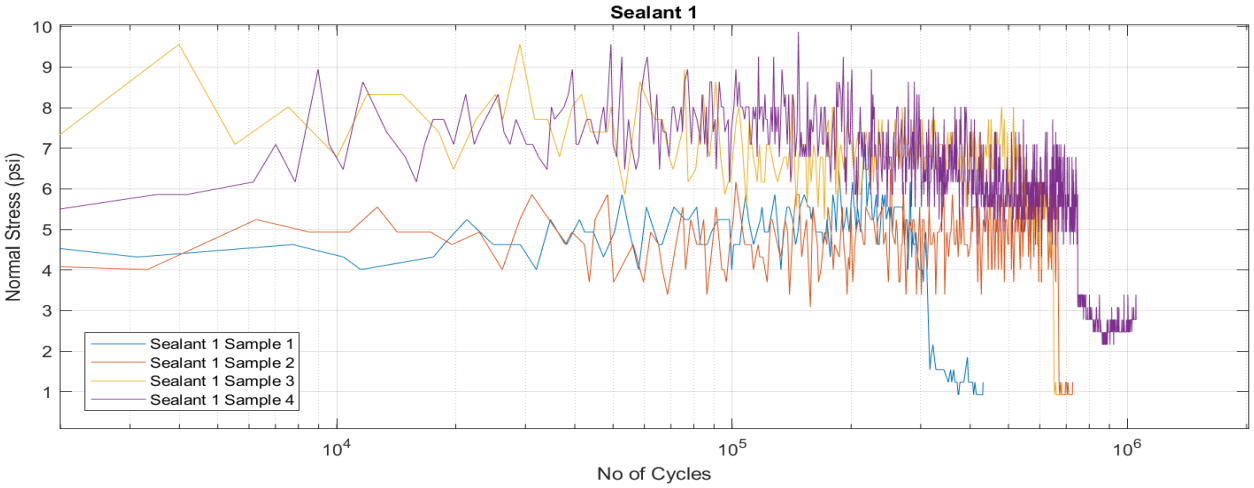

Figure 71. Fatigue test result comparison for Sealant 1 (commercial sealant)

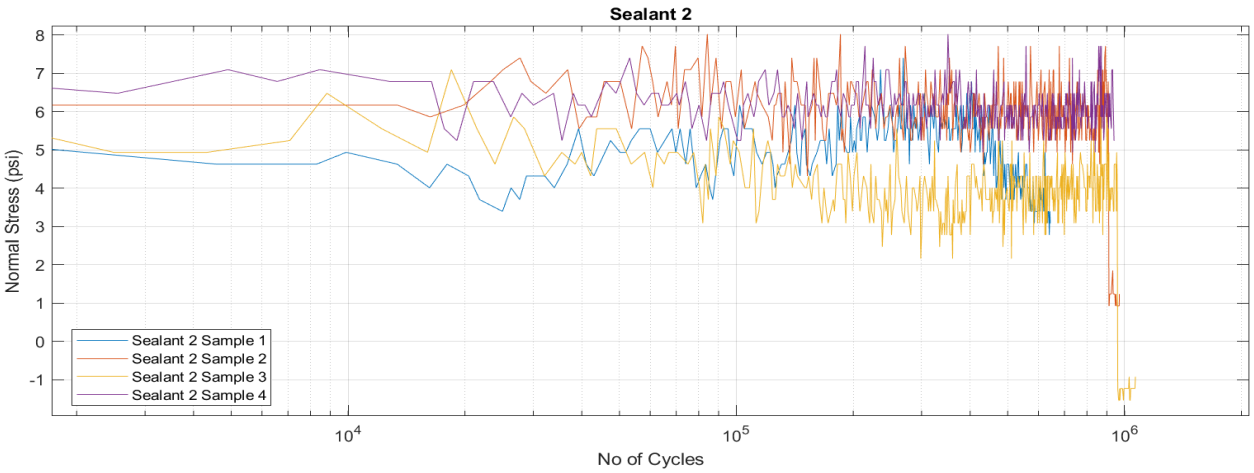

Figure 72. Fatigue test result comparison for Sealant 2 (commercial sealant)

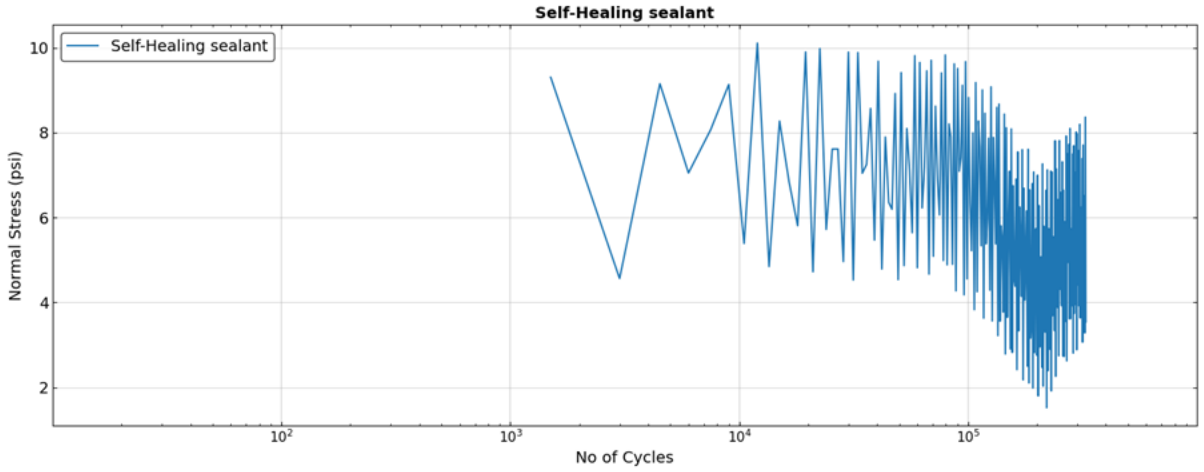

a)

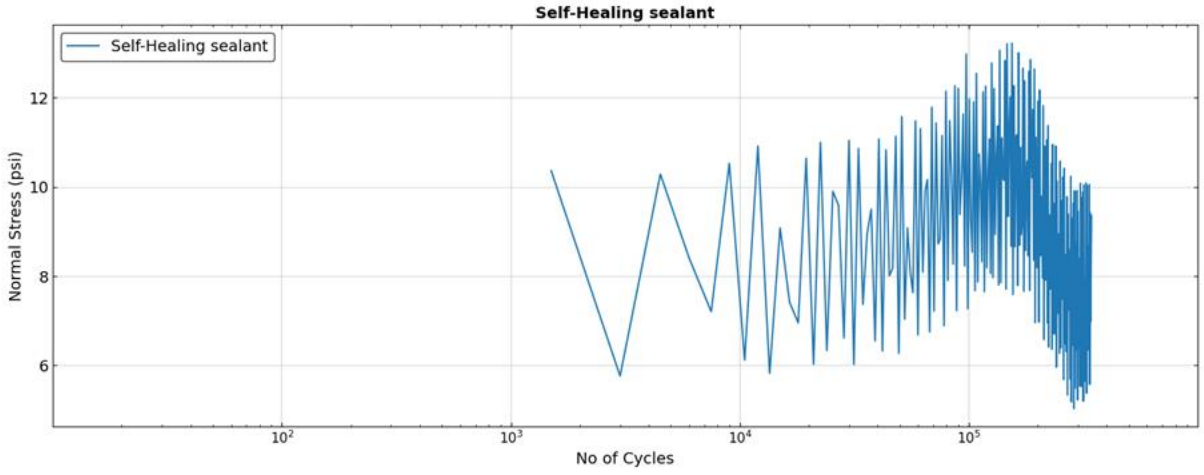

b)

Figure 73. Normal stress vs. number of cycles plot for self-healing sealants: a) LP55-E-R1-DMP1, b) LP55-R-1-DMP1-TEA1

CHAPTER 4

Summary and Conclusions

To improve the durability performance of concrete pavement sealants, an elastomer with self-healing ability was designed by incorporating dynamic disulfide bonds. Disulfide bond exchange is employed due to commercial availability of disulfide compounds with some of them having the ability to exchange bonds at room temperature. The objective was to 1) create a sealant using simple synthetic procedures and commercially available prepolymers, 2) analyze the effects of monomer type, type of initiator/catalyst and its concentrations on the polymer network and influence on the material properties and polymer self-healing, and 3) evaluate the performance of the new self-healing sealant under typical environmental and load conditions experienced by pavement joints.

Various formulations were tested and among them, an elastomer prepared from bisphenol-A epoxy resin and thiol-terminated polysulfides emerged as the most promising due to its capability for self-healing under ambient conditions. Further experimental investigation was employed to evaluate its suitability and efficacy for potential application in concrete pavement joints. The effects of catalyst type and concentration on polymer network and mechanical properties were studied. Two types of tertiary amines were tested as initiators for the epoxy-thiol reaction: 2,4,6-tris(dimethylaminomethyl)phenol (DMP) and triethylamine (TEA). DMP has been previously reported as an efficient initiator for epoxy-thiol reaction. Unlike prior research that used elevated temperatures for curing (75 ℃ for 24 h), our samples were cured at room temperature over a period of three weeks. TEA was tested as an initiator in an effort to improve self-healing efficiency. There has been interest in TEA as an effective catalyst for disulfide exchange or thiol-disulfide exchange. Three different formulations were tested to evaluate performance in concrete pavement joints: 1) with only DMP, 2) with only TEA, and 3) combination of DMP and TEA. With these three chosen formulations, the objective was to capture the impact of various catalysts and ensuring that the materials possess mechanical properties comparable to other commercially available sealants.

The performance of the three self-healing sealants was evaluated according to following requirements: 1) the sealant should cure within 21 days, 2) sealants should withstand elongation higher than 600%, 3) tensile strength should be limited to 0. 31 MPa at 150% strain to reduce the stress on the concrete/silicone bond, 4) specimens should not develop any cracks or separation between the concrete and the sealant when tested at -29 ℃ for five cycles of 100% extension each, 5) the hardness should not be less than 30 when tested at 23 ℃ using Type 00 durometer, 6) a sealant must be able to withstand exposure to UV. In addition to this, commercially available silicone sealant is used as a reference.

Curing under ambient conditions was monitored using spectroscopy and isothermal calorimetry. Dynamic mechanical analysis (DMA) was used to measure storage/loss modulus and determine glass transition temperature (T_g). In the context of self-healing polymers, a lower T_g is advantageous because it promotes

the movement of polymer segments, thus facilitating the self-healing response. In the self-healing experiments, dogbone specimens were removed from the mold and cut in half using a straight razor blade. Samples were then realigned back into the molds, taking care that halves are in contact to allow healing for 24 hours under SLC, 21 ℃, RH 50%. Following the self-healing, samples were tested in tension. The healing efficiency for each sample was defined as the percentage of restored elongation. To demonstrate the applicability of the elastomer in concrete pavement joints, the following experiments were conducted: adhesion to concrete in standard ambient conditions, adhesion to concrete after exposure to moisture, the effect of cold temperatures on adhesion, the effect of UV light, hardness, and fatigue testing. The effect of moisture and compression on the self-healing of joints was also tested.
The primary findings of the study are as follows:

- After 21 days of curing under ambient conditions the sealant did not contain any uncured material according to ASTM D5893 evaluation procedure. In addition to visual evaluation, curing under ambient conditions was monitored using spectroscopy and isothermal calorimetry. After 21 days at room temperature there were no unreacted thiols or epoxies in the polymer network.

- Type of catalyst had a significant effect on epoxy-thiol curing reaction. Using 1% of TEA decreased curing time from 24 hours when 1% of DMP was used to 16 h.

- Dynamic mechanical analysis showed that the glass transition temperature of the self-healable sealant was slightly lower (-35 ℃) compared to the commercial silicone sealant (-28 ℃). Storage modulus at room temperature varied between 1 MPa and 1.45 MPa for the three tested self-healable sealants and it was in the range of the silicone sealant (1.3 MPa).

- Tensile tests showed that by using combination of DMP and TEA as catalysts it is possible to design a sealant with ultimate elongation of approximately 500%. The measured elongation did not meet the requirement of 600% percent by ASTM D5893.

- Side reactions such as epoxy homopolymerization during the relatively long induction period of 12 h and plasticization when DMP was used led to decrease in tensile strength compared to samples prepared with TEA only.

- The sealants with DMP and combination of DMP and TEA had the tensile stress of approximately 200 kPa at 150% strain and met the performance requirement that limits this stress to 310 kPa.

- Adhesion tests after exposure to moisture and cold temperatures showed that sealants prepared with DMP and combination of DMP and TEA maintained adhesion to the concrete surface after the specified exposure condition, meeting the ASTM D5893 for water-immersed bond. However, the sealant prepared with TEA showed signs of damage and did not meet the performance requirement.

- The data and observations from fatigue testing indicate that the self-healing sealant failed after undergoing 850,000 cycles. The performance was comparable to a reference silicone sealant which failed adhesively after 950,000 cycles.

- After exposure to UV light and water spray, the self-healable sealants degraded significantly. This was expected as polysulfide sealants are inherently sensitive to UV light and require UV blockers to achieve resistance to UV degradation.

- Self-healing experiments showed that by using DMP and TEA as catalysts it is possible to design a sealant with self-healing efficiency of 78%. The sealants that contained either DMP or TEA had self-healing efficiency of 20% and 41%. The elongation of self-healed samples was 179% (contains only DMP), 56% (contains only TEA), and 360% (contains both DMP and TEA).

- Self-healing sealant joints exhibited cohesive failure after reaching a relatively high elongation of more than 1000% and tensile strength between 75 kPa and 250 kPa. In comparison to the commercial silicone which failed after reaching 350% elongation, self-healable sealant adhesion to concrete was better.

- Through exploring the effects of compressive force on sealant self-healing in joints, the study revealed a substantial increase in self-healing efficiency-when the applied displacement was increased from 10% to 20% of the joint width, the self-healing efficiency increased by over 100%.

- The most promising formulation is LP55-E-R1-DMP1-TEA1. It had higher self-healing efficiency and elongation compared with the other two formulations. The stress at 150% strain was lower than 310 kPa which was not the case with LP55-E-R1-TEA1 sample. It exhibited good adhesion to concrete, both after water exposure and exposure to cold temperatures. The hardness and fatigue response were similar to the reference commercial silicone sealant.

The self-healing sealants exhibited satisfactory performance across several aspects. However, before implementation, critical concerns regarding residual deformation must be addressed. These issues must be resolved to ensure the sealant's effectiveness and durability in real-world applications.

Limitations and future work

The effectiveness of the self-healing process relies on the capability of the two surfaces to come into contact. For the sealants we designed and tested here, it is assumed that this contact is facilitated by the temperature change causing closure of the joint. Using effects of compression as a result of atmospheric temperature change as a trigger for self-healing involves challenges related to the temporal control of the self-healing process. The ideal scenario where damaged interfaces are brought into contact immediately after the material rupture is not realistic in practical applications. It is crucial to consider the aging effect, as over time the number of dissociated groups within the broken interface decreases.

Issues related to the dimensional stability and stability of mechanical properties at elevated temperatures could be an issue. As dynamic mechanical analysis showed there is decrease in storage modulus with temperature which is caused by the nature of lightly cross-linked polymer network. However, increasing the rigidity of the polymer network would decrease the mobility of polymer chains which would make self-healing more challenging. Future research should explore other mechanisms and stimuli to enhance self-healing. Activation of self-healing processes through light exposure offers a means of achieving remote control over the polymer self-healing. Effects such as photoinduced metathesis of disulfides can initiate self-healing when a material is exposed to light. The photothermal effect observed in nanostructures of some metallic materials could be used to transform luminous energy into heat and trigger the self-healing of polymers by incorporating small amounts of metal nanoparticles into the polymer matrix.

Polysulfides are known for their susceptibility to residual deformation or creep. As shown during adhesion testing that involved extension and recompression of the joint, residual deformation was almost 80% due to testing conditions (low displacement rate applied to extend the sealant) that exacerbate creep behavior. Additional work on adjusting sealant formulation such as increasing cross-linking density and introducing monomers with permanent bonds to replace dynamic disulfide bonds is needed to improve sealants resistance to creep. Future work should also focus on further understanding and characterizing the stress-strain response of the sealant in tension/compression, particularly in the transition from “elastic” to plastic behavior. Analyzing parameters such as applied strain rate, temperature, and imposed extension is essential to establish the conditions under which the sealant can fully recover from the applied strain.

Another challenge we faced was establishing performance requirement for the cold-applied two component polysulfide sealant. Currently, there are no standard specifications or state issued performance requirements for polysulfide sealants that exist, for example, for silicone sealants. Due to cost consideration and competition from silicone and polyurethane sealants two-components polysulfide sealants are not typically used to seal joints in concrete pavements, therefore there is lack of standardized tests and performance requirements. Nevertheless, the potential evolution of cold-applied polysulfide sealants in the future to fulfill the industry's demand for improved performance and durability is likely to serve as motivation for the development of more standardized tests.

References

American Concrete Pavement Association (ACPA). (1993). Joint and Crack Sealing and Repair for Concrete Pavements. *Technical Bulletin TB012P*.

American Concrete Pavement Association (ACPA). (1995). Joint and Crack Sealing and Repair for Concrete Pavements. *Technical Bulletin* TB012P. Skokie, IL.

American Concrete Pavement Association (ACPA). (2018a). Concrete Pavement Joint Sealing/Filling. *Technical Bulletin* TB010. Rosemont, IL.

American Concrete Pavement Association (ACPA). (2018b). Joint and Sealant Movement Estimator. Rosemont, IL.

Aguirresarobe, R. H., Martin, L., Fernandez-Berridi, M. J., & Irusta, L. (2017). Autonomic healable waterborne organic-inorganic polyurethane hybrids based on aromatic disulfide moieties. *Express Polymer Letters*, *11*(4), 266.

Ahmad, M., Luo, J., Xu, B., Purnawali, H., King, P. J., Chalker, P. R., Fu, Y., Huang, W., & Miraftab, M. (2011). Synthesis and characterization of polyurethane-based shape-memory polymers for tailored Tg around body temperature for medical applications. *Macromolecular Chemistry and Physics*, *212*(6), 592–602.

Al-Qadi, I. L., & Abo-Qudais, S. A. (1995). Joint width and freeze/thaw effects on joint sealant performance. *Journal of Transportation Engineering*, *121*(3), 262–266.

Al-Qadi, I. L., Abo-Qudais, S., & Khuri, R. E. (1999). Method to evaluate rigid-pavement joint sealant under cyclic shear and constant horizontal deflections. *Transportation Research Record*, *1680*(1), 30–35.

Al-Qadi, I. L., Loulizi, A., Aref, S., Masson, J.-F., & McGhee, K. M. (2005). Modification of bending beam rheometer specimen for low-temperature evaluation of bituminous crack sealants. *Transportation Research Record*, *1933*(1), 96–106.

ARA. (2013). Arizona SPS-2 PCC Joint Seal Performance in ARA Technical Memorandum. *Applied Research Associates, Albuquerque, NM*.

ASTM D5893. (2016). Standard Specification for Cold Applied , Single Component , Chemically Curing Silicone Joint Sealant for Portland Cement Concrete. *ASTM International, West Conshohocken, PA*.

Babaahmadi, M., Sabzi, M., Mahdavinia, G. R., & Keramati, M. (2017). Preparation of amorphous nanocomposites with quick heat triggered shape memory behavior. *Polymer*, *112*, 26–34.

Bakhsh, K.N., Zollinger, D. G., & Jung, Y.S. (2013). *Evaluation of joint sealant effectiveness on moisture infiltration and erosion potential in concrete pavement*.

Biel, T. D., & Lee, H. (1997). Performance study of portland cement concrete pavement joint sealants. *Journal of Transportation Engineering*, *123*(5), 398–404.

Brown, H. E. (1991). *Joint sealant materials for concrete pavement repairs.* Virginia Transportation Research Council.

Brydson, J. A. (1999). *Plastics materials* (Seventh ed). Oxford: Butterworth-Heinemann.

Caihua, L. (2003). Applications of Filling Joint Materials on Cement Concrete Pavement. *Sci, & Tech, Information of Water Transportation*, *4*, 21.

Capelot, M., Montarnal, D., Tournilhac, F., & Leibler, L. (2012). Metal-catalyzed transesterification for healing and assembling of thermosets. *Journal of the American Chemical Society*, *134*(18), 7664–7667. https://doi.org/10.1021/ja302894k

Carbonell-Blasco, P., Martín-Martínez, J. M., & Antoniac, I. V. (2013). Synthesis and characterization of polyurethane sealants containing rosin intended for sealing defect in annulus for disc regeneration. *International Journal of Adhesion and Adhesives*, *42*, 11–20.

Chang, L.M., & Lee, Y.J. (2002). Evaluation of performance of bridge deck expansion joints. *Journal of Performance of Constructed Facilities*, *16*(1), 3–9.

Chen, D.H., Won, M., & Hong, F. (2009). Investigation of settlement of a jointed concrete pavement. *Journal of Performance of Constructed Facilities*, *23*(6), 440–446.

Chen, T., Qiu, J., Zhu, K., & Li, J. (2016). Electro-mechanical performance of polyurethane dielectric elastomer flexible micro-actuator composite modified with titanium dioxide-graphene hybrid fillers. *Materials & Design*, *90*, 1069–1076.

Chen, G., Tan, Y., et al. (2004). Study on low temperature performance evaluation system of normal temperature construction joint sealant. *Highway*, 119–122.

Choi, P., Senadheera, S., & Won, M. C. (2017). *Research on Joint Sealant Materials to Improve Installation and Performance*. Texas Tech University. Center for Multidisciplinary Research in Transportation.

Chongqi, S., Pan S., et al. (2007). Study on Fatigue and Aging Resistance of Joint Filling Materials for Cement Concrete Pavement. *Highway*, 172–174.

Cho, Y. K. (2013). *Advanced Cleaning Device to Remove Debris and Chemicals for Crack/Joint Sealing in Pavement*.

de Gennes, P. (1971). Reptation of a polymer chain in the presence of fixed obstacles. *J Chem Phys*, *55*, 572–579.

Denissen, W., Rivero, G., Nicolaÿ, R., Leibler, L., Winne, J. M., & Du Prez, F. E. (2015). Vinylogous urethane vitrimers. *Advanced Functional Materials*, *25*(16), 2451–2457. https://doi.org/10.1002/adfm.201404553

Dispenza, K. (2014). Concrete pavement preservation. *Concrete Producer*, *32*(5).

Eacker, M. J., & Bennett, A. R. (2000a). *Evaluation of various concrete pavement joint sealants*.

ECHEMI.COM. (n.d.). Retrieved January 31, 2023, from https://www.echemi.com/products/pid_Seven3449-trisdimethylaminomethylphenol.html

Evans, L., Smith, K. L., & Romine, A. R. (1999). *Materials and Procedures for Repair of Joint Seals in Portland Cement Concrete Pavements--Manual of Practice*. United States. Federal Highway Administration.

Fan, Z., Zhang, P., Wang, H.-Z., Cheng, X., & Wang, J. (2006). Study on Heat-Resistant Property of Organic-Silicone Sealant. *Journal of Aeronautical Materials*, *26*(3), 203.

Federal Highway Administration (FHWA). (2019). Tech Brief: Joint Sealing. FHWA-HIF-18-019. Washington, DC.

Feng, Q. I. N. (2009). Experimental study on shrinkage properties of cement-stabilized macadam base course with rubber powder. *New Building Material*, *36*(12), 32–35.

Fernández-Francos, X., Konuray, A. O., Belmonte, A., De La Flor, S., Serra, À., & Ramis, X. (2016). Sequential curing of off-stoichiometric thiol-epoxy thermosets with a custom-tailored structure. *Polymer Chemistry*, *7*(12), 2280–2290. https://doi.org/10.1039/c6py00099a

Fincher, H. E. (1983). *Evaluation of rubber expansion joints for bridges*. Indiana Department of Highways, Research and Training Center.

Gao, W., Bie, M., Liu, F., Chang, P., & Quan, Y. (2017). Self-Healable and Reprocessable Polysulfide Sealants Prepared from Liquid Polysulfide Oligomer and Epoxy Resin. *ACS Applied Materials and Interfaces*, *9*(18), 15798–15808. https://doi.org/10.1021/acsami.7b05285

Gao, W., Bie, M., Quan, Y., Zhu, J., & Zhang, W. (2018). *Self-healing , reprocessing and sealing abilities of polysulfide-based polyurethane*. *151*, 27–33. https://doi.org/10.1016/j.polymer.2018.07.047

Gao, W., Li, S., Cao, X., Li, W., & Han, B. (2021). Self-healable MnO2-cured polysulfide sealant and the effect of fillers on its self-healing ability. *Journal of Applied Polymer Science*, *138*(20). https://doi.org/10.1002/app.50428

Guimard, N. K., Oehlenschlaeger, K. K., Zhou, J., Hilf, S., Schmidt, F. G., & Barner-Kowollik, C. (2012). Current trends in the field of self-healing materials. *Macromolecular Chemistry and Physics*, *213*(2), 131–143. https://doi.org/10.1002/macp.201100442

Gurjar, A. H., Tang, T., & Zollinger, D. G. (1997). *Evaluation of Joint Sealants of Concrete Pavements*. Texas Transportation Institute, Texas A & M University System.

Gurjar, A., Kim, H. B., Moody, E., & Buch, N. J. (1998). Laboratory investigation of factors affecting bond strength in joint sealants. *Transportation Research Record*, *1627*(1), 13–21.

Gurjar, A., Zollinger, D. G., & Tang, T. (1996). Strain and age effects on behavior of a concrete pavement joint sealant material. *Transportation Research Record*, *1529*(1), 95–100.

Gu, X., & Mather, P. T. (2012). Entanglement-based shape memory polyurethanes: synthesis and characterization. *Polymer*, *53*(25), 5924–5934.

Hawkins, B. K., loannides, A. M., & Minkarah, I. A. (2001). To seal or not to seal? A field experiment to resolve an age-old dilemma. *Transportation Research Record*, *1749*(1), 38–45.

Huang, S., Kong, X., Xiong, Y., Zhang, X., Chen, H., Jiang, W., Niu, Y., Xu, W., & Ren, C. (2020). An overview of dynamic covalent bonds in polymer material and their applications. *European Polymer Journal*, *141*(September), 110094. https://doi.org/10.1016/j.eurpolymj.2020.110094

Ioannides, A. M., Long, A. R., & Minkarah, I. A. (2004). Joint sealant and structural performance at the Ohio route 50 test pavement. *Transportation Research Record*, *1866*(1), 28–35.

Jancar, J., Douglas, J. F., Starr, F. W., Kumar, S. K., Cassagnau, P., Lesser, A. J., Sternstein, S. S., & Buehler, M. J. (2010). Current issues in research on structure–property relationships in polymer nanocomposites. *Polymer*, *51*(15), 3321–3343.

Jianjun, C., Gang, G., Binhua, W., Xiaoping, D., Wanxia, H., & Mingjing, T. (2004). Preparation of PP/TiO2 nano-composite and analysis for its mechanism of aging resistance. *Engineering Plastics Application*, *7*, 15.

Jin, K., Heath, W. H., & Torkelson, J. M. (2015). Kinetics of multifunctional thiol-epoxy click reactions studied by differential scanning calorimetry: Effects of catalysis and functionality. *Polymer*, *81*, 70–78. https://doi.org/10.1016/j.polymer.2015.10.068

Ji, S., Wei, C., Ying, Y., & Huaping, X. (2015). Visible-Light-Induced Self-Healing Diselenide-Containing Polyurethane Elastomer. *Advanced Materials*, *27*, 7740–7745.

Keshavaraj R, Tock RW, Vallabhan CVG. (1994). Effects of moisture on structural silicone rubber sealants used in window glazing applications. *Constr Build Mater*, 8:227–32. https://doi.org/10.1016/S0950-0618(09)90006-X.

Kaiser, S., Novak, P., Giebler, M., Gschwandl, M., Novak, P., Pilz, G., Morak, M., & Schlögl, S. (2020). The crucial role of external force in the estimation of the topology freezing transition temperature of vitrimers by elongational creep measurements. In *Polymer* (Vol. 204). https://doi.org/10.1016/j.polymer.2020.122804

Kloxin, C. J., & Bowman, C. N. (2013). Covalent adaptable networks: Smart, reconfigurable and responsive network systems. *Chemical Society Reviews*, *42*(17), 7161–7173. https://doi.org/10.1039/c3cs60046g

Krishnakumar, B., Singh, M., Parthasarthy, V., Park, C., Sahoo, N. G., Yun, G. J., & Rana, S. (2020). Disulfide exchange assisted self-healing epoxy/PDMS/graphene oxide nanocomposites. *Nanoscale Advances*, *2*(7), 2726–2730. https://doi.org/10.1039/d0na00282h

Kunjun Sun. (2007). Study on Properties of New Anti - seepage Joint Material. *(Yang Ling: Northwest Agriculture and Forestry University)*.

Lacasse, M. A., Bryce, J. E., & Margeson, J. C. (1995). Evaluation of cyclic fatigue as a means of assessing the performance of construction joint sealants: silicone sealants. In *Science and Technology of Building Seals, Sealants, Glazing, and Waterproofing: Fourth Volume*. ASTM International.

Lamarre, A., Fini, E. H., & Abu-Lebdeh, T. M. (2016). Investigating effects of water conditioning on the adhesion properties of crack sealant. *Am. J. Eng. Applied Sci*, *9*, 178–186.

Lee, D. J. (1994). *Bridge bearings and expansion joints*. CRC Press.

Li, G., & Wang, A. (2016). Cold, warm, and hot programming of shape memory polymers. *Journal of Polymer Science Part B: Polymer Physics*, *54*(14), 1319–1339.

Li, H., Yi, Z., et al. (2015). Research Progress of Silicone Sealing Materials for Concrete Joints. *Concrete*, 156–160.

Li, K., Peng, J., Zhang, M., Heng, J., Li, D., & Mu, C. (2015). Comparative study of the effects of anatase and rutile titanium dioxide nanoparticles on the structure and properties of waterborne polyurethane. *Colloids and Surfaces A: Physicochemical and Engineering Aspects*, *470*, 92–99.

Lima, J. M., & de Brito, J. (2009). Inspection survey of 150 expansion joints in road bridges. *Engineering Structures*, *31*(5), 1077–1084.

Li, Q. (2011). *Development of testing system for analysis of transverse contractionjoints in Portland cement concrete pavement*. University of Florida.

Li, Q., Crowley, R. W., Bloomquist, D. B., & Roque, R. (2012). The creep testing apparatus (CRETA): A new testing device for measuring the viscoelasticity of joint sealant. *Journal of Testing and Evaluation*, *40*(3), 387–394.

Li, Q., Crowley, R. W., Bloomquist, D. B., & Roque, R. (2014a). Newly developed adhesive strength test for measuring the strength of sealant between joints of concrete pavement. *Journal of Materials in Civil Engineering*, *26*(12), 4014097.

Liu, X., & Wang, S. (2006). Fatigue Characteristics of Sealing Materials for Airport Concrete Pavement. *Journal of Traffic and Transportation Engineering*, *5*, 44–47.

Liu, X., Wang, S., Kong, D., et al. (2003). Applied Research on New Sealing Materials for Airport Concrete Pavement. *Journal of Air Force Engineering University; Natural Science Edition 4*, 31–33.

Liu, X., Wang, X., Liu, G., et al. (2008). Experimental Study on Elastic Recovery Characteristics of Sealing Materials for Airport Concrete Pavement. *New Building Materials*, 74–77.

Liu, G., Bai, E., Xu, J., Wang, T., & Chang, S. (2019). The Durability and Performance Test methods of the New Type of Pavement Filling Material-An Holistic Review. *IOP Conference Series: Earth and Environmental Science*, *304*(5), 52123.

Liu, J., Wu, S., & Chen, M. (2008a). The capability and application of sealing material for expansion joint [J]. *Water Sciences and Engineering Technology*, *4*.

Lima, M. J. & de Brito, J. (2009). Inspection survey of 150 expansion joints in road bridges. *Engineering Structures*, *31*(5), 1077–1084. https://doi.org/https://doi.org/10.1016/j.engstruct.2009.01.011

Loureiro, R. M., Amarelo, T. C., Abuin, S. P., Soulé, E. R., & Williams, R. J. J. (2015). Kinetics of the epoxy-thiol click reaction initiated by a tertiary amine: Calorimetric study using monofunctional components. *Thermochimica Acta*, *616*, 79–86. https://doi.org/10.1016/j.tca.2015.08.012

Lu, L., Zhao, D., Fan, J., & Li, G. (2022). *A brief review of sealants for cement concrete pavement joints and cracks*. https://doi.org/10.1080/14680629.2021.1898452

Lu, Z., Wu, A., Ou, X., Zhang, S., Niu, J., Ji, S., & Ling, Y. (2017). Enhanced anti-aging and mechanical properties of polyamide 1010 by sol-hydrothermal synthetic titanium dioxide-coated kaolinite addition. *Journal of Alloys and Compounds*, *693*, 381–388.

Lv, C., Wang, J., Li, Z., Zhao, K., & Zheng, J. (2019). Degradable, reprocessable, self-healing PDMS/CNTs nanocomposite elastomers with high stretchability and toughness based on novel dual-dynamic covalent sacrificial system. In *Composites Part B: Engineering* (Vol. 177). https://doi.org/10.1016/j.compositesb.2019.107270

Lynch, L. N., Chehovits, J. G., & Luders, D. G. (2002). Ten-Year Field Performance Evaluation of Joint Reseating Project. *Transportation Research Record*, *1795*(1), 40–48.

Lynch, L. N., Chehovits, J. G., Luders, D. G., & Belangie, M. (2013). Joint Resealing Project at Fairchild Air Force Base, Washington: Twenty-One-Year Field Performance. *Transportation Research Record*, *2361*(1), 98–105.

Lynch, L. N., & Janssen, D. J. (1999). Material characterization of silicone sealants. *Transportation Research Record*, *1680*(1), 44–46.

Lynch, L., Steffes, R., Chehovits, J., Voigt, G., Evans, L., & Al-Qadi, I. L. (2000). Joint-and Crack-Sealing Challenges. *Transportation in the New Millennium*.

Malla, R. B., Shaw, M. T., Shrestha, M. R., & Boob, S. (2006). *Sealing of small movement bridge expansion joints*.

Malla, R. B., Shaw, M. T., Shrestha, M. R., & Brijmohan, S. B. (2007). Development and laboratory analysis of silicone foam sealant for bridge expansion joints. *Journal of Bridge Engineering*, *12*(4), 438–448.

Malla, R. B., Shrestha, M. R., Shaw, M. T., & Brijmohan, S. B. (2011a). Temperature aging, compression recovery, creep, and weathering of a foam silicone sealant for bridge expansion joints. *Journal of Materials in Civil Engineering*, *23*(3), 287–297.

Malla, R. B., Swanson, B. J., & Shaw, M. T. (2011b). Laboratory evaluation of a silicone foam sealant bonded to various header materials used in bridge expansion joints. *Construction and Building Materials*, *25*(11), 4132–4143.

Masson, J. F. (1999). Bituminous sealants for pavement joints and cracks: building the basis for a performance-based specification. *Rilem Symposium on Durability of Building and Construction Sealants*, 315–328.

Meng, Q., & Hu, J. (2009). A review of shape memory polymer composites and blends. *Composites Part A: Applied Science and Manufacturing*, *40*(11), 1661–1672.

Miller, J. S., & Bellinger, W. Y. (2003). *Distress identification manual for the long-term pavement performance program*. United States. Federal Highway Administration. Office of Infrastructure ….

Montarnal, D., Capelot, M., Tournilhac, F., & Leibler, L. (2011). Silica-like malleable materials from permanent organic networks. *Science*, *334*(6058), 965–968. https://doi.org/10.1126/science.1212648

Morian, D. A., & Stoffels, S. (1998). Joint seal practices in the United States: Observations and considerations. *Transportation Research Record*, *1627*(1), 7–12.

Mphahlele, K., Ray, S. S., & Kolesnikov, A. (2017). Self-healing polymeric composite material design, failure analysis and future outlook: A review. *Polymers*, *9*(10), 1–22. https://doi.org/10.3390/polym9100535

Nevejans, S., Ballard, N., Miranda, J. I., Reck, B., & Asua, J. M. (2016). The underlying mechanisms for self-healing of poly(disulfide)s. *Physical Chemistry Chemical Physics*, *18*(39), 27577–27583. https://doi.org/10.1039/c6cp04028d

Odum-Ewuakye, B., & Attoh-Okine, N. (2006). Sealing system selection for jointed concrete pavements–A review. *Construction and Building Materials*, *20*(8), 591–602.

Paolillo, S., Bose, R. K., Santana, M. H., & Grande, A. M. (2021). Intrinsic self-healing epoxies in polymer matrix composites (Pmcs) for aerospace applications. *Polymers*, *13*(2), 1–32.

Pepels, M., Filot, I., Klumperman, B., & Goossens, H. (2013). Self-healing systems based on disulfide–thiol exchange reactions. *Polymer Chemistry*, *4*, 4955–4965.

Peterson, A. M., Kotthapalli, H., Rahmathullah, M. A. M., & Palmese, G. R. (2012). Investigation of interpenetrating polymer networks for self-healing applications. *Composites Science and Technology*, *72*(2), 330–336. https://doi.org/10.1016/j.compscitech.2011.11.022

Price, A. R. (1984). *The performance in service of bridge deck expansion joints*. Transport and Road Research Laboratory.

PubChem. (n.d.). Retrieved January 31, 2023, from https://pubchem.ncbi.nlm.nih.gov/compound/Triethylamine

Ramadani, R. F., Erastus Mosha, & Ramadani, R. F. (2014). https://doi.org/10.16526/j.cnki.11-4762/tp.2014.11.051

Rekondo, A., Martin, R., Ruiz De Luzuriaga, A., Cabañero, G., Grande, H. J., & Odriozola, I. (2014). Catalyst-free room-temperature self-healing elastomers based on aromatic disulfide metathesis. *Materials Horizons*, *1*(2), 237–240. https://doi.org/10.1039/c3mh00061c

Rogers, A. D., Lee-Sullivan, P., & Bremner, T. W. (1999a). Selecting concrete pavement joint sealants. I: Proposed test protocol. *Journal of Materials in Civil Engineering*, *11*(4), 302–308.

Seentrakoon, B., Junhasavasdikul, B., & Chavasiri, W. (2013). Enhanced UV-protection and antibacterial properties of natural rubber/rutile-TiO2 nanocomposites. *Polymer Degradation and Stability*, *98*(2), 566–578.

Shen, D., Shi, S., Xu, T., Huang, X., Liao, G., & Chen, J. (2018). Development of shape memory polyurethane based sealant for concrete pavement. *Construction and Building Materials*, *174*, 474–483. https://doi.org/https://doi.org/10.1016/j.conbuildmat.2018.04.154

Shou, C., Shang, P., & Song, N. (2007). Effect of Interface State of Cement Concrete Pavement Cutting Joints on Properties of Joint Sealants [J]. *Highway Engineering*, *32*, 188–190.

Smith, K. L., & Romine, A. R. (1999). *LTPP Pavement Maintenance Materials: SHRP Crack Treatment Experiment Final Report*. United States. Federal Highway Administration. Office of Infrastructure ….

Soliman, H., Shalaby, A., & Eng, P. (2007). Evaluation of joint and crack sealants based on cyclic loading and rheological properties. *Proc., 2007 Annual Conf. of the Transportation Association of Canada (TAC)*.

SS-S-200E. (1992). *Sealant joint, two-componenet, jet-blast-resistant, cold-applied, for portland cement concrete pavement* (pp. 0–21). US Military Specs.

State of California Department of Transportation. (2008). *MAINTENANCE TECHNICAL ADVISORY GUIDE Volume II - Rigid Pavement Preservation Second Edition*. *II*.

Thakur, S., & Karak, N. (2015). Tuning of sunlight-induced self-cleaning and self-healing attributes of an elastomeric nanocomposite by judicious compositional variation of the TiO 2–reduced graphene oxide nanohybrid. *Journal of Materials Chemistry A*, *3*(23), 12334–12342.

Tons, E. (1959). A Theoretical Approach to Design of a Road Joint Seal. *Highway Research Board Bulletin*, *229*.

Van Der Zwaag, S. (2014). *Self-Healing Materials: An Alternative Approach to 20 Centuries of Materials Science* (Vol. 30, Issue 6). Springer. https://doi.org/10.1515/ci.2008.30.6.20

Vidil, T., Tournilhac, F., Musso, S., Robisson, A., & Leibler, L. (2016). Control of reactions and network structures of epoxy thermosets. *Progress in Polymer Science*, *62*, 126–179. https://doi.org/10.1016/j.progpolymsci.2016.06.003

Wabo Bridge Seal. Retrieved February 19, 2024, from https://www.watsonbowmanacme.com/products/wabo-fs-bridge-seal

Wallbank, E. J. (1989). *The performance of concrete in bridges. A survey of 200 highway bridges*.

Wang, S., & Urban, M. W. (2020). Self-healing polymers. *Nature Reviews Materials*, *5*(8), 562–583. https://doi.org/10.1038/s41578-020-0202-4

Wang, J., L. L. and B. W. (2012). Study on Water Sealing Test Method of Joint Sealant for Cement Concrete Pavement. *Highway Traffic Technology*, 8–14.

Wang, S., & Zhang, J. (2014). Effect of titanium dioxide (TiO2) on largely improving solar reflectance and cooling property of high density polyethylene (HDPE) by influencing its crystallization behavior. *Journal of Alloys and Compounds*, *617*, 163–169.

Cai, C. (2012). Experimental Study on Waterproofing Materials for Deformation Joints of Highway Culvert in Cold Regions. *Xi'an: Chang' an University*.

Wang, H., Li, C., & Chao, B. (2011a). Research progress of concrete pavement joint filler materials in China. *Chinese Journal of Building Waterproofing*, 31–34.

White, C. C., Hunston, D. L., Tan, K. T., Hettenhouser, J., & Garver, J. D. (2013). An accelerated exposure and testing apparatus for building joint sealants. *Review of Scientific Instruments*, *84*(9), 95113.

White, C., Hunston, D., & Tan, K. (2012). A Test Method for Monitoring Modulus Changes during Durability Tests on Building Joint Sealants. In *Durability of Building and Construction Sealants and Adhesives: 4th Volume*. ASTM International.

Wool, R. P., & O'Connor, K. M. (1981). A theory of crack healing in polymers. *Journal of Applied Physics*, *52*(10), 5953–5963. https://doi.org/10.1063/1.328526

Worms, T. Shalaby, T., & Kavanagh, L.N. (2005). *Accelerated laboratory evaluation of joint sealants under cyclic loads*. Transportation Association of Canada. 2005 Annual Conference and Exhibition of the Transportation Association of Canada : Transportation - Investing in Our Future; Transportation Association of Canada.

Wu, H., Jin, B., Wang, H., Wu, W., Cao, Z., Wu, J., & Huang, G. (2020). A Degradable and Self-Healable Vitrimer Based on Non-isocyanate Polyurethane. In *Frontiers in Chemistry* (Vol. 8). https://doi.org/10.3389/fchem.2020.585569

Xie, T. (2011). Recent advances in polymer shape memory. *Polymer*, *52*(22), 4985–5000.

Xu, J., Zhu, L., Nie, Y., Li, Y., Wei, S., Chen, X., Zhao, W., & Yan, S. (2022). Advances and Challenges of Self-Healing Elastomers: A Mini Review. *Materials*, *15*(17), 1–21. https://doi.org/10.3390/ma15175993

Xu, L., Shang, P., Xu, X. W., Herrick, A. M., Sgro, A., & Shou, C. Q. (2011). Studies on synthesis and properties of novel polyurethane pavement joint sealant modified with polydimethysiloxane. *Materials Research Innovations*, *15*(2), 150–155.

Zhan, B., Li, Q. S., Hong, W., Xia, Y. Z., Wang, G. W., & Xing, G. Z. (2013a). Preparation and properties of epoxy resin modified waterborne polyurethane. *Applied Mechanics and Materials*, *320*, 607–610.

Zhang, B., Yuan, C., Zhang, W., Dunn, M. L., Qi, H. J., Liu, Z., Yu, K., & Ge, Q. (2019). Recycling of vitrimer blends with tunable thermomechanical properties. *RSC Advances*, *9*(10), 5431–5437. https://doi.org/10.1039/c9ra00015a

Zhang, G. Z., Fan, Z. K., Quan, Y. W., & Chen, Q. M. (2013). The preparation and physical properties of polysulfide-based elastomers through one-pot thiol-ene click reaction. *Express Polymer Letters*, *7*(7), 577–584. https://doi.org/10.3144/expresspolymlett.2013.55

Zhang, H., Cai, C., Liu, W., Li, D., Zhang, J., Zhao, N., & Xu, J. (2017). Recyclable Polydimethylsiloxane Network Crosslinked by Dynamic Transesterification Reaction. *Scientific Reports*, *7*(1), 1–9. https://doi.org/10.1038/s41598-017-11485-6

Zhang, J., Wang, Z., Ding, G., Quan, Y., & Chen, Q. (2012). *The Effect of Epoxy Resin to Reduce the Compression Set of Polysulfide Sealant*. *125*, 390–395. https://doi.org/10.1002/app

Zhang, P., Ogunmekan, B., Ibekwe, S., Jerro, D., Pang, S.-S., & Li, G. (2016). Healing of shape memory polyurethane fiber-reinforced syntactic foam subjected to tensile stress. *Journal of Intelligent Material Systems and Structures*, *27*(13), 1792–1801.

Zohrevand, A., Ajji, A., & Mighri, F. (2014). Morphology and properties of highly filled iPP/TiO2 nanocomposites. *Polymer Engineering & Science*, *54*(4), 874–886.

Appendix

A1. Tensile testing-SLC

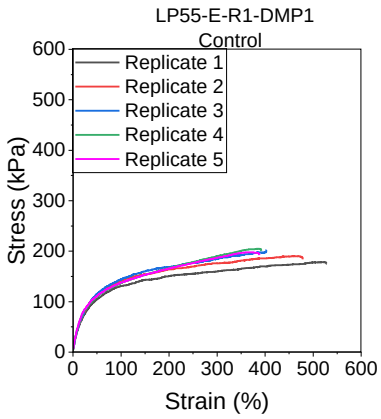

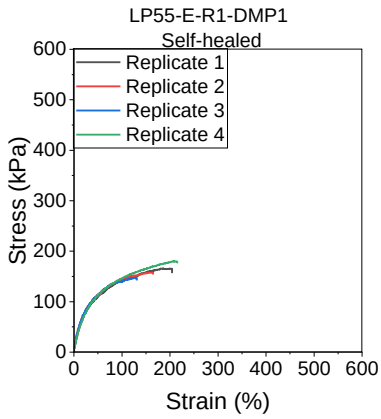

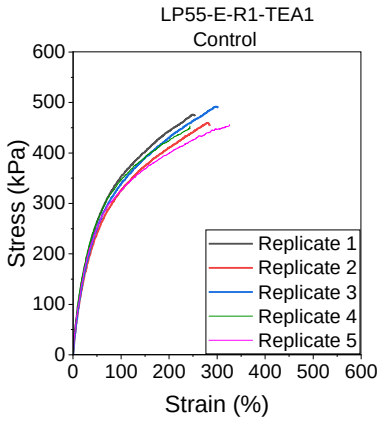

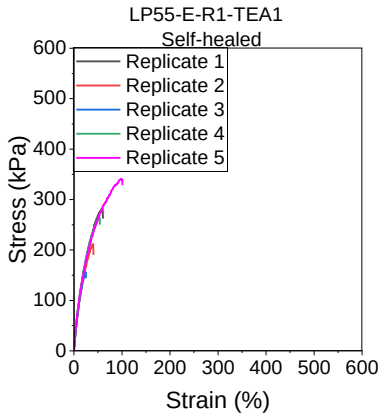

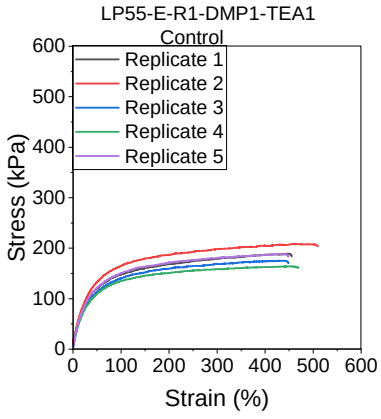

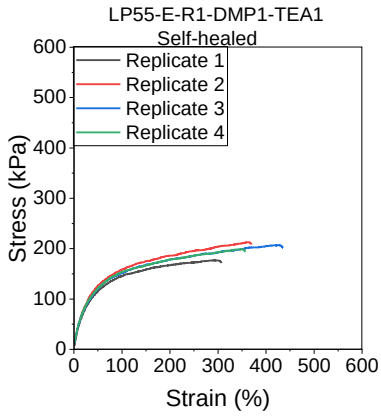

A2. Adhesion to concrete-SLC

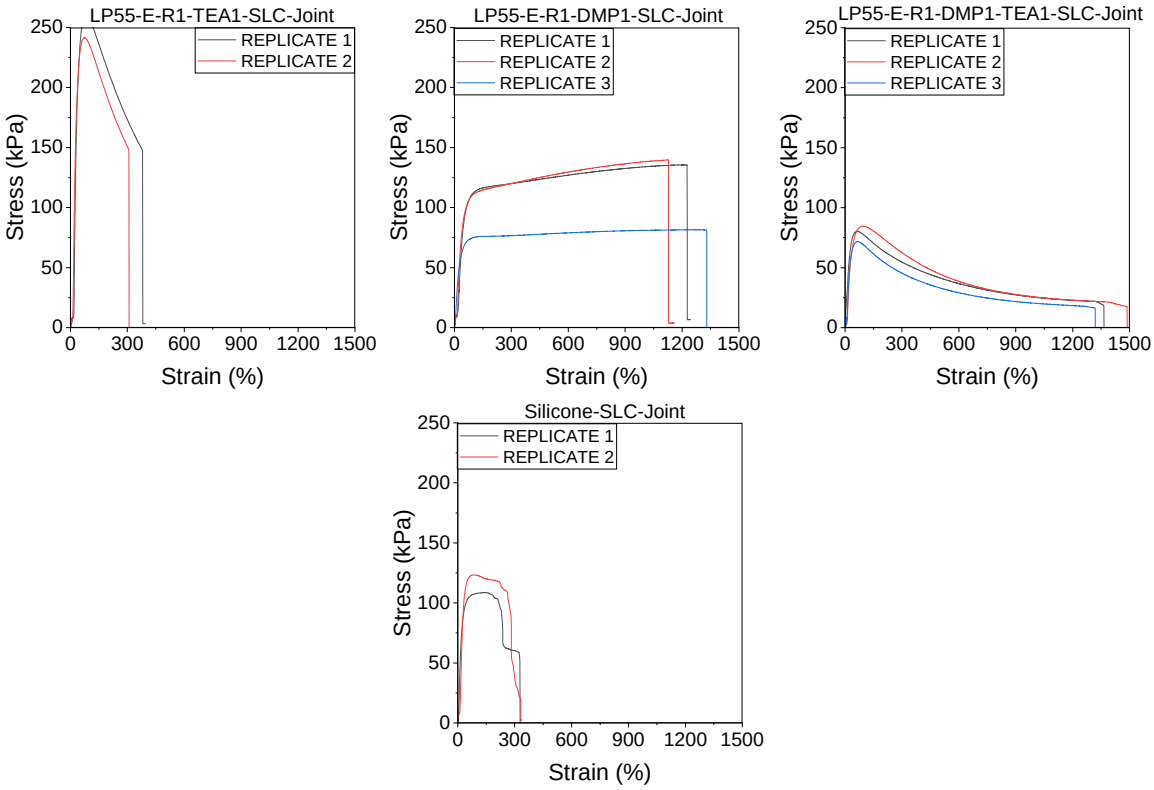

A3. Adhesion to concrete and self-healing in joints after water immersion

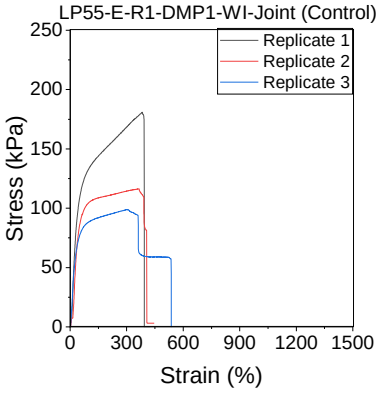

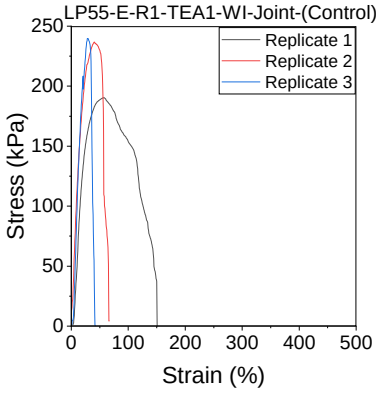

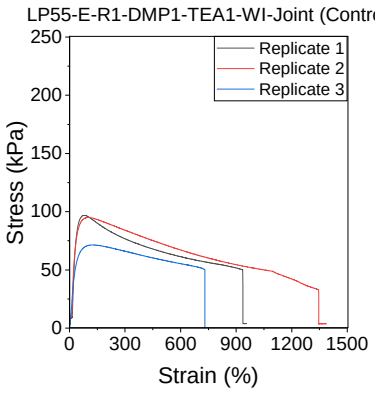

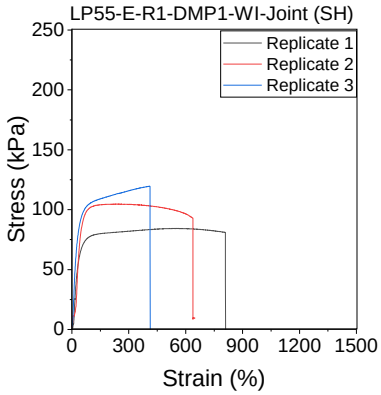

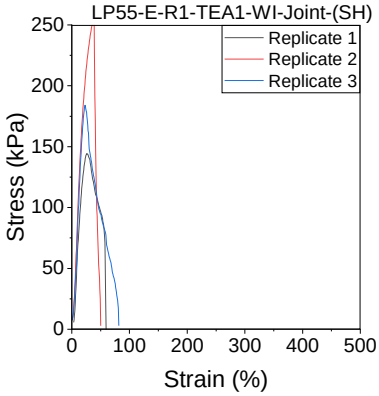

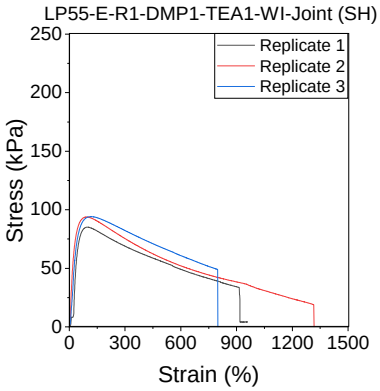

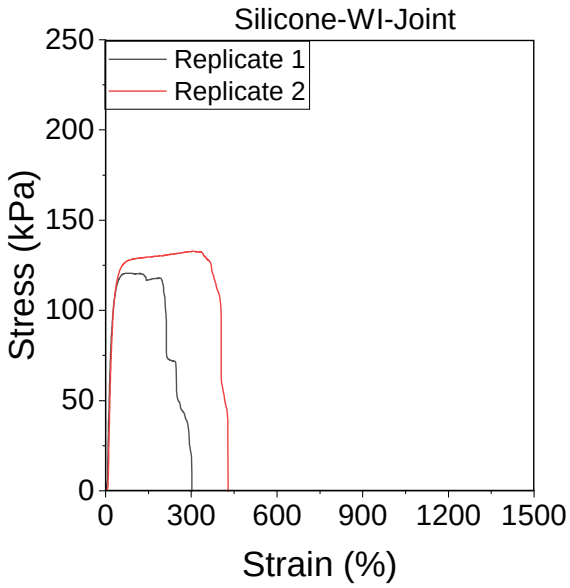

A4. Effect of compressive force on self-healing